

**SPRAY PAINTING MANIPULATOR MODELLING , SIMULATION AND  
CONTROL**

by

**B.Hakan GÜROCAK**

**B.S. in M.E., Middle East Technical University, 1986**

**Submitted to the Institute for Graduate Studies in  
Science and Engineering in partial fulfillment of  
the requirements for the degree of**

**Master of Science**

**in**

**Mechanical Engineering**

Bogazici University Library



39001100310575

14

**Boğaziçi University**

**1989**

### ACKNOWLEDGEMENTS

I wish to express my gratitude to Prof.Dr. Ahmet KUZUCU in acknowledgement of his valuable advices,insightful suggestions and supports.

I also greatly appreciate Doç.Dr. Osman TÜRKAY and Doç.Dr. Ali Rıza KAYLAN for their contributions in completion of my study.

Hakan GÜROCAK

## SPRAY PAINTING MANIPULATOR MODELLING, SIMULATION AND CONTROL

## ABSTRACT

In this study, a computer simulation program package for a six revolute joint spray painting robot having pitch-yaw-roll type wrist configuration has been developed. For this purpose, direct kinematics and inverse kinematics problems besides construction of manipulator Jacobian matrix have been investigated. A recursive dynamic modelling algorithm based on Newton-Euler formulation has been adopted to the six revolute joint spray painting robot. Furthermore, for the control of the robot, computed torque technique and minimum energy approach with specified final time and state are the methods employed.

In addition to several scenarios as the path to be followed during operation, one of the most critical problems of spray painting robots: Trajectory determination for a spray painting robot performing three dimensional surface operations has been investigated through on-line teach-in with off-line path planning approach.

# SPREY BOYA MANİPÜLATÖRÜ MODELLEMESİ, BİLGİSAYARLA BENZETİMİ VE DENETİMİ

## KISA ÖZET

Bu çalışmada, altı serbestlik dereceli, dönel eklemlili, pitch-yaw-roll tipi bilek yapısına sahip bir boya robotunun bilgisayarla benzetimi için bir program geliştirilmiştir. Bu sebeple, robot Jacobian matrisinin oluşturulmasının yanısıra, düz ve ters kinematik problemleri incelenmiştir. Ayrıca, Newton-Euler formülasyonuna dayalı bir dinamik modelleme yöntemi de altı serbestlik dereceli robota uyarlanmıştır. Denetim amacı ile seçilen algoritma en az enerji, optimum kontrol algoritmasıdır.

Bununla birlikte, boyama sırasında takip edilecek birkaç örnek yörüngenin yanısıra, spreyc boya robotlarının en önemli problemlerinden biri olan: Üç boyutlu yüzey işlemleri yapmakta olan bir spreyc boya robotu için yörünge belirlenmesi problemi de on-line öğretim ve off-line yörünge hesaplama yaklaşımı ile irdelenmiştir.

## TABLE OF CONTENTS

	<u>Page</u>
ACKNOWLEDGEMENTS	<i>iii</i>
ABSTRACT	<i>iv</i>
KISA ÖZET	<i>v</i>
LIST OF FIGURES	<i>viii</i>
LIST OF TABLES	<i>xi</i>
LIST OF SYMBOLS	<i>xii</i>
I. INTRODUCTION	1
II. SPRAY PAINTING	4
III. MATHEMATICAL MODELLING OF THE 6R SPRAY PAINTING ROBOT ARM	9
3.1. Structure of a 6R spray painting robot	9
3.2. Kinematics of the robot arm	10
3.2.1. Direct kinematics	13
3.2.2. Inverse kinematics	19
3.3.3. Jacobian of the robot arm	25
3.3. Dynamic modelling of 6R spray painting Robot	30
IV. CONTROL OF THE ROBOT	48
4.1. Computed torque technique	48
4.1.1. Updating policy	50
4.1.2. Minimum energy approach with specified final time & state	53

V.	TRAJECTORY DETERMINATION	55
	5.1. Introduction	55
	5.2. Space curves as the "path"	56
	5.3. Teach-in with ON-LINE programming on the surface to be painted	60
	5.4. OFF-LINE trajectory planning	63
	5.5. Overlapped polynomials as the "path"	67
VI.	SIMULATION OF BEHAVIORS OF THE 6R ROBOT	71
	6.1. Structure of the simulation program (flowchart)	71
	6.2. Main program	72
	6.3. Subroutines	74
	6.4. User interaction	75
VII.	SIMULATION RESULTS	76
	7.1. Scenarios	76
	7.2. Scenario 1 (Spatial line)	76
	7.3. Scenario 2 (Conic helix)	78
	7.4. Scenario 3 (Spatial parabola)	82
	7.5. Teach-in on conic helix	85
	7.6. Teach-in on a rectangular surface	86
	7.7. Graphics	88
VIII.	CONCLUSIONS	110
	BIBLIOGRAPHY	113

## LIST OF FIGURES

	<u>Page</u>
Figure 2.1. - Automatic spray gun	5
Figure 2.2. - Spray patterns	5
Figure 2.3. - Air cap	6
Figure 2.4. - Spray gun, when arced	8
Figure 3.1. - Workspace of a 6R robot	11
Figure 3.2. - Structural configuration	11
Figure 3.3. - Coord. frames attached to the 6R robot	12
Figure 3.4. - Denavit-Hartenberg parameters	15
Figure 3.5. - Coordinate frames in 3D space	18
Figure 3.6. - Translation of a point on the surface	20
Figure 3.7. - Linear and angular velocities of hand	26
Figure 3.8. - Motion with respect to moving frames	33
Figure 3.9. - Forces and Moments on the links	36
Figure 4.1. - Trace of inertia matrix w.r.t. position	51
Figure 4.2. - Approximated trace of inertia matrix	52
Figure 4.3. - Concentric stratum in the workspace	52
Figure 5.1. - Space curve	56
Figure 5.2. - Moving trihedral	58
Figure 5.3. - Translation of knots in world coord. into joint coordinates.	64
Figure 5.4. - Third order polynomial	68
Figure 5.5. - Polynomials attached sequentially	68
Figure 5.6. - Overlapped polynomials	69

	<u>Page</u>
Figure 6.1. - Flowchart	73
Figure 7.1. - Spatial line	77
Figure 7.2. - Conic helix	78
Figure 7.3. - Spatial parabola	82
Figure 7.4. - Teach-in on the conic helix	85
Figure 7.5. - Teach-in on a rectangular surface	86
Figure 7.6. - First three joint disp.for conic helix	88
Figure 7.7. - Wrist joint disp.for conic helix	89
Figure 7.8. - First three joint vel.for conic helix	90
Figure 7.9. - Wrist joint vel.for conic helix	91
Figure 7.10 - First three joint torques for conic helix	92
Figure 7.11 - Wrist joint torques for conic helix	93
Figure 7.12 - Pos. err. of first three j. on con.helix	94
Figure 7.13 - Pos.err. of wrist joints on con.helix	95
Figure 7.14 - Speed err. of first three j. on con.helix	96
Figure 7.15 - Speed err. of wrist joints on con. helix	97
Figure 7.16 - Teach-in on con.hel. first 3 joint disp.	98
Figure 7.17 - Teach-in on con.hel. wrist joint disp.	99
Figure 7.18 - Teach-in on con.hel. first three j. vel.	100
Figure 7.19 - Teach-in on con.hel. wrist joint vel.	101
Figure 7.20 - Teach-in first three joint disp.on rect.	102
Figure 7.21 - Teach-in wrist joint disp. on rect. pla.	103
Figure 7.22 - Pos.err. of first three joints on rec. pl.	104
Figure 7.23 - Pos.err. of wrist joints on rec. plate	105

	<u>Page</u>
Figure 7.24 - Torque of 1st, pos. err. of 1st & 5th j. on spatial line	106
Figure 7.25 - Speed of the 1st, spe. err. of the 1st & 6th joints on the spatial line	107
Figure 7.26 - 1st & 4th joint disp., vel. of the 2nd joint on spatial parabola	108
Figure 7.27 - Pos. & spe. err. of the 5th & 4th joints, and torque of the first joint on spatial parabola	109

## LIST OF TABLES

	<u>Page</u>
Table 3.1. - Den.Hartenberg par. for the 6R robot.	16
Table 5.1. - Typical applications of teach-in.	61
Table 7.1. - Dimensions of the selected robot.	87

## LIST OF SYMBOLS

$a_i$	Distance between the origins of $(i-1)$ th and $i$ th coordinate frames along $x_i$
$\vec{a}_i$	Linear acceleration of link $i$
$\vec{a}_{g_i}$	Linear acceleration of center of mass of link $i$
$A$	System matrix
$A_i^{i-1}$	Homogeneous transformation matrix relating $(i-1)$ th and $i$ th frames
$B$	Input or Control vector
$b$	Bi-normal vector of the end-effector
$\vec{b}_{i-1}$	Vector defined with respect to the base frame which is aligned in each joint's axis
$d_i$	Distance between $x_{i-1}$ and $x_i$ along $z_{i-1}$
$\vec{f}(q_i, q_j, \dot{q})$	Vector for centrifugal and Coriolis effects
$\vec{f}_i$	Force exerted on link $i$ by $i-1$
$\vec{F}_i$	Total force exerted on link $i$
$\vec{g}$	Gravitational acceleration
$\vec{g}(\vec{q})$	Vector for the gravitational terms
$\vec{h}(\vec{q})$	Vector for external forces and moments on the end-effector
$I_i$	Inertia tensor of link $i$ with respect to its center of mass expressed in the fixed base frame.
$\bar{I}_i$	Inertia tensor of link $i$ with respect to its center of mass expressed in $i$ th link's own coordinate frame.

$J$	Inertia matrix, quadratic performance index
$\rightarrow k$	Summation of vectors $\vec{h}$ , $\vec{f}$ and $\vec{g}$
$m_i$	Mass of link $i$
$\vec{m}_i$	Moment exerted on link $i$
$\rightarrow M_i$	Total moment exerted on link $i$
$\vec{n}$	Normal vector of the end-effector
$\rightarrow P$	Position vector of the tip with respect to the base frame
$\vec{q}$	Vector of generalized coordinates
$\vec{q}_d, \dot{\vec{q}}_d, \ddot{\vec{q}}_d$	Vectors for desired joint coordinates, velocities and accelerations, respectively
$\vec{r}_i$	Vector from the base coordinate origin to the origin of the $i$ th frame
$\vec{r}_i^*$	Vector from the origin of $(i-1)$ th frame to that of $i$ th frame
$R_i^{i-1}$	Rotation matrix relating $(i-1)$ th frame to $i$ th
$\vec{s}_i$	Vector from the origin of base coordinate frame to the center of mass of link $i$
$\rightarrow t$	Tangent vector of the path
$t$	Time
$T$	Horizon time
$T$	Arm matrix
$\vec{u}$	Input control vector
$\rightarrow v_i$	Linear velocity of link $i$
$\rightarrow v_{gi}$	Linear velocity of center of mass
$V$	Viscous friction matrix

$\vec{x}$	State vector
$\vec{x}_{i-1,e}$	Position vector for $i$ th joint
$(x_i, y_i, z_i)$	Body attached coordinate frame of link $i$
$\alpha_i$	Angle between the $z_{i-1}$ and $z_i$ axis about $x_i$ (right-hand rule)
$\vec{\alpha}_i$	Angular acceleration vector
$\kappa$	Curvature of a space curve
$\rho$	Torsion of a space curve
$\theta_i$	Angle between the $x_{i-1}$ and $x_i$ axes measured about $z_{i-1}$ (right-hand rule)
$\vec{\tau}$	Vector for input torques by the link actuators
$\vec{\omega}_i$	Angular velocity of link $i$

## I. INTRODUCTION

Industrial robots are in use throughout the world for a multitude of tasks. With a pressing need for increased productivity and the delivery of end products of uniform quality, industry is turning more and more toward computer-based automation. At the present time, most automated manufacturing tasks are carried out by special-purpose machines designed to perform predetermined functions in a manufacturing process. But nowadays, robots are capable of performing a variety of manufacturing functions with improved quality. They may work in a more flexible working environment at a lower production cost. They also record accurately what is being done and provide information that can be used to improve management control. Besides those advantages, recently, computer controlled robots became indisputably more important in the industry in that; they can carry out various operations in hostile environmental conditions without being effected at all.

Spray painting is done with toxic materials that are extremely harmful to the worker's health. Therefore, they are required to work completely covered with hoods and sealed garments. In addition, it's been proved that in most of the

applications spray painting costs more than that has been estimated because of the material wasted as overspray mist, mainly due to the lack of skill of the operator in performing the task. The need for replacement of human in the paint booths with a substitute and precision constraints for economical justification together with the well-known advantages of manipulators resulted in specially designed and equipped spray painting robots.

Robotic applications in spray painting is interesting in that; the investment is economically justified only due to the precision increased, therefore the material saved. That means a high performance, suitable manipulator.

In spray painting process, there is usually a complex path involved which cannot be determined analytically once at a time. This path has to be a continuous one rather than a point to point defined task.

Spray painting has its own special requirements to be fulfilled. For a better and economical result, the spray gun must be kept being normal to the path, retaining a constant offset distance from the surface throughout the operation. In addition, the end-effector, that is; the spray gun must be traversing the surface to be painted, with a constant speed, leading to a uniform thickness coating on the surface. Hence, there is a need for a suitable technique that will meet all requirements of spray painting.

In this study, a computer simulation program that

fulfills the special requirements due to spray painting and trajectory determination problems has been developed.

Chapter 2 gives a brief explanation about spray painting process and the apparatus necessary.

In chapter 3, derivation of mathematical model of the 6R robot with explanations about its structure in relation to spray painting, kinematics of the robot including direct and inverse kinematics, together with the construction of manipulator Jacobian and adapted Newton-Euler recursive algorithm for dynamic modelling are present.

Chapter 4 contains the proposed control algorithms for trajectory following.

In chapter 5, formulations for defining the path to be followed, on-line teach-in on the surface to be painted with off-line trajectory planning schemes and overlapped polynomials as the path are included.

Structure of the simulation program package with detailed explanations of the main structure and subroutines are presented in chapter 6.

Chapter 7 concludes the study with several scenarios employed and the results obtained.

## II. SPRAY PAINTING

Spray painting or coating is the process of applying a paint or a coating material on to a surface by atomization. That is, transforming the liquid used, into fine spray by some means. The fundamental characteristic which determines the 'sprayability' of a paint is its viscosity. Today's finishes have extremely complex chemical formulations. All of them will usually require the addition of thinners or reducers to get a viscosity appropriate for spraying.

Spray painting is achieved by means of what is called as a *spray gun*. It is a tool which uses compressed air to atomize paint or other sprayable material and apply it to a surface. Air and the material enter the gun through separate passages and are mixed at the air cap in a controlled pattern. There are many types of spray guns. Even though all of them have many parts and components in common, each gun type is suited for only a certain defined range of jobs. Industrial spraying robots employ pressure fed automatic guns since there is a large amount of material used during production spraying.

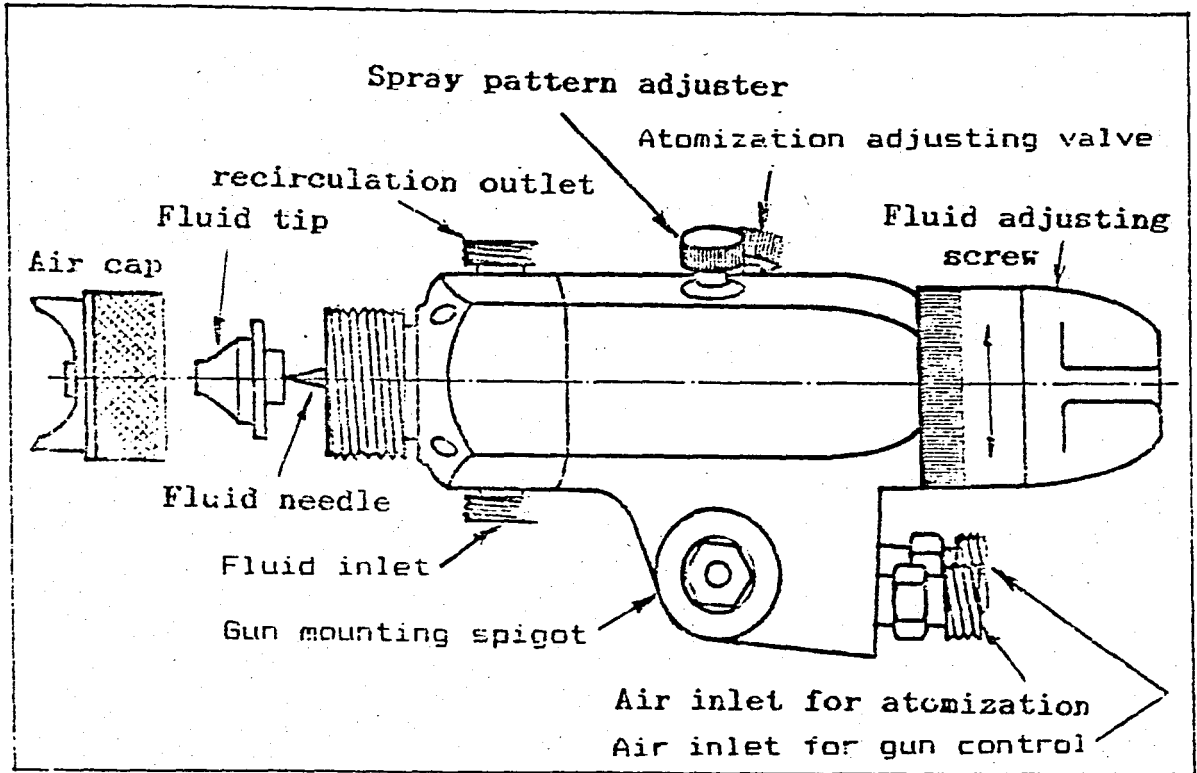


Figure 2.1. - Automatic spray gun

The air cap directs compressed air into the material stream to atomize it and form different spray patterns.

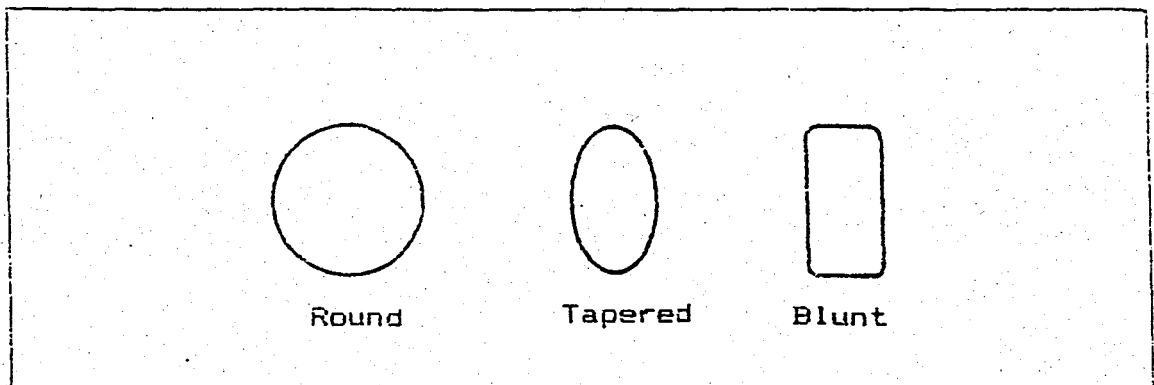


Figure 2.2. - Spray patterns

Automatic spray guns use multiple jet caps which provide better atomization and greater uniformity in pattern.

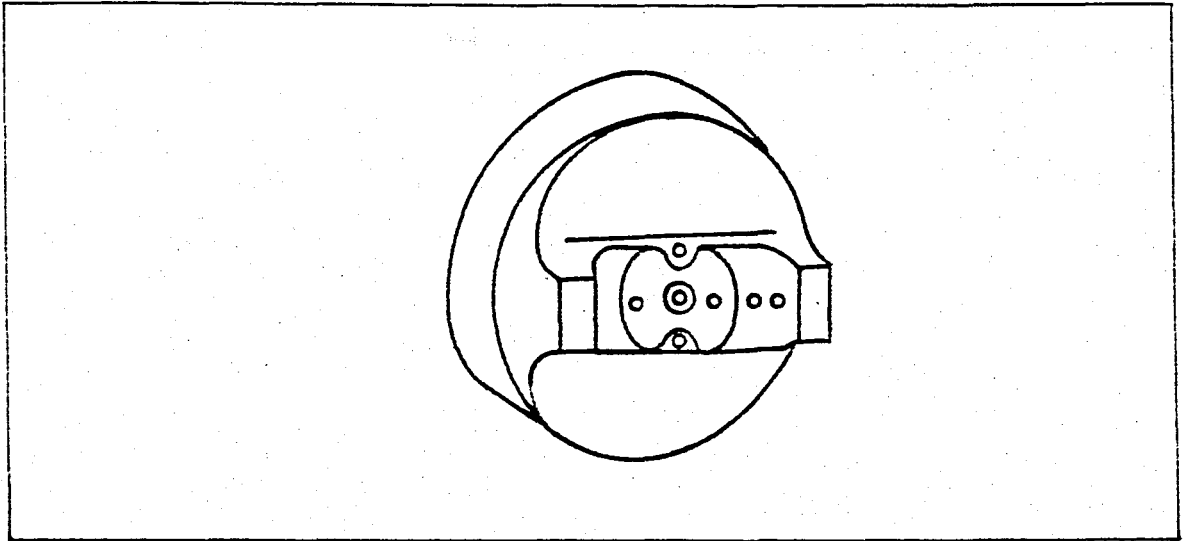


Figure 2.3. - Air cap

Spray pattern adjuster valve is for controlling the air to the horn holes which regulates the size and shape of the spray pattern. The fluid flow rate is on the other hand, controlled by the fluid needle opening.

Spray painting processes can be classified into four major groups:

*i)* Air spray;

Atomization is done by blowing compressed air toward the fluid injected through fluid tip.

*ii)* Airless spray;

Atomization is achieved by forcing the material

with high pressure through a small orifice which causes it to split down into fine particles.

*iii) Air-assisted airless spray;*

Atomization is done just as it is in the airless spray method. But the air stream blown to the fluid injected envelopes the material preventing it from overspraying.

*iv) Electrostatic spraying;*

Material is directed to the surface by the magnetic field in between the surface and the gun. The surface attracts the particles.

The proper spraying technique for spray gun stroke and positioning necessitates four important factors to be met at the same time. The spray gun must be so held that the pattern will be perpendicular to the surface and away from it by a constant offset distance, at all times. The spray gun must traverse the surface with a constant speed and the stroke must be a continuous motion until the other end of the surface is reached. Finally, at each consequent stroke, the spray pattern must overlap the preceding one 50 per cent. Less than that will result in streaks on the finished surface.

During spraying, the gun should never be arcing which results in uneven application of paint and excessive overspray at each end of the stroke. When the gun is arced 45 degrees away from the surface approximately 65 per cent of

paint is wasted.[1]

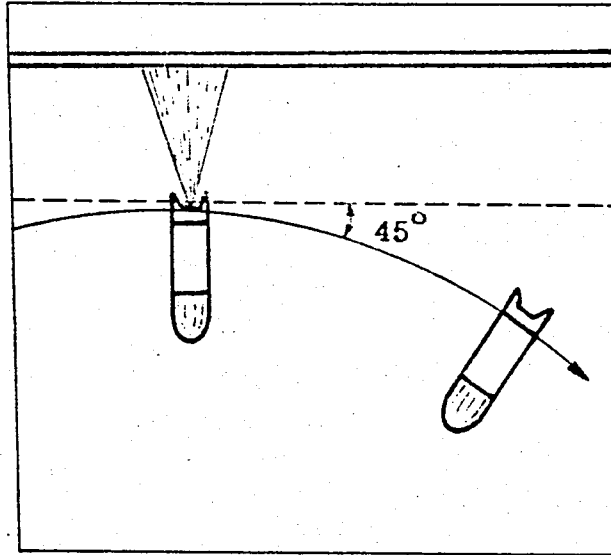


Figure 2.4. - Spray gun,when arced

### III. MATHEMATICAL MODELLING OF THE 6R SPRAY PAINTING ROBOT

#### 3.1. STRUCTURE OF A PAINTING ROBOT

One of the several fabrication applications of robots is the spray painting and finishing process. Robots used for spray painting must work in paint booths that are often small since they were initially designed for human use. But spraying robots generally have a light weight, which can be powered by relatively small actuators. Therefore, they are compact so as to fit the workspace [2].

The most important problem in spray painting is the amount of concentration of volatile solvents in the air. These mixtures can become concentrated enough to explode and are easily ignited by an electric spark. The safety regulations necessitate the voltage be less than that required to cause a spark in the air. Therefore, in practice, spray painting robots use hydraulic or pneumatic drive systems rather than electric motors. Hydraulics is preferred because it is intrinsically safe and rigid. The electronic control systems are usually installed in a separate ventilated chamber. The position and speed data of each link are fed back by the individual encoders fixed at each joint, through a complex microprocessor architecture to a computer which is fast enough to process the

inputs. Then, it performs the necessary calculations to define the next state of each link and enables the controllers to generate the required signals to the actuators, to move the arm there.

Spray painting requires the use of continuous-path robots. To achieve the necessary flexibility, speed and accuracy, five, six, or seven axis servo controlled robots are used. However, *six axis with revolute joints* is the most favorite among all. Accuracy requirements are not as strict as it is for the assembly or welding robots. Repeatability of  $\pm 0.125$  inch is common.

The *wrist* sub-assembly is made of the last three revolute joints which put the spray gun into the desired orientation. The first three joints on the other hand are, to position the wrist in the workspace (Fig 3.2). The *pitch-yaw-roll* type wrist is common among many industrial applications of spray painting robots.

### 3.2. KINEMATICS OF THE ROBOT ARM

An industrial robot can be modelled as an open-loop articulated chain with several rigid bodies often referred as *links* connected in series by either revolute or prismatic joints driven by actuators. One end of the chain is attached to a supporting base while the other is free and equipped with a tool, suitable to perform the desired task. The

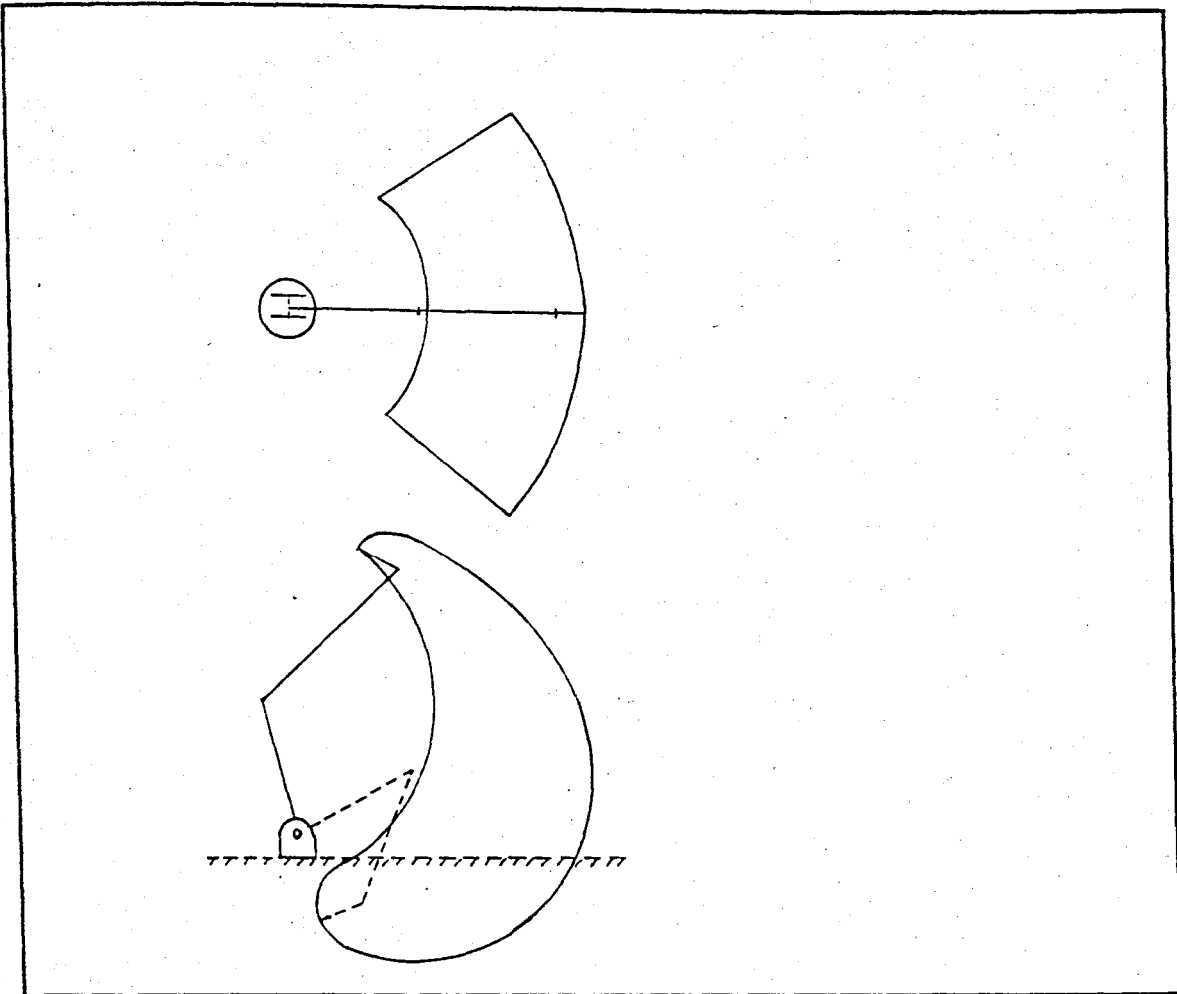


Figure 3.1. - Workspace of a 6R robot

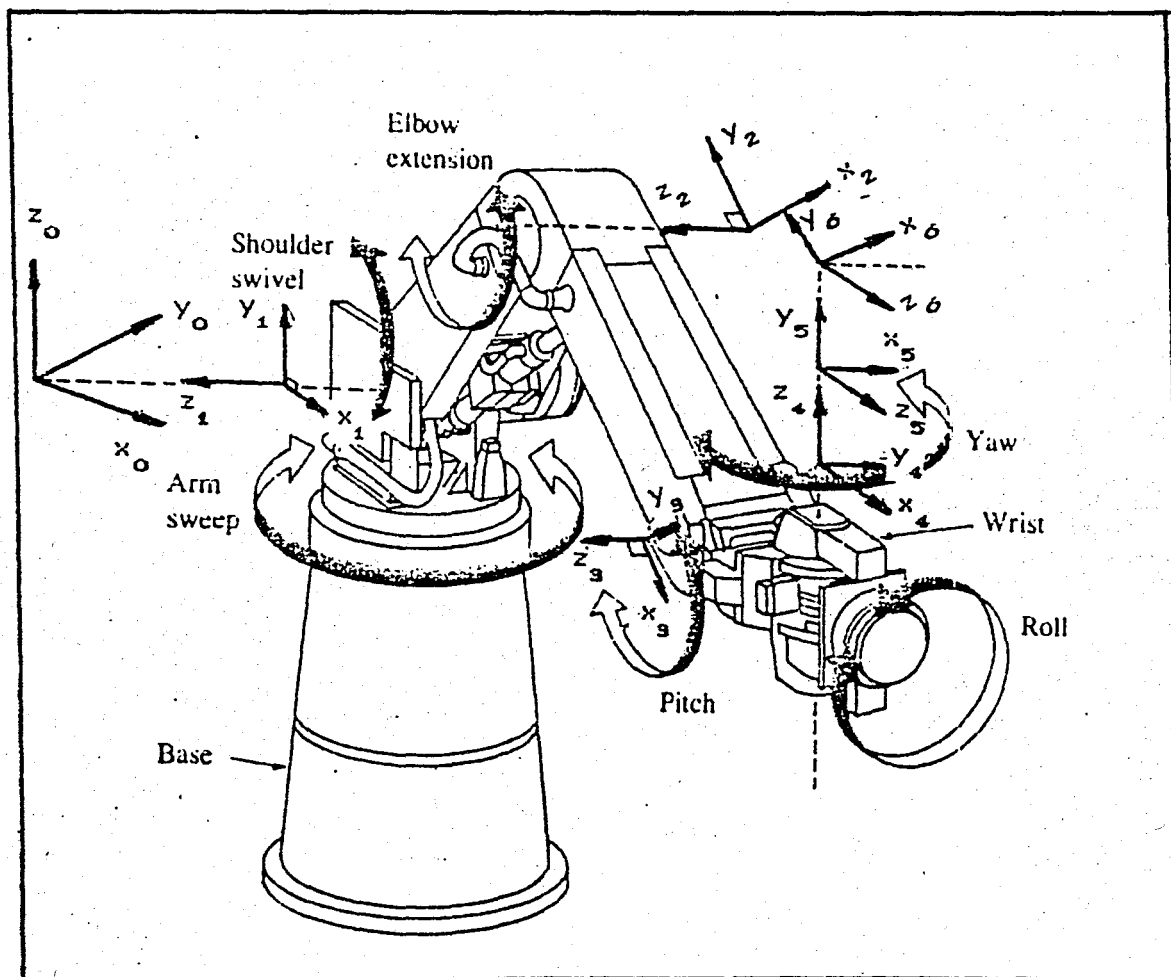


Figure 3.2 - Structural configuration.

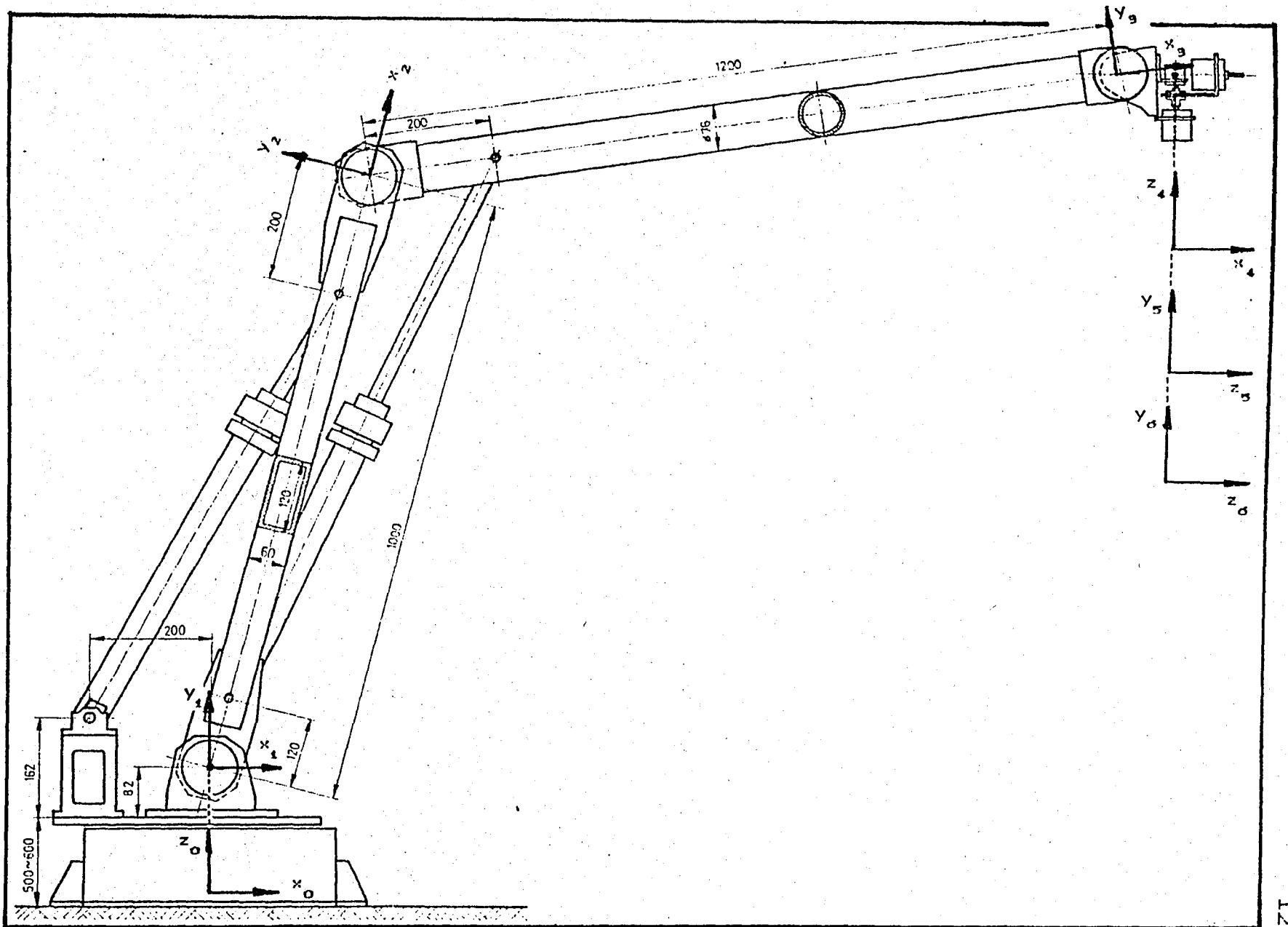


Figure 3.3. - Coordinate frames attached to the 6R robot

positioning of the tool which is generally named as the end-effector in the desired orientation is the consequence of the relative motions of joints connecting the links [3].

Robot arm kinematics particularly investigates the relations between joint-variable space and the cartesian-coordinate space which describes the position and orientation of the end-effector. The kinematics problem consists of two subproblems as the answers to two fundamental questions,

- 1) How to find the position and orientation of the end-effector of a given manipulator whose geometric link parameters together with the joint displacements have been specified ? This is called *Direct kinematics*.
- 2) How to find the necessary joint displacements to be able to reach the prescribed position and orientation of the end-effector ? This is referred as *Inverse kinematics*.

### 3.2.1. Direct Kinematics Problem

In most robotic applications the major interest is focused on the spatial description of the end-effector, that is; determination of the position and orientation of hand with respect to a fixed base coordinate frame when a set of joint displacements were given.

In order to represent the location of the links forming the robot arm, vectors and matrix algebra are used. This is advantageous to develop a systematic and generalized approach. Since each joint in between the adjacent links enable them to move with respect to each other. Each link needs to be attached a body-attached coordinate frame at the joint. Then, the direct kinematics problem reduces to finding transformation matrices that relate the body-attached coordinate frames to the fixed base frame. The transformation matrix relates the adjacent frames to each other through the employment of four parameters called as *Denavit-Hartenberg parameters*. The (4x4) transformation matrix comprises of two parts: A (3x3) rotation matrix that operates on a position vector in a 3D Euclidean space and maps its coordinates in a rotated coordinate frame. And a (3x1) position vector which counts for the translational transformation of origins of two coordinate frames to be related. This vector is augmented to (4x1) by adding a '1' as the fourth element.

Denavit-Hartenberg parameters are:

$\theta_i$  :The joint angle from the  $X_{i-1}$  axis to the  $X_i$  axis about the  $Z_{i-1}$  axis.(using the righthand rule)

$d_i$  :The distance from the origin of the  $(i-1)$ th coordinate frame to the intersection of the  $Z_{i-1}$  axis with the  $X_i$  axis along the  $Z_{i-1}$  axis.

$a_i$  :The offset distance from the intersection of the  $Z_{i-1}$  axis with the  $X_i$  axis to the origin of the  $i$ th frame along the  $X_i$  axis(or shortest distance between the  $Z_{i-1}$  and  $Z_i$  axis).

$\alpha_i$  :The offset angle from the  $Z_{i-1}$  axis to the  $Z_i$  axis about the  $X_i$  axis.(using righthand rule)

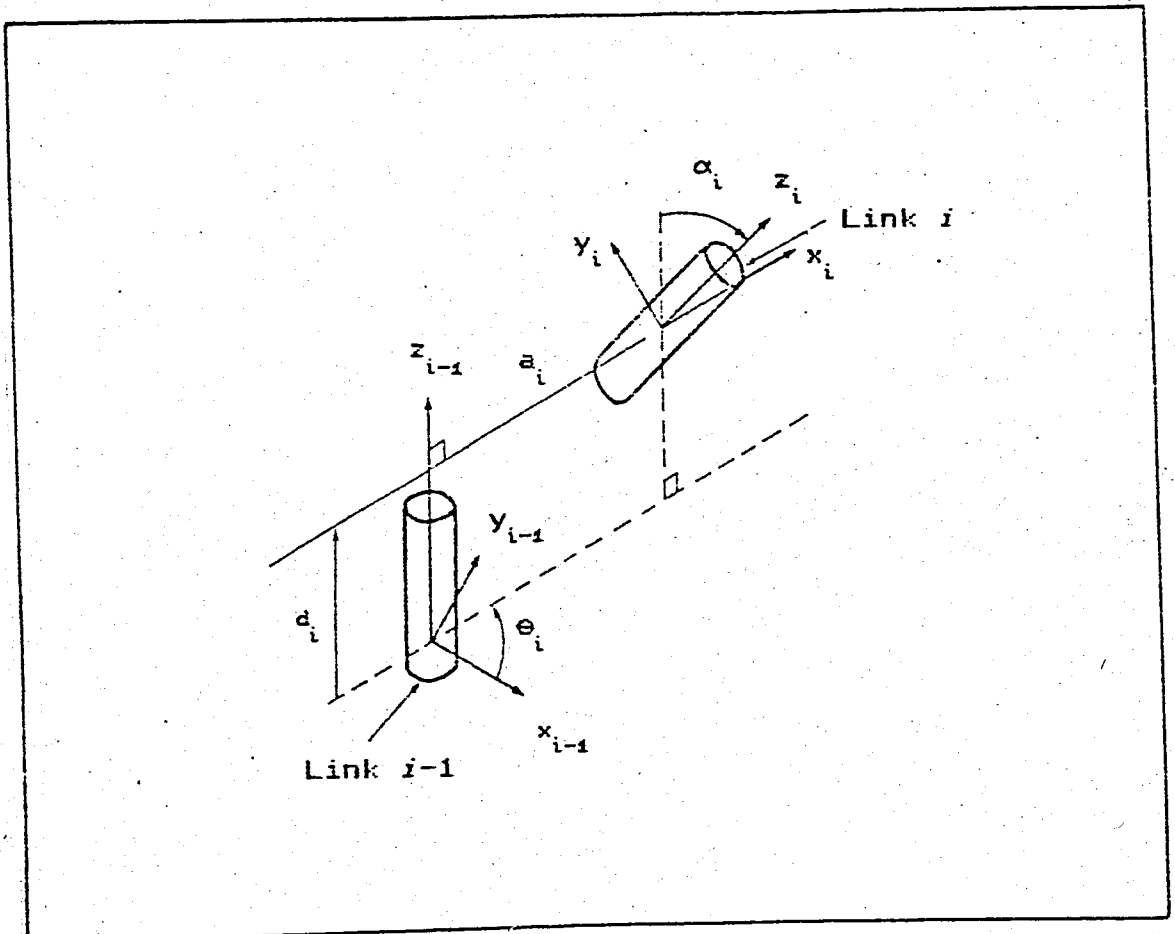


Figure 3.4. - Denavit-Hartenberg parameters

For the revolute joints  $d_i, a_i$  and  $\alpha_i$  parameters remain constant while  $\theta_i$  becomes the joint variable that changes in time as the link moves.

The non-singular homogeneous transformation matrix that transforms from the  $i$ th frame to the  $(i-1)$ th is [3] :

$$A_{i-1}^i = \begin{bmatrix} \cos\theta_i & -\cos\alpha_i \sin\theta_i & \sin\alpha_i \sin\theta_i & a_i \cos\theta_i \\ \sin\theta_i & \cos\alpha_i \cos\theta_i & -\sin\alpha_i \cos\theta_i & a_i \sin\theta_i \\ 0 & \sin\alpha_i & \cos\alpha_i & d_i \\ 0 & 0 & 0 & 1 \end{bmatrix} \quad (3.1)$$

The inverse of the transformation matrix is denoted by:  $A_i^{i-1}$

The Denavit-Hartenberg parameters for the 6R spray painting robot are:

link #	$a_i$	$d_i$	$\alpha_i$	$\theta_i$
1	0	$l_0$	90	$\theta_1$
2	$l_2$	0	0	$\theta_2$
3	$l_3$	0	0	$\theta_3$
4	$l_4$	0	-90	$\theta_4$
5	0	0	90	$\theta_5$
6	0	0	0	$\theta_6$

Table 3.1. Den.Hartenberg parameters for the 6R robot.

Then the homogeneous (4x4) transformation matrices become:

$$A_{0}^1 = \begin{bmatrix} c_1 & 0 & s_1 & 0 \\ s_1 & 0 & -c_1 & 0 \\ 0 & 1 & 0 & 0 \\ 0 & 0 & 0 & 1 \end{bmatrix} \quad A_{1}^2 = \begin{bmatrix} c_2 & -s_2 & 0 & l_2 c_2 \\ s_2 & c_2 & 0 & l_2 s_2 \\ 0 & 0 & 1 & 0 \\ 0 & 0 & 0 & 1 \end{bmatrix}$$

$$A_{2}^3 = \begin{bmatrix} c_3 & -s_3 & 0 & l_3 c_3 \\ s_3 & c_3 & 0 & l_3 s_3 \\ 0 & 0 & 1 & 0 \\ 0 & 0 & 0 & 1 \end{bmatrix} \quad A_{3}^4 = \begin{bmatrix} c_4 & 0 & -s_4 & l_4 c_4 \\ s_4 & 0 & c_4 & l_4 s_4 \\ 0 & -1 & 0 & 0 \\ 0 & 0 & 0 & 1 \end{bmatrix}$$

$$A_{4}^5 = \begin{bmatrix} c_5 & 0 & s_5 & 0 \\ s_5 & 0 & -c_5 & 0 \\ 0 & 1 & 0 & 0 \\ 0 & 0 & 0 & 1 \end{bmatrix} \quad A_{5}^6 = \begin{bmatrix} c_6 & -s_6 & 0 & 0 \\ s_6 & c_6 & 0 & 0 \\ 0 & 0 & 1 & 0 \\ 0 & 0 & 0 & 1 \end{bmatrix}$$

where  $c_i = \cos \theta_i$ ,  $s_i = \sin \theta_i$ , ( $i=1,2,3,\dots,6$ ) and  $l_2, l_3$  and  $l_4$  are the link lengths.

In order to describe the position and orientation of the end-effector with respect to the fixed base frame as a function of joint displacements,  $n$  consecutive transformation matrices have to be chain multiplied for an  $n$  degree of freedom manipulator.

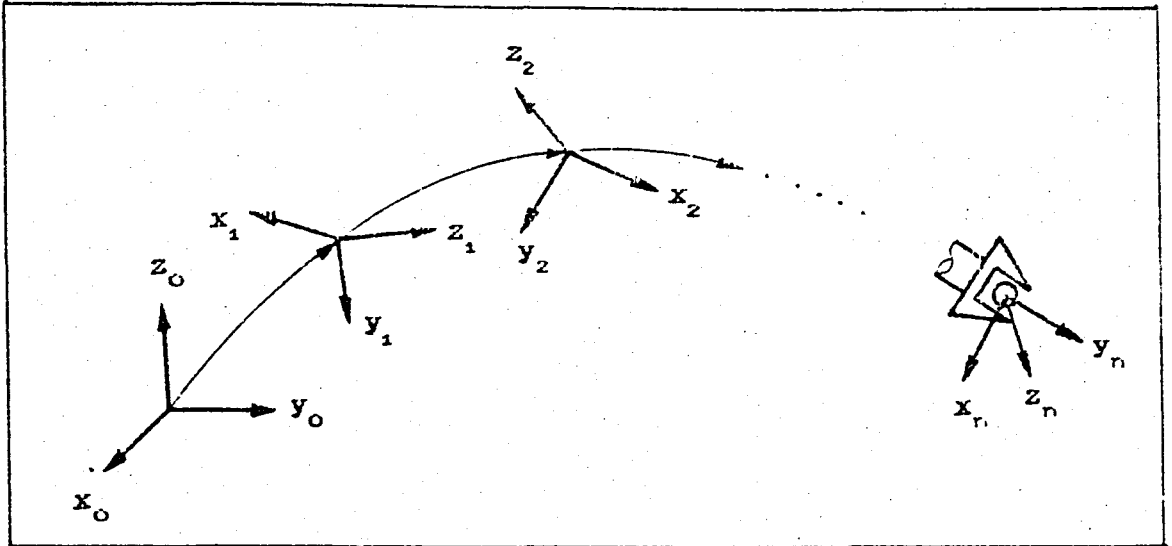


Figure 3.5. - Coordinate frames in 3D space

Then,

$$T = A_0^1 A_1^2 A_2^3 A_3^4 A_4^5 A_5^6 \quad (3.2)$$

is the *kinematic equation* of the 6R spray painting robot, and governs the fundamental kinematic behavior of the robot. Here matrix  $T$  is called as the *arm matrix* and describes the position and orientation of the end-effector with respect to the base frame.

$$T = \begin{bmatrix} t_x & b_x & n_x & P_x \\ t_y & b_y & n_y & P_y \\ t_z & b_z & n_z & P_z \\ 0 & 0 & 0 & 1 \end{bmatrix} \quad (3.3)$$

where,

- t :tangent vector of the hand,
- b :bi-normal vector of the hand,
- n̄ :normal vector of the hand.

### 3.2.2. Inverse Kinematics Problem

The independent variables in a robot arm are the joint variables, and a task (path in spray painting) is usually stated in terms of a reference coordinate frame which is the fixed base frame. The inverse kinematics solutions are used frequently to find the necessary joint displacements which will lead the end-effector to the specified position on the path in the desired orientation. The position of a point and the desired orientation on the path are specified in the standard form of the arm matrix  $T$  and are known values [4]. Schematically, the 6R spray painting robot has the joint-axis configuration as shown in (Fig 3.3)

In (Fig. 3.6), the position of the point 'P' with respect to the base frame is defined by the position vector  $\vec{r}_1$ . To be able to solve the inverse kinematics problem the position of point 'P' must be transferred to the intersection of three motion axis of the wrist (point A). So that after this linear transformation not the vector  $\vec{r}_1$  but vector  $\vec{r}_2$  will be the position vector of point 'P' on the path .

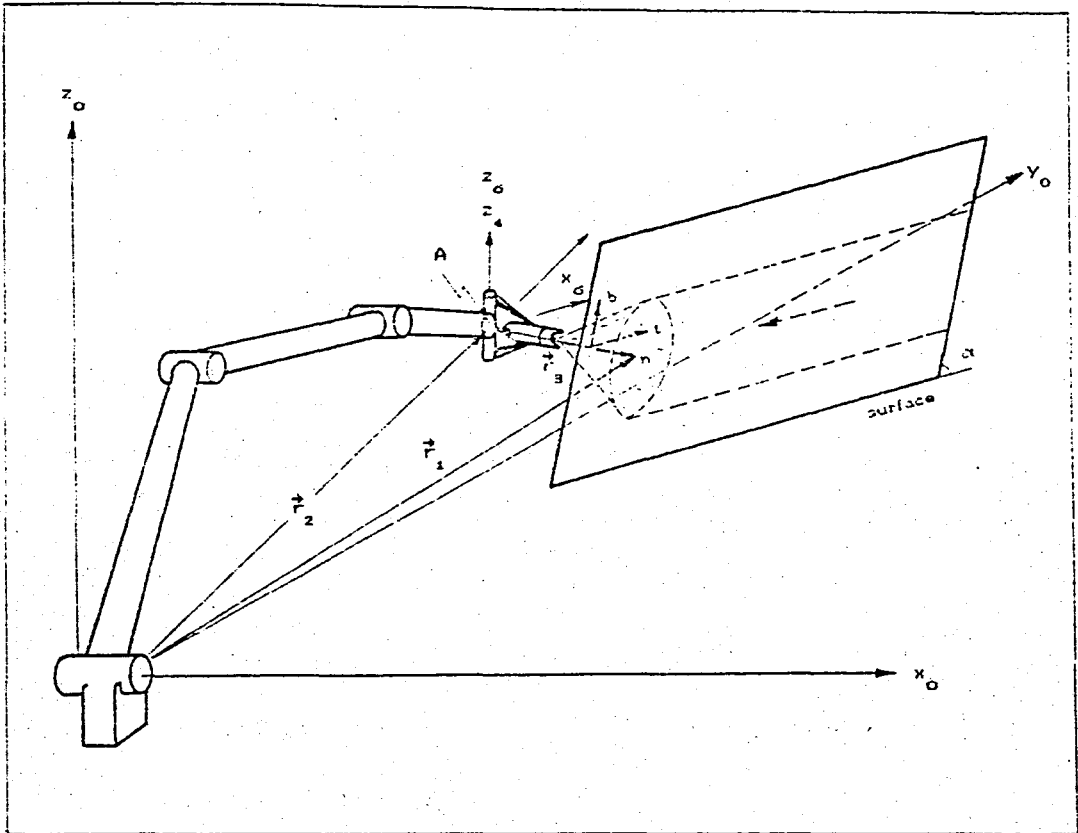


Figure 3.6. - Translation of a point on the surface

$$\vec{r}_2 = \vec{r}_1 + \vec{r}_g \quad (3.4)$$

where  $\vec{r}_g$  is a vector in the same direction as the normal of the path at point 'P' and has a magnitude of paint spray-cone length + the length of the last link, that is; the gun. As a result, the base link's rotational displacement will be so as to position the robot to the point A which automatically positions the gun at right angles, just right across the point P on the surface and a prescribed spray-cone length offset from it. After a closer observation one can immediately see that:

$$\theta_1 = \tan^{-1}\left(\frac{P_{y_a}}{P_{x_a}}\right) \quad \text{and} \quad \theta_1 = \theta_1 + 180 \quad (3.5)$$

Translation of the point 'P' on the surface to the three joint-axis intersection also enables us to have all remaining joint displacements  $\theta_2, \theta_3, \theta_4$  except  $\theta_5$  be co-planar, which results in some geometric simplifications.

As described before, the kinematic equation of the 6R robot is:

$$A_0^1 A_2^1 A_3^2 A_4^3 A_5^4 A_6^5 = T \quad (3.6)$$

premultiplying both sides by  $(A_0^1)^{-1}$  gives:

$$A_2^1 A_3^2 A_4^3 A_5^4 A_6^5 = (A_0^1)^{-1} T \quad (3.7)$$

equating the 3rd row,3rd column elements of both sides gives:

$$c_5 = s_1 n_x - c_1 n_y \quad (3.8)$$

Then premultiplication of the matrices  $(A_0^1)^{-1}$ ,  $(A_1^2)^{-1}$ ,  $(A_2^3)^{-1}$ ,  $(A_3^4)^{-1}$  by (3.6) gives:

$$(A_0^1)^{-1} (A_1^2)^{-1} (A_2^3)^{-1} (A_3^4)^{-1} T = (A_4^5) (A_5^6) \quad (3.9)$$

After the successive multiplications of the above matrices the elements of the 3rd row,3rd column of both sides are equated,so as to give:

$$-s_{294} (c_1 n_x + s_1 n_y) + c_{294} n_z = 0 \quad (3.10)$$

or

$$\theta_{294} = \tan^{-1} \frac{n_z}{c_1 n_x + s_1 n_y} \quad (3.11)$$

where

$$\theta_{294} = \theta_2 + \theta_3 + \theta_4 \quad (3.12)$$

Equating the 1st row,4th column and 2nd row,4th column of the above matrices respectively,gives:

$$c_1 P_x + s_1 P_y = c_{294} l_4 + c_{29} l_3 + c_2 l_2 \quad (3.13)$$

$$P_z = s_{294} l_4 + s_{29} l_3 + s_2 l_2 \quad (3.14)$$

where  $l_2, l_3$  and  $l_4$  are link lengths of the corresponding links. To solve for  $\theta_3$ , (3.13) and (3.14) are solved simultaneously. Let

$$P'_x = c_1 P_x + s_1 P_y - c_{294} l_4 \quad (3.15)$$

and

$$P'_y = P_z - s_{294} l_4 \quad (3.16)$$

Then

$$P'_x = c_{29} l_3 + c_2 l_2 \quad (3.17)$$

$$P'_y = s_{29} l_3 + s_2 l_2 \quad (3.18)$$

Square and add both sides of the above equation, then:

$$\theta_3 = \cos^{-1} \frac{P_x'^2 + P_y'^2 - l_3^2 - l_2^2}{2 l_2 l_3} \quad (3.19)$$

Similarly, if (3.17) and (3.18) are solved for  $\theta_2$  :

$$\theta_2 = \tan^{-1} \frac{(c_{s_1} l_1 + l_2) P_y - s_{s_1} l_1 P_x}{(c_{s_1} l_1 + l_2) P_x + s_{s_1} l_1 P_y} \quad (3.20)$$

$$\theta_4 = \theta_{294} - \theta_2 - \theta_3 \quad (3.21)$$

To find the displacement  $\theta_6$  of the last link:

$$(A_2^3)^{-1} (A_1^2)^{-1} (A_0^1)^{-1} T = (A_4^3) (A_5^4) (A_6^5) \quad (3.22)$$

equating 3rd row, 2nd column elements and 3rd row, 1st column elements of the resulting matrices on both sides of the equation (3.22) gives :

$$-s_1 b_x + c_1 b_y = -s_5 s_6 \quad (3.23)$$

$$-s_1 t_x + c_1 t_y = s_5 c_6 \quad (3.24)$$

Dividing both sides of (3.23) by (3.24) yields :

$$\theta_6 = \tan^{-1} \left( \frac{s_1 b_x - c_1 b_y}{c_1 t_y - s_1 t_x} \right) \quad (3.25)$$

As long as the arm matrix  $T$  at a desired position is prescribed, the inverse kinematics problem can be solved in the order of  $\theta_1, \theta_5, \theta_{294}, \theta_3, \theta_2, \theta_4$  and  $\theta_6$  using (3.5), (3.8), (3.11), (3.19), (3.20), (3.21), (3.25), sequentially.

### 3.3.3. Jacobian of the 6R Robot Arm

In most of the robotic applications, not only the positioning but also the velocity at which the end-effector moves, is important.

In spray painting process, moving the spray gun at a desired constant speed in a specified direction on a prescribed path is critical [1].

In order to achieve a coordinated motion of each link leading to the motion requirements both positioning and velocity, of the hand at that instant, the differential relationship between the joint displacements and the end-effector location has been investigated. The infinitesimal motion relationship is determined by differentiating the kinematic equation of the manipulator. It is in the form of [3],[4] :

$$d\vec{p} = J d\vec{\theta} \quad (3.26)$$

where  $d\vec{p}$  and  $d\vec{\theta}$  are the infinitesimal displacements vector and  $J$  is the so called *Jacobian* matrix. For an  $n$  degree of freedom manipulator arm, the infinitesimal displacements vector is composed of the infinitesimal translation and rotation of the end-effector, as :

$$d\vec{p} = \begin{bmatrix} dx_e \\ d\phi_e \end{bmatrix} \quad (3.27)$$

where  $dx_e$  and  $d\phi_e$  are (3x1) vectors.

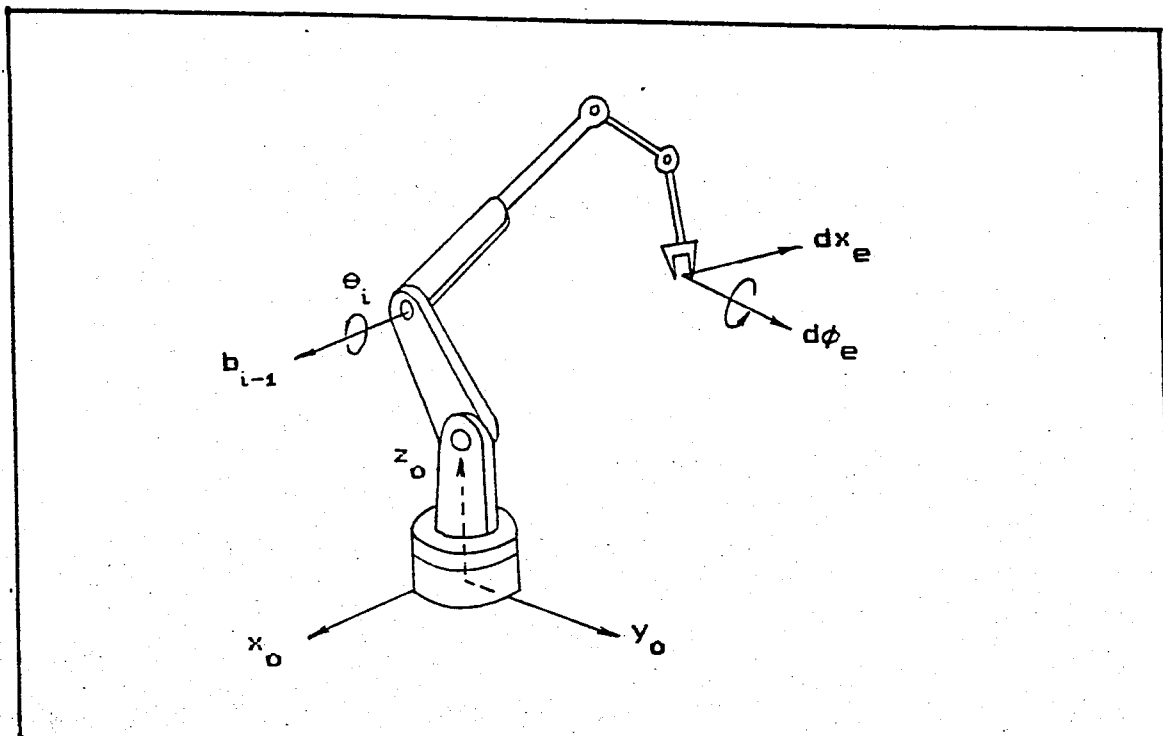


Figure 3.7. - Linear and angular velocity of hand

Dividing both sides of (3.27) by infinitesimal time  $dt$  gives

$$\dot{\vec{p}} = J \cdot \dot{\vec{\theta}} \quad (3.28)$$

where  $\dot{\vec{p}} = \begin{bmatrix} \dot{v}_e \\ \dot{w}_e \end{bmatrix}$  and  $\dot{\vec{\theta}} = [\dot{\theta}_1, \dot{\theta}_2, \dots, \dot{\theta}_3]^T$ . Here  $v_e$  and  $w_e$  are the linear and angular velocity vectors of the end-effector, respectively. And  $\dot{\vec{\theta}}$  is the joint velocities vector of the 6R robot. The Jacobian matrix is in the form of

$$J = \begin{bmatrix} J_{L1} & J_{L2} & J_{L3} & \dots & J_{L6} \\ J_{A1} & J_{A2} & J_{A3} & \dots & J_{A6} \end{bmatrix} \quad (3.29)$$

where  $J_{Li} : (3 \times 1)$  column vector associated with linear velocity.

$J_{Ai} : (3 \times 1)$  column vector associated with angular velocity.

The angular velocity of revolute joints create a linear velocity at the end-effector. And the resultant end-effector linear velocity is the linear combination of those velocities due to each revolute joint's motion.

Similarly, the angular velocity of the end-effector is the linear combination of each revolute joint's angular motion. Consequently, each column corresponding to an individual joint of the Jacobian matrix for the 6R spray painting robot is as follows :

$$\begin{aligned} J_{Li} &= b_{i-1} * r_{i-1,0} \\ J_{Ai} &= b_{i-1} \quad i=1,2,\dots,6 \end{aligned} \quad (3.30)$$

Here  $b_{i-1}$  vector is defined with respect to the base frame and is aligned in the direction of each joint's motion axis that is the  $Z_i$  axis. \* sign is the cross-product. It is given by the equation :

$$\vec{b}_{i-1} = R^1 R^2 \dots R_{i-2}^{i-1} \vec{b} \quad (3.31)$$

where  $\vec{b} = [0 \ 0 \ 1]^T$  is the direction of axis of motion of the base joint ( $Z_0$ ) and  $i=1,2,\dots,6$ .

$\vec{r}_{i-1,e}$  is the position vector and can be computed using (4x4) transformation matrices of the body-attached coordinate frames. Let  $\vec{X}_{i-1}$  be the (4x1) augmented vector of  $\vec{r}_{i-1,e}$  position vector.

$$\vec{X}_{i-1,e} = (A_0^1 \ A_1^2 \ \dots \ A_{n-1}^n \ \vec{X}) = (A_0^1 \ A_1^2 \ \dots \ A_{i-2}^{i-1} \ \vec{X}) \quad (3.32)$$

where  $\vec{X} = [0 \ 0 \ 0 \ 1]^T$  is the augmented position vector representing the origin of its own coordinate frame.

For the 6R spray painting robot :

$$\begin{aligned} \vec{b} &= [0 \ 0 \ 1]^T & \vec{b}_0 &= R_0^1 \vec{b} \\ & & \vec{b}_1 &= R_0^1 R_1^2 \vec{b} \\ & & \vec{b}_2 &= R_0^1 R_1^2 R_2^3 \vec{b} \\ & & \vec{b}_3 &= R_0^1 R_1^2 R_2^3 R_3^4 \vec{b} \\ & & \vec{b}_4 &= R_0^1 R_1^2 R_2^3 R_3^4 R_4^5 \vec{b} \\ & & \vec{b}_5 &= R_0^1 R_1^2 R_2^3 R_3^4 R_4^5 R_5^6 \vec{b} \end{aligned} \quad (3.33)$$

The position vectors from each joint to the end-effector are :

$$\bar{X} = [0 \ 0 \ 0 \ 1]^T, \quad A_0^6 = A_0^1 A_1^2 A_2^3 A_3^4 A_4^5 A_5^6$$

$$\begin{aligned} X_{1,e} &= A_0^6 \bar{X} \\ X_{2,e} &= A_0^6 \bar{X} - A_1^0 \bar{X} \\ X_{3,e} &= A_0^6 \bar{X} - A_1^0 A_1^2 \bar{X} \\ X_{4,e} &= A_0^6 \bar{X} - A_1^0 A_1^2 A_2^3 \bar{X} \\ X_{5,e} &= A_0^6 \bar{X} - A_1^0 A_1^2 A_2^3 A_3^4 \bar{X} \\ X_{6,e} &= A_0^6 \bar{X} - A_1^0 A_1^2 A_2^3 A_3^4 A_4^5 A_5^6 \bar{X} \end{aligned} \quad (3.34)$$

then, the 6R spray painting robot's Jacobian will be in the following form :

$$J = \begin{bmatrix} b_0^* r_0 & b_1^* r_1 & b_2^* r_2 & b_3^* r_3 & b_4^* r_4 & b_5^* r_5 & b_6^* r_6 \\ \hline b_0 & b_1 & b_2 & b_3 & b_4 & b_5 & b_6 \end{bmatrix} \quad (3.35)$$

A subroutine (JAC2) has been written to calculate the manipulator Jacobian matrix which is utilized to find the necessary angular velocities of each link, to achieve the desired linear speed of the end-effector on the path at a given instant.

$$\dot{\theta} = [\dot{\theta}_1, \dot{\theta}_2, \dot{\theta}_3, \dots, \dot{\theta}_6]^T \quad \text{and} \quad \dot{V} = [V_x, V_y, V_z, w_x, w_y, w_z]^T$$

$$\dot{\theta} = J \cdot \dot{V} \quad (3.36)$$

where  $V_x, V_y$  and  $V_z$  are the linear velocity components of the end-effector,  $w_x, w_y$  and  $w_z$  are the angular velocities of pitch-yaw-roll motions of the wrist, respectively.

### 3.3. DYNAMIC MODELLING OF THE 6R SPRAY PAINTING ROBOT

The dynamic equations of motion of a manipulator are a set of highly-coupled, non-linear differential equations describing the dynamic behavior of the manipulator. Such equations of motion are of vital importance for computer simulations, design of controller and evaluation of the design and structure of a robot arm. In addition, dynamic performance of a manipulator directly depends on the efficiency of the dynamic model and control algorithm [5].

The actual dynamic model of a robot arm can be obtained from known physical laws such as the laws of Newtonian mechanics or Lagrangian mechanics leading to the development of the dynamic equations of motion for the various articulated joints of the manipulator in terms of specified geometric and inertial parameters of the links. There are several approaches available in the literature towards dynamic modelling. Mainly, they are the Lagrangian-Euler (L-E) and Newton-Euler (N-E) methods and some approximate ones. These motion equations are equivalent to each other in the sense that they describe the dynamic

behavior of the same physical robot arm. However, the structure of these equations may differ as they are obtained for various reasons and purposes. Some are for fast computation of nominal torques, others are for facilitating control analysis while others are meant to improve computer simulation of robot motions.

In this study, the recursive (N-E) algorithm of [6] has been adapted to 6R spray painting robot for it has the advantage of both speed and conformability to computer simulation. The derivation is simple, although messy, and involves vector cross-product terms. The resultant dynamic equations, excluding the dynamics of the controller and gear friction, are a set of forward and backward recursive equations. These equations are applied to the robot links sequentially. The forward recursion from the base link to the end-effector propagates kinematics information in the form of proper coefficients for angular velocities, angular accelerations, linear accelerations, total forces and moments exerted at the center of mass of each link. The backward recursion from the end-effector to the base link propagates the forces and moments exerted on each link. Unlike the (L-E) formulation employing (4x4) transformation matrices very frequently slowing down the computations, the (N-E) recursive algorithm is very systematical allowing a shorter computation time. Furthermore, the calculations are carried out in each link's own body-attached coordinate frame

leading to a great elimination of messy coordinate transformations needed by other methods.

The equation of motion of a robot arm for an  $n$  degree of freedom manipulator is in the form of :

$$\vec{\tau} = J(\vec{q})\ddot{\vec{q}} + V\dot{\vec{q}} + \vec{f}(\vec{q}_i, \dot{\vec{q}}_j, \vec{q}) + \vec{g}(\vec{q}) + \vec{h}(\vec{q}) \quad (3.37)$$

where (for 6R robot),

$\vec{q}$  : 6x1 vector of joint variables,

$J(\vec{q})$  : 6x6 symmetric, non-singular moment of inertia matrix,

$V$  : 6x6 diagonal viscous friction matrix,

$\vec{f}(\vec{q}_i, \dot{\vec{q}}_j, \vec{q})$  : 6x1 vector of centrifugal and coriolis effects,

$\vec{g}(\vec{q})$  : 6x1 vector of gravitational effects,

$\vec{h}(\vec{q})$  : 6x1 vector of the external forces and moments exerted on the end-effector,

$\vec{\tau}$  : 6x1 vector of input torques to the links by the actuators at the joints.

The following method is to form the inertia matrix  $J$  and the gravity, hand, and centrifugal effects vectors  $\vec{g}$ ,  $\vec{h}$ ,  $\vec{f}$  respectively. Here, the viscous friction matrix  $V$  has been neglected because it has comparatively small magnitudes.

This method can only be used to define the above matrix and vectors, if the position and angular velocity vectors  $\vec{q}$  and  $\dot{\vec{q}}$  are known at a specified instant.

Kinematic investigation of the robot arm necessitates attaching a coordinate frame to each link which moves together with the link. If the adjacent three coordinates are taken, a vector equation can be written as [7] :

$$\vec{r}_{i+1} = \vec{r}_i + \vec{r}_{i+1}^* \quad (3.38)$$

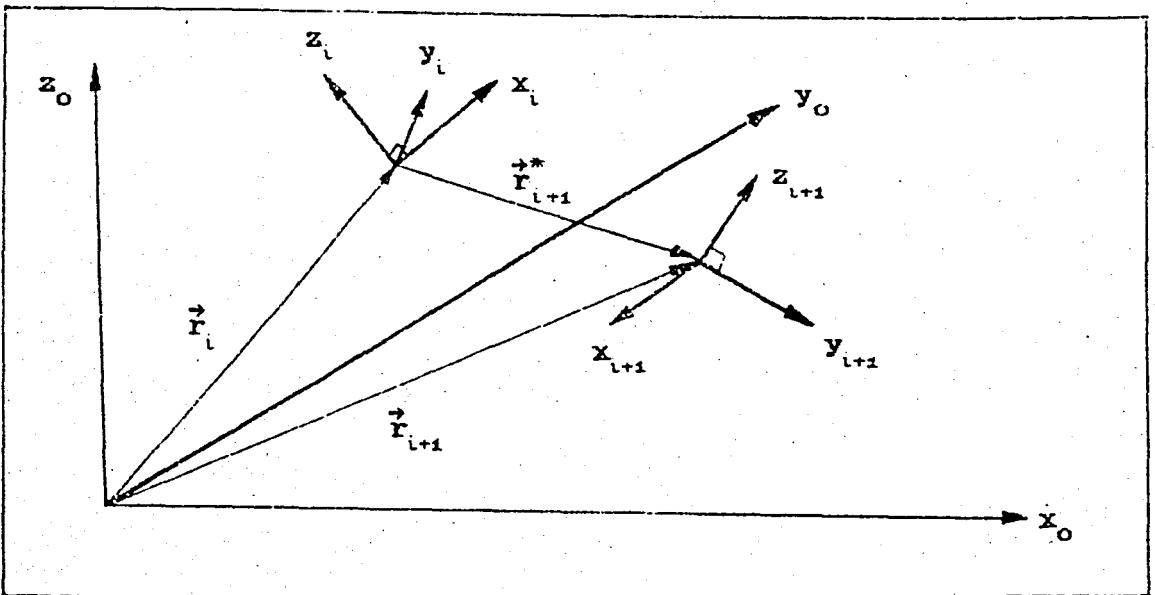


Figure 3.8. - Motion with respect to moving frames

The linear velocity of the  $(i+1)$ th coordinate frame with respect to the base frame  $(x_0, y_0, z_0)$  is given by the differentiation of (3.38),

$$\vec{v}_{i+1} = \vec{v}_i + \vec{\omega}_i * \vec{r}_{i+1} + \left( \frac{d\vec{r}_{i+1}^*}{dt} \right)_i \quad (3.39)$$

where

$\vec{\omega}_i$  : Angular velocity of the  $i$ th frame with respect to

the base frame.

$\left(\frac{d\vec{r}_{i+1}^*}{dt}\right)_i$  : Rate of change of  $\vec{r}_{i+1}^*$  with respect to the  $i$ th frame.

Differentiation of (3.39) gives the linear acceleration of the  $i$ th frame with respect to the base one as :

$$\vec{a}_{i+1} = \vec{a}_i + (\vec{\alpha}_i * \vec{r}_{i+1}^*) + \vec{\omega}_i * (\vec{\omega}_i * \vec{r}_{i+1}^*) + 2\vec{\omega}_i * \left(\frac{d\vec{r}_{i+1}^*}{dt}\right) + \left(\frac{d^2\vec{r}_{i+1}^*}{dt^2}\right)_i \quad (3.40)$$

where

$\alpha_i$  : Angular acceleration of  $i$ th frame with respect to the base frame.

The third term in (3.40) is the centrifugal acceleration. Furthermore, the fourth term is the coriolis acceleration.

The angular velocity of link  $(i+1)$  with respect to the base frame is :

$$\vec{\omega}_{i+1} = \vec{\omega}_i + \vec{\omega}_{i+1}^* \quad (3.41)$$

where  $\vec{\omega}_{i+1}^*$  is the angular velocity of  $(i+1)$ th frame with respect to the base one. Upon differentiating (3.41) ones more,

$$\vec{\alpha}_{i+1} = \vec{\alpha}_i + (\vec{\omega}_i * \vec{\omega}_{i+1}^*) + \left(\frac{d\vec{\omega}_{i+1}^*}{dt}\right)_i \quad (3.42)$$

In case of 6R spray painting robot, all joints are rotational. So, if the  $(i+1)$ th link is rotating with an angular velocity  $\dot{q}_{i+1}$  with respect to the  $i$ th link about  $Z_i$  then,

$$\vec{w}_{i+1}^* = Z_i \dot{q}_{i+1} \quad (3.43)$$

$$\left(\frac{d\vec{w}_{i+1}^*}{dt}\right)_i = Z_i \ddot{q}_{i+1} \quad (3.44)$$

$$\left(\frac{d\vec{r}_{i+1}^*}{dt}\right)_i = \vec{w}_{i+1}^* * \vec{r}_{i+1}^* \quad (3.45)$$

$$\left(\frac{d^2\vec{r}_{i+1}^*}{dt^2}\right)_i = \left(\frac{d\vec{w}_{i+1}^*}{dt}\right)_i * \vec{r}_{i+1}^* + \vec{w}_{i+1}^* * (\vec{w}_{i+1}^* * \vec{r}_{i+1}^*) \quad (3.46)$$

are the relative terms in the equations (3.39-3.42). Substitution of the relative terms (relative with respect to the moving frame) reforms the equations (3.39-3.42) as :

$$\vec{V}_{i+1} = \vec{V}_i + \vec{w}_{i+1}^* * \vec{r}_{i+1}^* \quad (3.47)$$

$$\vec{a}_{i+1} = \vec{a}_i + \dot{\alpha}_{i+1} * \vec{r}_{i+1}^* + \vec{w}_{i+1}^* * (\dot{\vec{w}}_{i+1}^* * \vec{r}_{i+1}^*) \quad (3.48)$$

$$\dot{\vec{w}}_{i+1}^* = \dot{\vec{w}}_i + Z_i \dot{q}_{i+1} \quad (3.49)$$

$$\dot{\alpha}_{i+1} = \dot{\alpha}_i + Z_i \ddot{q}_{i+1} + \dot{\vec{w}}_i * (Z_i \dot{q}_{i+1}) \quad (3.50)$$

In order to find the kinematic variables ( $\vec{V}_g$  and  $\vec{a}_g$ ) of the center of mass, the third frame; that is the  $(i+1)$ th frame is fixed at the link's mass center. Distance from the



Here,

$\vec{F}_i$ : total external force exerted on link  $i$ ,

$\vec{M}_i$ : total external moment exerted on link  $i$ ,

$m_i$ : total mass of link  $i$ ,

$I_i$ : Inertia matrix of link  $i$  about its center of mass with respect to the base frame.

As it can be seen from the above set of equations, the robot arm dynamics can be solved through sequential application of the recursive equations to the links. But one obvious drawback of them is that all inertial matrices  $I_i$  and the geometric parameters ( $\vec{r}_{i+1}^0, \vec{s}_{gi}$ , etc.) are referenced to the base coordinate frame. As a result, they change as the robot moves. But using the method given by [6],[8] it is possible to have all those matrices and vectors constant during motion by referring the dynamics of each link to its own coordinate frame, hence leading to a shorter computational time requirement. The modified equations become :

$$R_{i+1}^0 \vec{w}_{i+1} = R_{i+1}^i (R_{i+1}^0 \vec{w}_i + \dot{z}_0 \dot{q}_{i+1}) \quad (3.56)$$

$$R_{i+1}^0 \vec{\alpha}_{i+1} = R_{i+1}^i (R_{i+1}^0 \vec{\alpha}_i + \dot{z}_0 \ddot{q}_{i+1} + R_{i+1}^0 \vec{w}_i * \dot{z}_0 \dot{q}_{i+1}) \quad (3.57)$$

$$R_{i+1}^0 \vec{v}_{i+1} = R_{i+1}^i (R_{i+1}^0 \vec{v}_i) + R_{i+1}^0 \vec{w}_{i+1} * R_{i+1}^0 \vec{f}_{i+1}^* \quad (3.58)$$

$$R_{i+1}^0 \vec{a}_{i+1} = R_{i+1}^i (R_{i+1}^0 \vec{a}_i) + R_{i+1}^0 \vec{\alpha}_{i+1} * R_{i+1}^0 \vec{f}_{i+1}^* + (R_{i+1}^0 \vec{w}_{i+1} *$$

$$R_{i+1}^0 \vec{f}_{i+1}^*) \quad (3.59)$$

Here  $\vec{z}_0 = [0 \ 0 \ 1]^T$  and  $R_{i+1}^0 \vec{f}_{i+1}^* = [a_i \ d_i \sin \alpha_i \ d_i \cos \alpha_i]^T$  where  $a_i$  and  $d_i$  are Denavit-Hartenberg parameters of that link. The equations seem to involve too many multiplications of

matrices and vectors but actually they don't. Because,  $R_{i+1}^0 \vec{w}_{i+1}$  for example doesn't mean the multiplication of  $R_{i+1}^0$  by  $\vec{w}_{i+1}$  but it is the notation used in [6] to show that the vector  $\vec{w}_{i+1}$  is defined with respect to that link's own coordinate frame.

To be able to solve the inverse dynamics problem which is to solve the equation of motion for the forces and moments, the expressions of the angular and linear accelerations have to be written in a modified manner, [9] since the linear and angular accelerations are assumed to be unknown.

The angular accelerations of link  $i$  can be expressed as :

$$R_i^0 \vec{\alpha}_i = \sum_{j=1}^i \Psi_{ij} \ddot{q}_j + \vec{\alpha}_i \quad (3.60)$$

where  $\Psi_{ij}$  and  $\vec{\alpha}_i$  are the so called angular acceleration coefficients. Substitution of (3.60) into (3.57) gives :

$$\Psi_{ij} = R_i^{i-1} \Psi_{i-1,j} \quad 1 < j < i-1 \quad (3.61)$$

$$\Psi_{ii} = R_i^{i-1} \vec{z}_0 \quad (3.62)$$

$$\vec{\alpha}_i = R_i^{i-1} \vec{\alpha}_{i-1} + R_i^{i-1} (R_{i-1}^0 \vec{w}_{i-1} * \vec{z}_0 \dot{q}_i) \quad (3.63)$$

$\Psi_{ij}$  is in the form of a  $6 \times 6$  matrix whose diagonal elements are  $\Psi_{ii}$  which are calculated first. Then  $\Psi_{ij}$ 's can be found sequentially.  $\vec{\alpha}_i$  is a  $6 \times 1$  vector where for  $i=1$ ,  $\vec{\alpha}_1 = [0 \ 0 \ 0]^T$ .

Forward recursion starts by (3.56)

$$\begin{aligned}
 R_{11}^{0\rightarrow} &= R_1^0 (\dot{z}_0 q_1) \\
 R_{22}^{0\rightarrow} &= R_2^1 (R_{11}^{0\rightarrow} + \dot{z}_0 q_2) \\
 R_{33}^{0\rightarrow} &= R_3^2 (R_{22}^{0\rightarrow} + \dot{z}_0 q_3) \\
 &\vdots \\
 R_{66}^{0\rightarrow} &= R_6^5 (R_{55}^{0\rightarrow} + \dot{z}_0 q_6)
 \end{aligned} \tag{3.64}$$

The  $\Psi_{ij}$  matrix has the form :

$$\Psi = \begin{bmatrix}
 \Psi_{11} & & & & & \\
 \Psi_{21} & \Psi_{22} & & & & \\
 \Psi_{31} & \Psi_{32} & \Psi_{33} & & & \\
 \Psi_{41} & \Psi_{42} & \Psi_{43} & \Psi_{44} & & \\
 \Psi_{51} & \Psi_{52} & \Psi_{53} & \Psi_{54} & \Psi_{55} & \\
 \Psi_{61} & \Psi_{62} & \Psi_{63} & \Psi_{64} & \Psi_{65} & \Psi_{66}
 \end{bmatrix} \quad \text{symmetric}$$

The linear acceleration of each link can also be written as

$$R_i^{0\rightarrow} \ddot{a}_i = \sum_{j=1}^i \beta_{ij} \ddot{q}_j + \ddot{\eta}_i \tag{3.65}$$

where  $\beta_{ij}$  and  $\ddot{\eta}_i$  are the linear acceleration coefficients. The recursive equations for  $\beta_{ij}$  and  $\ddot{\eta}_i$  are found by substituting (3.65), (3.60) into (3.59).

$$\vec{\beta}_{ij} = R_i^{i-1} \vec{\beta}_{i-1,j} + \vec{\psi}_{ij} * R_i^{0*} \vec{r}_i \quad (3.66)$$

$$\vec{\beta}_{ii} = \vec{\psi}_{ii} * R_i^{0*} \vec{r}_i \quad (3.67)$$

$$\vec{\eta}_i = R_i^{i-1} \vec{\eta}_{i-1} + \vec{\theta}_i * R_i^{0*} \vec{r}_i + R_i^{0*} \vec{w}_i * (R_i^{0*} \vec{w}_i * R_i^{0*} \vec{r}_i) \quad (3.68)$$

where  $\vec{\beta}_{ij}$  forms a 6x6 matrix and  $\vec{\eta}_i$  is a 6x1 vector. Calculations are carried out in the same manner. For  $i=1$ ,  $\vec{\eta}_1 = [0 \ 0 \ 0]^T$ .

$$\beta = \begin{bmatrix} \beta_{11} & & & & & \\ \beta_{21} & \beta_{22} & & & & \\ \beta_{31} & \beta_{32} & \beta_{33} & & & \\ \beta_{41} & \beta_{42} & \beta_{43} & \beta_{44} & & \\ \beta_{51} & \beta_{52} & \beta_{53} & \beta_{54} & \beta_{55} & \\ \beta_{61} & \beta_{62} & \beta_{63} & \beta_{64} & \beta_{65} & \beta_{66} \end{bmatrix} \quad \text{symmetric}$$

The linear acceleration and velocity of mass center of link  $i$  can be represented as :

$$R_i^{0*} \vec{V}_{gi} = R_i^{0*} \vec{V}_i + R_i^{0*} \vec{w}_i * R_i^{0*} \vec{s}_i \quad (3.69)$$

$$R_i^{0*} \vec{a}_{gi} = R_i^{0*} \vec{a}_i + R_i^{0*} \dot{\alpha}_i * R_i^{0*} \vec{s}_i + R_i^{0*} \vec{w}_i * (R_i^{0*} \vec{w}_i * R_i^{0*} \vec{s}_i) \quad (3.70)$$

or,

$$R_i^{0*} \vec{a}_{gi} = \sum_{j=1}^i \lambda_{ij} \vec{q}_j + \vec{\gamma}_i \quad (3.71)$$

The coefficients  $\lambda_{ij}$  and  $\gamma_i$  are obtained by substituting (3.60), (3.65) and (3.71) into (3.70).

$$\vec{\lambda}_{ij} = \vec{\psi}_{ij} * R_{iS_i}^{0\vec{}} + \vec{\beta}_{ij} \quad (3.72)$$

$$\vec{\gamma}_i = \vec{\theta}_i * R_{iS_i}^{0\vec{}} + R_{iW_i}^{0\vec{}} * (R_{iW_i}^{0\vec{}} * R_{iS_i}^{0\vec{}}) \quad (3.73)$$

Equations of motion for link  $i$  referred to its own coordinate frame, can be written as :

$$R_{iS_i}^{0\vec{}} F_i = m_i R_{iS_i}^{0\vec{}} \vec{a}_{gi} \quad (3.74)$$

$$R_{iS_i}^{0\vec{}} M_i = \bar{I}_i R_{iS_i}^{0\vec{}} \vec{\alpha}_i + R_{iW_i}^{0\vec{}} * (\bar{I}_i R_{iW_i}^{0\vec{}}) \quad (3.75)$$

where,

$$\bar{I}_i = \begin{bmatrix} I_{xx} & -I_{xy} & -I_{xz} \\ -I_{yx} & I_{yy} & -I_{yz} \\ -I_{zx} & -I_{zy} & -I_{zz} \end{bmatrix} \quad (3.76)$$

is the *inertia tensor* of a link, referred to its own coordinate frame. Here,  $I_{xx}$ ,  $I_{yy}$  and  $I_{zz}$  are the so called *principle moments of inertia*. While the remaining terms are called the *products of inertia*. When the link's own coordinate frame is attached to its center of gravity, the product terms vanish and the inertia tensor becomes :

$$\bar{I}_i = \begin{bmatrix} I_{xxi} & 0 & 0 \\ 0 & I_{yyi} & 0 \\ 0 & 0 & I_{zz_i} \end{bmatrix} \quad (3.77)$$

$i=1,2,\dots,6$

or,

$$R_i^0 \vec{F}_i = L_i \vec{q}_i + \vec{f}_i \quad (3.78)$$

$$R_i^0 \vec{M}_i = N_i \vec{q}_i + \vec{n}_i \quad (3.79)$$

$L_i$  and  $N_i$  being  $3 \times 6$  matrices,  $\vec{q}_i$  and  $\vec{n}_i$  being  $3 \times 1$  vectors. And  $m_i$  is the mass of  $i$ th link.

$$L_i = m_i \begin{bmatrix} \lambda_{i1} & \lambda_{i2} & \dots & \lambda_{ii} & 0 & \dots & 0 \\ \dots & \dots & \dots & \dots & \dots & \dots & \dots \\ \dots & \dots & \dots & \dots & \dots & \dots & \dots \end{bmatrix} \quad (3.80)$$

$$N_i = I_i \begin{bmatrix} \Psi_{i1} & \Psi_{i2} & \dots & \Psi_{ii} & 0 & \dots & 0 \\ \dots & \dots & \dots & \dots & \dots & \dots & \dots \\ \dots & \dots & \dots & \dots & \dots & \dots & \dots \end{bmatrix} \quad (3.81)$$

for the 6R robot,  $i=1,2,\dots,6$ . The matrices have the form :

$$L_1 = m_1 \begin{bmatrix} * & 0 & 0 & 0 & 0 & 0 \\ * & 0 & 0 & 0 & 0 & 0 \\ * & 0 & 0 & 0 & 0 & 0 \end{bmatrix} \quad L_2 = m_2 \begin{bmatrix} * & * & 0 & 0 & 0 & 0 \\ * & * & 0 & 0 & 0 & 0 \\ * & * & 0 & 0 & 0 & 0 \end{bmatrix} \quad L_3 = m_3 \begin{bmatrix} * & * & * & 0 & 0 & 0 \\ * & * & * & 0 & 0 & 0 \\ * & * & * & 0 & 0 & 0 \end{bmatrix}$$

$$L_4 = m_4 \begin{bmatrix} * & * & * & * & 0 & 0 \\ * & * & * & * & 0 & 0 \\ * & * & * & * & 0 & 0 \end{bmatrix} \quad L_5 = m_5 \begin{bmatrix} * & * & * & * & * & 0 \\ * & * & * & * & * & 0 \\ * & * & * & * & * & 0 \end{bmatrix} \quad L_6 = m_6 \begin{bmatrix} * & * & * & * & * & * \\ * & * & * & * & * & * \\ * & * & * & * & * & * \end{bmatrix}$$

where '\*' shows a non-zero element. In the same way;

$$N_1 = \begin{bmatrix} I_{xx} & & & & & \\ & I_{yy} & & & & \\ & & I_{zz} & & & \\ & & & & & \\ & & & & & \\ & & & & & \end{bmatrix} \begin{bmatrix} * & 0 & 0 & 0 & 0 & 0 \\ * & 0 & 0 & 0 & 0 & 0 \\ * & 0 & 0 & 0 & 0 & 0 \end{bmatrix}$$

$$N_2 = \begin{bmatrix} I_{xx} \\ I_{yy} \\ I_{zz} \end{bmatrix} \cdot \begin{bmatrix} * * 0 0 0 0 \\ * * 0 0 0 0 \\ * * 0 0 0 0 \end{bmatrix} \dots \dots N_6$$

$$l_i = m_i \cdot \vec{r}_i \tag{3.82}$$

$$\vec{n}_i = I_i \vec{\theta} + R_i^0 \vec{w}_i * (I_i R_i^0 \vec{w}_i) \tag{3.83}$$

where  $I_i \theta_i = 0$  for  $i=1$  in (3.83).

The forces and moments acting on link  $i$  are shown in Fig.(3.9). Then, for equilibrium;

$$\vec{F}_i = \vec{f}_i - \vec{f}_{i+1} + m_i \vec{g} \tag{3.84}$$

$$\vec{M}_i = \vec{m}_i - \vec{m}_{i+1} + (\vec{r}_{i-1} - \vec{c}_i) * \vec{f}_i - (\vec{r}_i - \vec{c}_i) * \vec{f}_{i+1} \tag{3.85}$$

where  $\vec{f}_i$  : force exerted on link  $i$  by link  $i-1$

$\vec{m}_i$  : moment exerted on link  $i$  by link  $i-1$

$\vec{g}$  : gravitational acceleration.

The recursive equations of reaction forces and moments with the replacement of  $(\vec{c}_i - \vec{r}_{i-1})$  by  $(\vec{r}_i^* + \vec{s}_i)$  (Fig.3.9) are :

$$\vec{f}_i = \vec{f}_{i+1} + \vec{F}_i - m_i \vec{g} \tag{3.86}$$

$$\vec{m}_i = \vec{m}_{i+1} + \vec{r}_i^* * \vec{f}_{i+1} + (\vec{r}_i^* + \vec{s}_i) * \vec{F}_i - (\vec{r}_i^* + \vec{s}_i) * m_i \vec{g} + M_i \tag{3.87}$$

When they are transferred to the link's own coordinates :

$$R_i^0 \vec{f}_i = R_i^{i+1} (R_{i+1}^0 \vec{f}_{i+1}) + R_i^0 \vec{F}_i - R_i^0 m_i \vec{g} \tag{3.88}$$

$$R_i^0 \vec{m}_i = R_i^{i+1} [R_{i+1}^0 \vec{m}_{i+1} + (R_{i+1}^0 \vec{F}_i^*) * (R_{i+1}^0 \vec{t}_{i+1})] + (R_i^0 \vec{F}_i^* + R_i^0 \vec{S}_i) * (R_i^0 \vec{F}_i - R_i^0 \vec{m}_i \vec{g}) + R_i^0 \vec{M}_i \quad (3.89)$$

All reaction forces and moments at the joints can be calculated by a *backward* recursion using (3.88) and (3.89) but, for a faster algorithm, they are converted into coefficients. Substituting (3.78) into (3.88) :

$$R_i^0 \vec{f}_i = T_i \ddot{\vec{q}} + \vec{t}_i - \vec{g}_{fi} + \vec{f}_{Hi} \quad (3.90)$$

The elements of which are expressed recursively as :

$$T_i = R_i^{i+1} T_{i+1} + L_i \quad (3.91)$$

$$\vec{t}_i = R_i^{i+1} \vec{t}_{i+1} + \vec{l}_i \quad (3.92)$$

Since backward recursion starts,  $i=6,5,\dots,1$ . For  $i=6$ , first terms are zero.

$$\begin{array}{l} T_6 = L_6 \\ T_5 = R_5^6 T_6 + L_5 \\ \vdots \\ T_1 = R_1^2 T_2 + L_1 \end{array} \quad \text{and} \quad \begin{array}{l} t_6 = \vec{l}_6 \\ t_5 = R_5^6 t_6 + \vec{l}_5 \\ \vdots \\ t_1 = R_1^2 t_2 + \vec{l}_1 \end{array}$$

$$\vec{g}_{fi} = R_i^{i+1} \vec{g}_{fi+1} + R_i^0 \vec{m}_i \vec{g} \quad (3.93)$$

$$\vec{f}_{Hi} = R_i^{i+1} \vec{f}_{Hi+1} \quad (3.94)$$

Since  $i=6$  is the last link that is; the spray gun, the terms  $\vec{f}_{\sigma+1}$  and  $\vec{m}_{\sigma+1}$  are the force and moment exerted by the gun to the surroundings, respectively. In the spray painting process  $\vec{m}_{\sigma+1}$  is zero whereas,  $\vec{f}_{\sigma+1}$  is taken as the thrust of pressurized paint liquid passing through the nozzle of the gun.

Therefore, the first terms of (3.91), (3.92) and (3.93) are omitted. For the last link ( $i=6$ ), the hand force is given as :

$$\vec{f}_{Hi} = R_{\sigma}^0 \vec{f}_{\sigma+1} \quad (3.95)$$

and

$$\vec{g}_{i\sigma} = R_{\sigma}^0 \vec{m}_{\sigma} \vec{g} \quad (3.96)$$

It is the gravitational force exerted on the last link referred to the base frame. As an example, it is calculated as follows :

$$\vec{g} = [0 \ 0 \ -9.81]^T \quad (\text{gravity vector}) ,$$

$m_{\sigma}$  is the mass of the spray gun.

$$R_{\sigma}^0 = R_1^0 R_2^1 R_3^2 R_4^3 R_5^4 R_6^5$$

In the same way, the reaction moments are :

$$R_i^0 \vec{m}_i = S_i \ddot{q} + C_i + D_i + N_i \quad (3.97)$$

$$S_i = R_i^{i+1} S_{i+1} + C_i + D_i + N_i \quad (3.98)$$

Here,  $S_i, C_i, D_i$  and  $N_i$  are  $3 \times 6$  matrices. In order to construct each column of the matrices  $C_i$  and  $D_i$  following equations are used:

$$C_i^k = R_i^{O \rightarrow * *} (R_i^{i+1} T_{i+1})^k \quad (3.99)$$

$$D_i^k = (R_i^{O \rightarrow * *} + R_i^{O \rightarrow \underline{S}}) * L_i^k \quad (3.100)$$

where  $k$  shows the  $k$  th column of the matrices mentioned and  $k=1,2,\dots,6$ .

$$S_i = R_i^{i+1} S_{i+1} + R_i^{O \rightarrow * *} R_i^{i+1} t_{i+1} + (R_i^{O \rightarrow * *} + R_i^{O \rightarrow \underline{S}}) * l_i + \vec{n}_i \quad (3.101)$$

$$\vec{g}_{mi} = R_i^{i+1} \vec{g}_{m_{i+1}} + R_i^{O \rightarrow * *} R_i^{i+1} \vec{g}_{f_{i+1}} + (R_i^{O \rightarrow * *} + R_i^{O \rightarrow \underline{S}}) * R_i^{O \rightarrow \underline{m}} \vec{g} \quad (3.102)$$

The first terms of (3.101) and (3.102) are omitted for  $i=6$ .

$$\vec{m}_{Hi} = R_i^{i+1} \vec{m}_{H_{i+1}} + R_i^{O \rightarrow * *} * \vec{f}_{Hi} \quad (3.103)$$

for  $i=6$ ,  $\vec{m}_{H6} = R_{66}^{O \rightarrow * *} * \vec{f}_{H6}$ .

Finally, the required torque that must be given by the actuator to the joint  $i$  is the projection of the reaction moment at that joint on to the joint axis, (Viscous friction has been neglected.)

$$\vec{t}_i = [R_{i-1}^i (R_{i-1}^{O \rightarrow \underline{m}})]^T \cdot \vec{Z}_0, \quad \vec{Z}_0 = [0 \ 0 \ 1]^T \quad (3.104)$$

If (3.90) and (3.97) are put in (3.104), the inertia matrix  $J$  and vectors  $\vec{f}$ ,  $\vec{g}$  and  $\vec{h}$  of (3.37) can be found from,

$$J = (R_{i-1}^i S_i)_{s_j} \quad i, j=1, 2, \dots, 6 \quad (3.105)$$

$$\vec{f}_i = (R_{i-1}^i \vec{s}_i)_{s_3} \quad i, j=1, 2, \dots, 6 \quad (3.106)$$

$$\vec{g}_i = (R_{i-1}^i \vec{g}_{mi})_{s_3} \quad i, j=1, 2, \dots, 6 \quad (3.107)$$

$$\vec{h}_i = (R_{i-1}^i \vec{m}_{Hi})_{s_3} \quad i, j=1, 2, \dots, 6 \quad (3.108)$$

where subscript 3 means the third row of that vector.

## IV. CONTROL OF THE 6R ROBOT

### 4.1. COMPUTED TORQUE TECHNIQUE

A controlled tracking of a prescribed path for a robot's end-effector can only be achieved by controlling each joint of the robot so that the desired trajectory is followed. Corrective compensation torques to the actuators of each joint must be applied to adjust for any deviations of the arm from the trajectory. In case of spray painting process, the speed of the gun which is the tool attached to the end-effector must also be controlled besides the position / orientation control of the arm.

Several robot arm control methods are available in the literature. One of the basic control schemes among them is the computed torque technique based on the (N-E) equations of motion. According to what is stated in [5], closed-loop digital control is made impossible if the complete (L-E) equations of motion are used because of over 2000 floating point multiplications and additions. Whereas (N-E) equations of motion are quite suitable for the derivation of an efficient control law in the joint-coordinate system [3],[6]. The control law is also computed recursively.

The computed torque technique is basically a feed forward control and the idea of which is to define control torque  $\tau$  using a structure identical to that of (N-E) dynamic model.(3.37)

$$\vec{\tau} = J \vec{\ddot{u}} + \vec{k} \quad (4.1)$$

where  $J$  is the inertia matrix and  $\vec{k}$  is the sum of the vectors  $\vec{f}$ ,  $\vec{h}$  and  $\vec{g}$ , of the (N-E) dynamic model. Substitution of (4.1) into (3.37) gives :

$$\vec{\ddot{q}} = \vec{\ddot{u}} \quad (4.2)$$

Which merely represents a set of  $n$  decoupled double-integrators, each of which can be controlled independently.

In case of 6R spray painting robot,  $u$  vector is a  $6 \times 1$  vector. The  $i$ th element of the control vector  $u$  is :

$$\vec{\ddot{q}}_i = \vec{\ddot{u}}_i \quad i=1,2,\dots,6 \quad (4.3)$$

$$u_i = J^{-1}[\tau_i - k_i] \quad (4.4)$$

The linear decoupled model (4.3) obtained above doesn't fully consider the non-linear structure of the equation of motion, because numerically computed values of  $J$  and  $\vec{k}$  are used directly at the updating instants and kept

constant until the next one. But still it is adequate enough both in accuracy and speed for control purposes.

#### 4.1.1. Updating Policy of the System Matrices

As it's been stated by the (N-E) recursive algorithm, the motion dynamics of the manipulator is inherently non-linear and can be described by a set of highly coupled, non-linear second order ordinary differential equations [8]. The non-linearities arise from the inertial loading, coupling between neighbouring joints, and the gravitational loading of the links. Furthermore, the dynamic parameters of the manipulator vary with the position of the joint variables which are already related by complex trigonometric transformations. Following these, it can easily be noted that so much computation in between the consecutive incremental motions of the arm on the path is not that practical, for it slows down the motion speed of the robot in industrial applications and takes a simulation program considerably long time to be run on a computer. Consequently, an updating policy for the basic system parameter matrices in (3.37) of the arm has been established.

The effect of the inertia matrix  $J$  in (3.37) is considerably large when compared with those of the vectors  $\vec{g}$ ,  $\vec{h}$  and  $\vec{f}$ . In order to see the changes of the inertia matrix

in the workspace of the 6R robot, the trace of the  $J$  matrix has been plotted as the arm moves from its most extended position to its most contracted one, on a linear path.

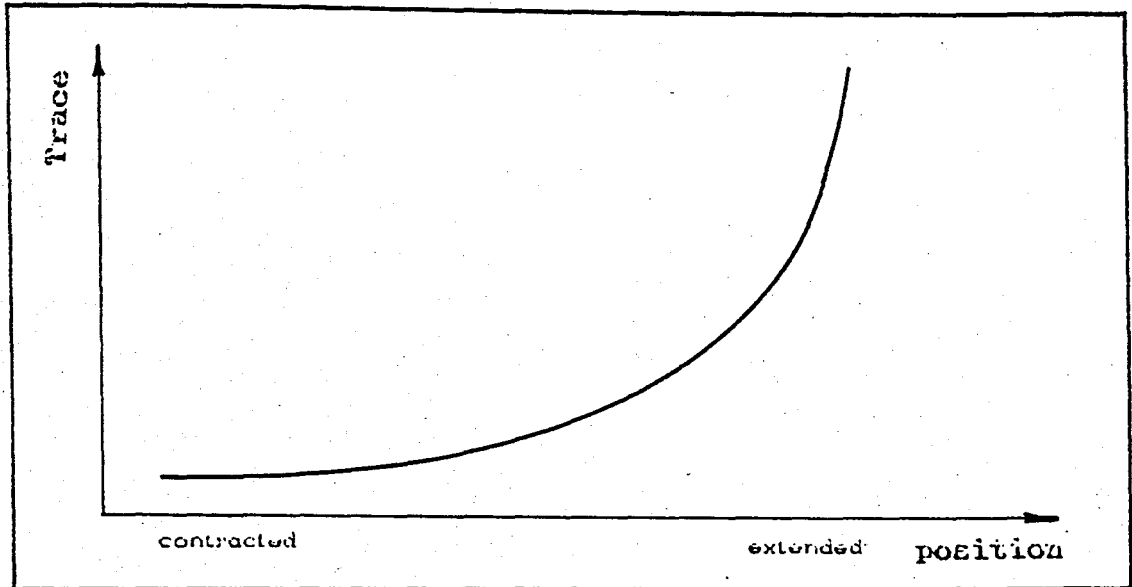


Figure 4.1. - Trace of inertia matrix w.r.t. position

As it can be seen from Fig.(4.1) the trace, therefore the values of the inertia matrix tend to remain constant as the arm is contracted. This proves the assumption of constant inertia matrix  $J$  in between the updating periods.

Fig.(4.2) clearly shows that, the inertia matrix is dependent on the position of the joint variables, or the position of the end-effector within the workspace of the robot. But, when the workspace is divided properly into sub-regions, the inertia matrix  $J$  almost retains constant values in each individual sub-regions. The curve in Fig.(4.2) can be approximated as :

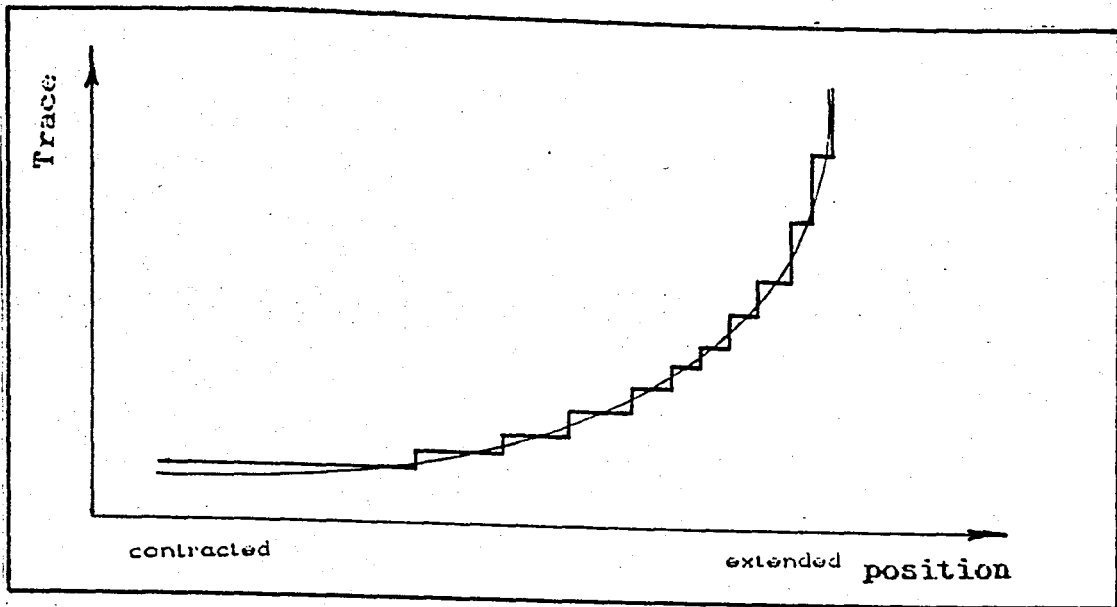


Figure 4.2. - Approximated trace of inertia matrix

This is nothing but dividing the workspace of the robot into concentric spherical stratum of different thicknesses. The robot is at the center (Fig.4.3). The stratum get thicker as the robot contracts because the inertia matrix retains almost constant values for a longer distance. But they get thinner and thinner as the arm extends because the inertia matrix and the vector  $\vec{k}$  needs to be updated more frequently. The algorithm is so as to update the system parameter matrices as the end-effector passes from one stratum to the other.

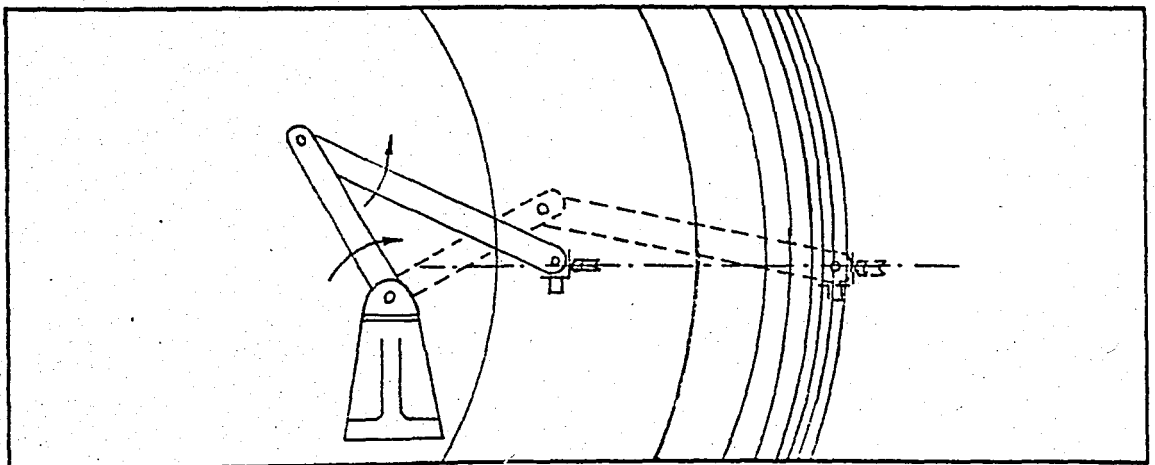


Figure 4.3. - Concentric stratum in the workspace

#### 4.1.2. Minimum Energy Approach with Specified Final Time and State

The equation of motion given by (3.1) is solved for the joint accelerations which put forward the decoupled linear model described by (4.3) when the desired trajectory for joint  $i$  is given by  $q_{di}(t)$ ,  $\dot{q}_{di}(t)$ ,  $\ddot{q}_{di}(t) = \gamma(t)$ , the state variables may be defined as [10]:

$$x_1 = q_{di} - q_i \quad \text{and} \quad x_2 = \dot{q}_{di} - \dot{q}_i \quad (4.5)$$

Then the state model becomes:

$$\frac{d}{dt} \begin{bmatrix} x_1 \\ x_2 \end{bmatrix} = \begin{bmatrix} 0 & 1 \\ 0 & 0 \end{bmatrix} \begin{bmatrix} x_1 \\ x_2 \end{bmatrix} + \begin{bmatrix} 0 \\ 1 \end{bmatrix} u_i + \begin{bmatrix} 0 \\ \gamma \end{bmatrix}, \quad t \in [t_k, t_{k+1}] \quad (4.6)$$

with an initial condition  $\vec{x}(t_0) = \vec{x}_k$ . The state model is in the form of :

$$\dot{\vec{x}} = A\vec{x} + B\vec{u} \quad (4.7)$$

The optimal control problem is solved by employing an energy optimal performance index. This stabilizes the system feedback matrices and reduces the number of control parameters involved [10]. The performance index is given by:

$$J = \frac{1}{2} \int_{t_0}^{t_0+T} \rho u_i^2 dt \quad (4.8)$$

where  $\rho$  is the weight coefficient for the control effort. The terminal condition is  $\dot{x}(t_f) = 0$ . The solution of the minimum energy terminal control problem defined by (4.6) and (4.8) with the final state constraints leads to the control law [10] as:

$$u_i = \frac{6}{T^2} (q_{di} - q_i) + \frac{4}{T} (\dot{q}_{di} - \dot{q}_i) \quad (4.9)$$

This is the decoupled control law for each joint. ( $i=1,2,\dots,6$ ). And  $T$  is the so called time-to-go and given by  $T = t_{k+1} - t_k$ . Substitution of (4.9) into (4.3) gives:

$$\ddot{q}_i + \frac{4}{T} \dot{q}_i + \frac{6}{T^2} q_i = \frac{6}{T^2} q_{di} + \frac{4}{T} \dot{q}_{di} + \ddot{q}_{di} \quad (4.10)$$

As a result the natural frequency of the system can be adjusted by only tuning the time-to-go, while damping ratio  $\zeta$  of the system is constant and equal to 0.82.

$$\zeta = \frac{b}{2\sqrt{km}} \quad , \quad k = \frac{6}{T^2} \quad , \quad m=1 \quad , \quad b = \frac{4}{T} \quad \text{then } \zeta = 0.82 \quad (4.11)$$

$$\omega_n = \sqrt{k/m} \quad \text{then } \omega_n = \sqrt{6}/T \quad (4.12)$$

## V. TRAJECTORY DETERMINATION

### 5.1. INTRODUCTION

Spray painting is the process of applying a paint on to a surface by atomization for finishing purposes.

Associated with the robotic applications to the spray painting processes, the problem of determining the appropriate path which is to be followed by the spray gun to perform the task, came across with the designers. Along with the determination of path, spray painting process has its own requirements that must be fulfilled for a better result. First of all, the spray gun must be so held that the pattern will be perpendicular to the surface at all times. Second, it must be kept a constant offset distance away from the surface in the direction of the normal to the surface at each instant. Next, the stroke must transverse the surface at a constant speed for uniform thickness coating and the overlapping of the patterns of two consecutive strokes must be 50 per cent. These show that; trajectory determination for a spray painting robot is not only a problem of finding a path but it is the description of time history of the position, orientation and speed of the end-effector with respect to the world coordinate frame.

## 5.2. SPACE CURVES AS THE " PATH "

Reference trajectory determination and planning for a manipulator performing 3D (three dimensional) surface operations generally involve a space curve as the path to be followed by the end-effector during operation.

A space curve is a three dimensional curve which is described by the position vector  $\vec{r}(u)$  joining the origin of base frame and any point  $(x,y,z)$  on the curve as :

$$\vec{r}(u) = x(u)\hat{i} + y(u)\hat{j} + z(u)\hat{k} \quad (5.1)$$

As the parameter 'u' changes, the terminal point of  $\vec{r}(u)$  describes a space curve, having parametric equations;

$$x=x(u) \quad y=y(u) \quad z=z(u) \quad (5.2)$$

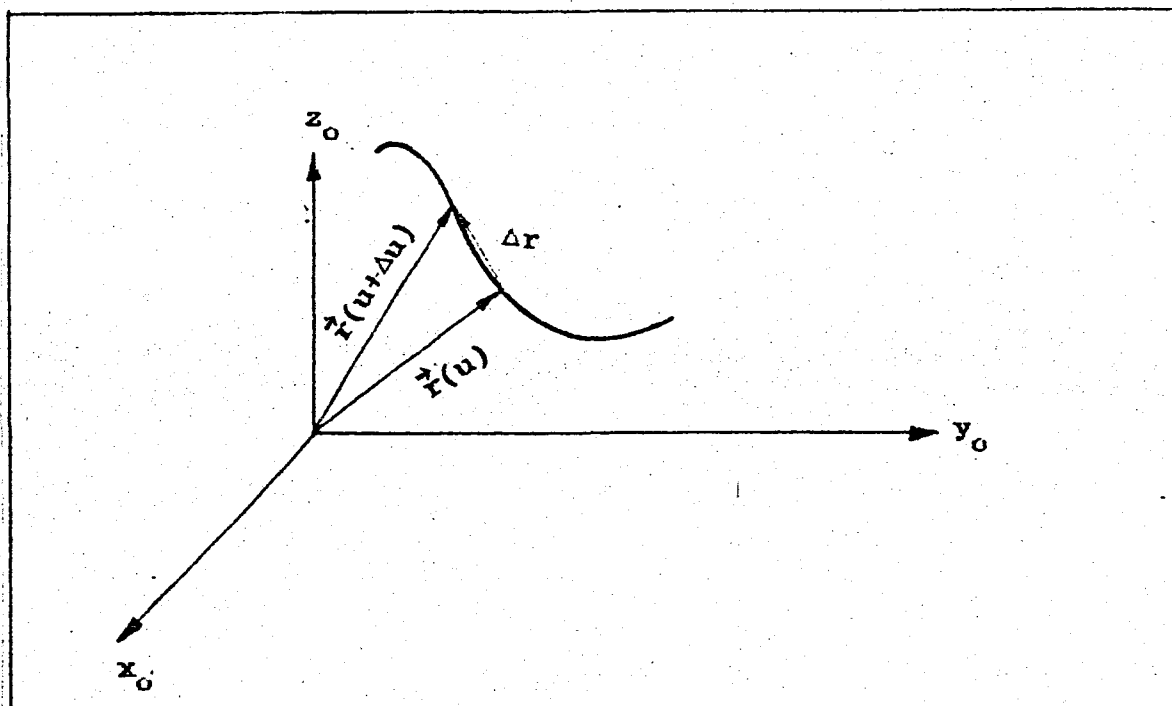


Figure 5.1. - Space curve

Then

$$\frac{\Delta \vec{r}}{\Delta u} = \frac{\vec{r}(u+\Delta u) - \vec{r}(u)}{\Delta u} \quad (5.3)$$

is a vector in the direction of  $\Delta \vec{r}$ . If,

$$\lim_{\Delta u \rightarrow 0} \frac{\Delta \vec{r}}{\Delta u} = \frac{d\vec{r}}{du} \quad (5.4)$$

exists, the limit will be a vector in the direction of the tangent to the space curve at  $(x, y, z)$  and is given by :

$$\frac{d\vec{r}}{du} = \frac{dx}{du} \hat{i} + \frac{dy}{du} \hat{j} + \frac{dz}{du} \hat{k} \quad (5.5)$$

If the parameter 'u' is taken as the time 't', then  $\vec{r}(t)$  represents the time history of the position vector.

Given the space curve 'C' defined by the vector  $\vec{r}(u)$ , then the tangent unit vector is found by taking 'u' the arc length, as:

$$\vec{T} = \frac{d\vec{r}}{ds} \quad (5.6)$$

The rate at which  $\vec{T}$  changes with respect to 's' is a measure of the curvature of 'C' and is given as  $d\vec{T}/ds$ . The direction of the vector  $d\vec{T}/ds$  at any given point on 'C' is normal to the curve at that point. If  $\vec{N}$  is a unit vector in

this normal direction then it is called the *principle normal* to the curve.

$$\frac{d\vec{T}}{ds} = \kappa \vec{N} \quad (5.7)$$

where  $\kappa$  is the curvature of 'C' specified at the point.

A unit vector  $\vec{B}$  perpendicular to the plane of  $\vec{T}$  and  $\vec{N}$  and such that  $\vec{B} = \vec{T} \times \vec{N}$  ( $\times$  is the cross-product) is called the *bi-normal* to the curve. The coordinate frame composed of the three unit vectors  $\vec{T}$ ,  $\vec{N}$  and  $\vec{B}$  is known as the *moving trihedral* [11].

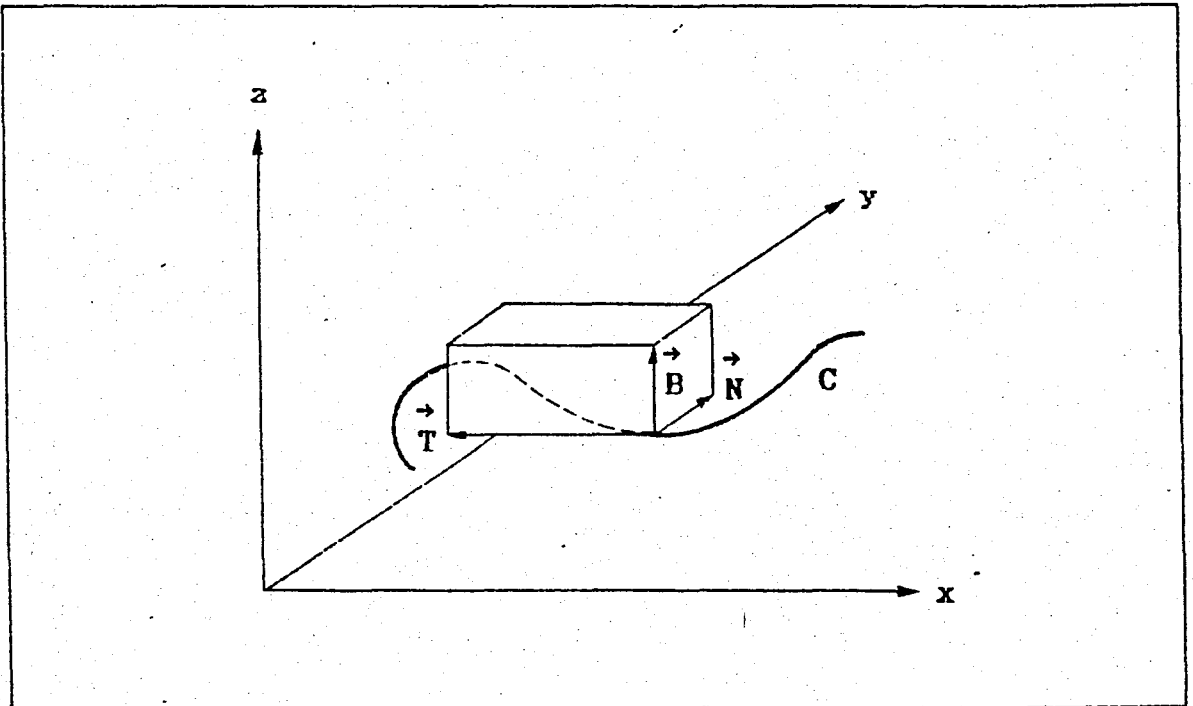


Figure 5.2. - Moving trihedral

A set of relations involving derivatives of the fundamental vectors  $\vec{T}$ ,  $\vec{N}$  and  $\vec{B}$  is known collectively as the

Frenet-Serret formulas and are given by:

$$\frac{d\vec{T}}{ds} = \kappa \vec{N} \quad (5.8)$$

$$\frac{d\vec{N}}{ds} = \rho \vec{B} - \kappa \vec{T} \quad (5.9)$$

$$\frac{d\vec{B}}{ds} = -\rho \vec{N} \quad (5.10)$$

where  $\rho$  is called as the torsion.

Consequently, the moving trihedral can be determined at every point on a space curve as long as the parametric equations  $x(u)$ ,  $y(u)$  and  $z(u)$  of the position vector  $\vec{r}(u)$  that is; the curve itself is known. In case of 6R spray painting robot, the 6th coordinate frame attached to the spray gun which shows the position and orientation of the end-effector, at the given point on the path is aligned in the same way as the moving trihedral. This satisfies the requirements of spray painting process.

In this study, a conic helix, a spatial parabola and a spatial line in the work space of a particular 6R robot have been chosen as the paths to be followed during operation.

### 5.3. TEACH-IN WITH ON-LINE PROGRAMMING

The programming process of a robot may be performed in many ways: by guiding the robot through the correct motions, textual language or even by graphics or voice. Some methods are more sophisticated than others and some are used commercially.

One of the ways of teaching a robot is lead-through teaching, where the programmer manually moves the manipulator through the cycle which is to be performed. The motions are recorded in the memory exactly as they are executed. This method is commonly used to teach the continuous path robots such as those of spray painting. Recording of each link's position as the operator manipulates the arm through the desired path, can be in two ways. It is done either when a trigger button on the handheld handle fixed at the end-effector of the robot is depressed or by sampling with a preset frequency as the operator traverses the surface to be painted.

The programmer need not be an expert in computer programming but he must be very familiar with the task that is to be performed. He may be a skilled worker on painting for teaching a spray painting robot.

The sampled points on the desired path are often called as *knots*. The position samples that is; the knots taken on the surface are generally distributed arbitrarily. If the

sampling is done by triggering, the programmer will certainly trigger at positions which are unequal distances apart from each other. On the other hand, if sampling is done with a preset frequency, the knots may still be unevenly distributed since the programmer can never retain a constant traversal speed at all times during teach-in. The uneven distribution of the knots may seem to be a disadvantage. However, most of the times it is of vital importance such as when teaching the cavities of an object or sudden directional changes of the path. The more accurate a path has to be, the closer the distance between the knots. The following table shows typical applications in practice [12].

Point Spacing in mm	Typical Application
0.5	very exact contours
2.0	welding, deburring
10.0	glue appl. ,welding
50.0	coating, spraying
100.0	spray painting
500.0	material handling
1000.0	material handling

Table 5.1. - Typical applications of teach-in

But an important drawback of the method is that, it requires a considerably large memory capacity to store the knots. Furthermore, the memory capacity limits the accuracy of the path. The number of knots to complete the path definition

will increase as the knots on a prescribed task get closer for better accuracy. The teach-in process may be interrupted because of the lack of memory before completing the cycle. As a solution, off-line programming may stand to be useful at the first glimpse. It offers considerable advantages; mainly: Programs can be moved from one robot to another, programming becomes the responsibility of a person more familiar with the overall operation than the plant floor-technician, and robots can be taught earlier, not during production.

In spite of many given advantages of the off-line programming it is still not widely in use. Because, off-line programming requires programming skills together with the necessary computational hardware, and they don't come cheap. Furthermore it necessitates an advanced level of technical knowledge. In addition, the use of pure off-line programming suffers from the inaccuracy of the robots. If the program calls for the end-effector to be at a particular location and the robot doesn't have the accuracy to position it there, some on-line teaching will then be inevitable again.

A useful means of providing the ability to easily define the task may be a hybrid method: Sampling knots on the desired path during manipulation of the robot through the cycle followed by an off-line trajectory planning.

#### 5.4. OFF-LINE TRAJECTORY PLANNING

Off-line trajectory planning schemes generally *interpolate* or *approximate* the desired path by a class of polynomial functions and generates a time based continuous, smooth path for the end-effector from its initial position to its destination. It describes what the end-effector will do between sampled knots.

Quite frequently, there exists a number of possible trajectories between the two given endpoints. It may be a path of straight line segments or a smooth polynomial trajectory that satisfies the position and orientation constraints.

In spray painting process, the knots are specified with the active manipulation of the robot arm on the surface to be painted, with respect to the world coordinate frame  $(x_0, y_0, z_0)$ , with the constraints that path, velocity and acceleration be continuous. But the servos at the joints handle the motions of joints with respect to the joint coordinate frames.

At each knot point, the position vector and the orientation matrix of the spray gun at that individual knot is converted into joint coordinates using inverse kinematics as the consecutive joint angular positions in time to complete the task. (Fig. 5.3)

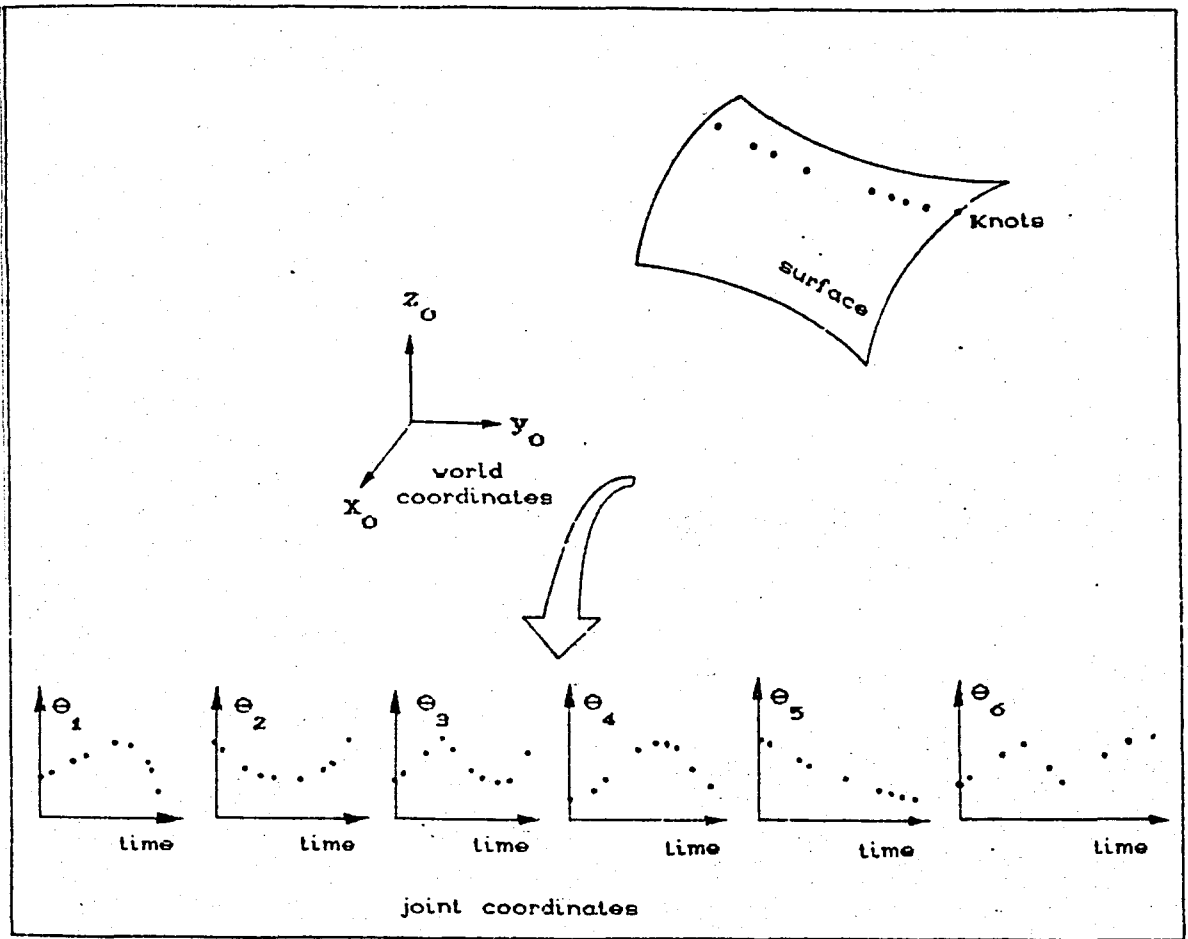


Figure 5.3. - Translation of knots in world coordinates into joint coordinates

Sampling the desired path by lead-through teaching brings out the problem of time scaling when the path is re-executed during production. The relative distribution of the knots in time can not be achieved by simply sampling the time as the position. Because during teaching, the time elapsed is virtual. It depends directly on the speed of the programmer. What happens for example, if he interrupts teaching temporarily ?

A parameter must be developed for timing between the knots. It must be such a parameter that its value corresponding to a knot must be greater than that of the preceding one, in a chain manner. That is; the values it takes can be assigned to the time axis of the 6 joint coordinate frames in Fig. 5.3, as one moves from one knot to another [13],[14],[15]. This parameter can be chosen as the straight line distance between two adjacent knots. This will facilitate a means of relative spacing between the knots. And will provide all the necessary requirements above. It is:

$$\Delta u = \sqrt{\Delta x^2 + \Delta y^2 + \Delta z^2} \quad (5.11)$$

where

$$\begin{aligned} \Delta x &= P_{xi} - P_{xi-1} \\ \Delta y &= P_{yi} - P_{yi-1} \\ \Delta z &= P_{zi} - P_{zi-1} \quad i=1,2,\dots,6 \end{aligned} \quad (5.12)$$

and  $P_x, P_y$  and  $P_z$  represent the components of the position vector of that knot with respect to the world coordinate frame. Once  $\Delta u$  between each knot is calculated, the scaling parameter is :

$$u_i = u_{i-1} + \Delta u \quad (5.13)$$

and  $u_1=0$  is taken as the origin of the scaled axis.

It is possible to use the straight line distance between knots for the off-line trajectory planning of spray painting process, as the scaling factor for time because, it is essential to have a constant speed during spray painting process. Which enables us to relate the time elapsed to the distance to be travelled as :

$$d = S t \quad (5.14)$$

where  $d$  : distance to be travelled,

$S$  : speed

$t$  : time elapsed.

Here the speed  $S$  has the role of a proportionality constant. This means that, distance travelled will be directly proportional to the time elapsed or vice versa since the speed is constant. Consequently, the 'time' axis of the above joint coordinate frames may be replaced by the relative distances to be travelled.

In some applications, it may be desirable to perform the task in a limited time, while other applications may necessitate a specified constant speed as critical in task completion. In any case, it is compulsory to scale the knots in time. If the limitation is on time in performing the task, time normalization may be done as follows :

$$t_i = t \frac{u_i}{u_n} \quad (5.15)$$

where  $t_i$  :time corresponding to  $i$ th knot,  
 $t$  :given task performance time limitation,  
 $u_i$  :scaling parameter corresponding to  $i$ th knot,  
 $u_n$  :scaling parameter corresponding to the last knot.

On the other hand,if speed is specified then,

$$t = \frac{d}{S} \quad (5.16)$$

and time normalization is achieved by using (5.15).

$d$  :total length of the path,

$S$  :specified speed.

### 5.5. OVERLAPPED POLYNOMIALS AS THE " PATH "

After time scaling,third order polynomials to approximate the desired path specified by the knots are employed in each joint's coordinate frame of the 6R spray painting robot.The polynomials are in the form :

$$\theta_{ij} = a_{9i} t_j^3 + a_{2i} t_j^2 + a_{1i} t_j + a_{0i} \quad (5.17)$$

where  $i$  is the joint number ( $i=1,2,\dots,6$ ),  $j$  is the knot number ( $1,2,\dots$ ) and  $\theta_{ij}$  is the joint coordinate of the  $i$ th joint corresponding to the  $j$ th knot. $a_{9i}, a_{2i}, a_{1i}$  and  $a_{0i}$  are the coefficients of the polynomial.

In order to determine all coefficients of a polynomial four knots are enough.

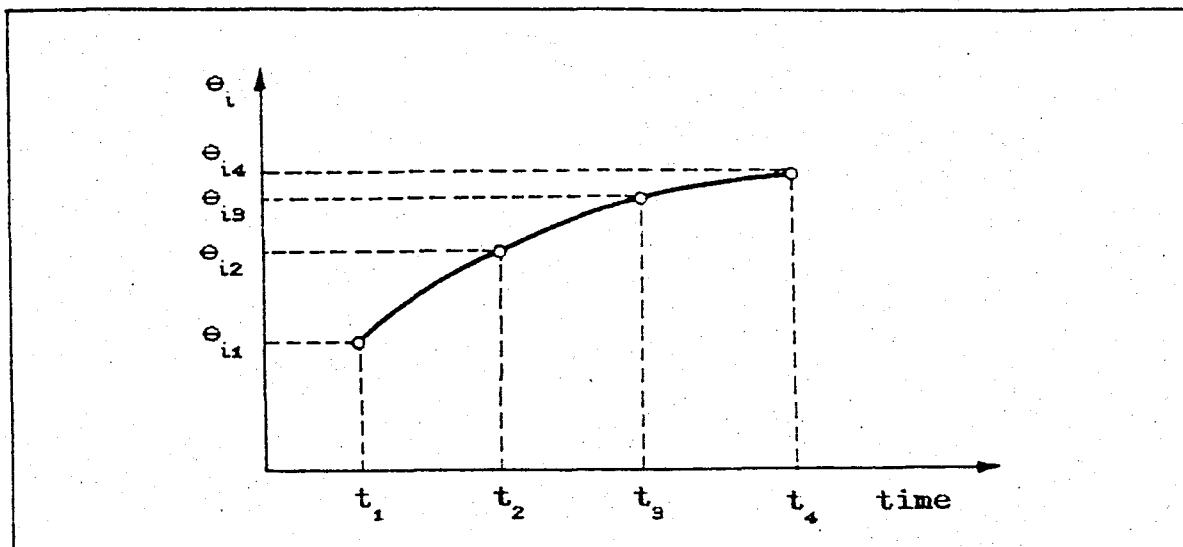


Figure 5.4. - Third order polynomial

So, if the adjacent 'four knots' are used, having the terminating knot of the preceding group in common with the first one of the current group in chain manner, a path continuous in position can be obtained.

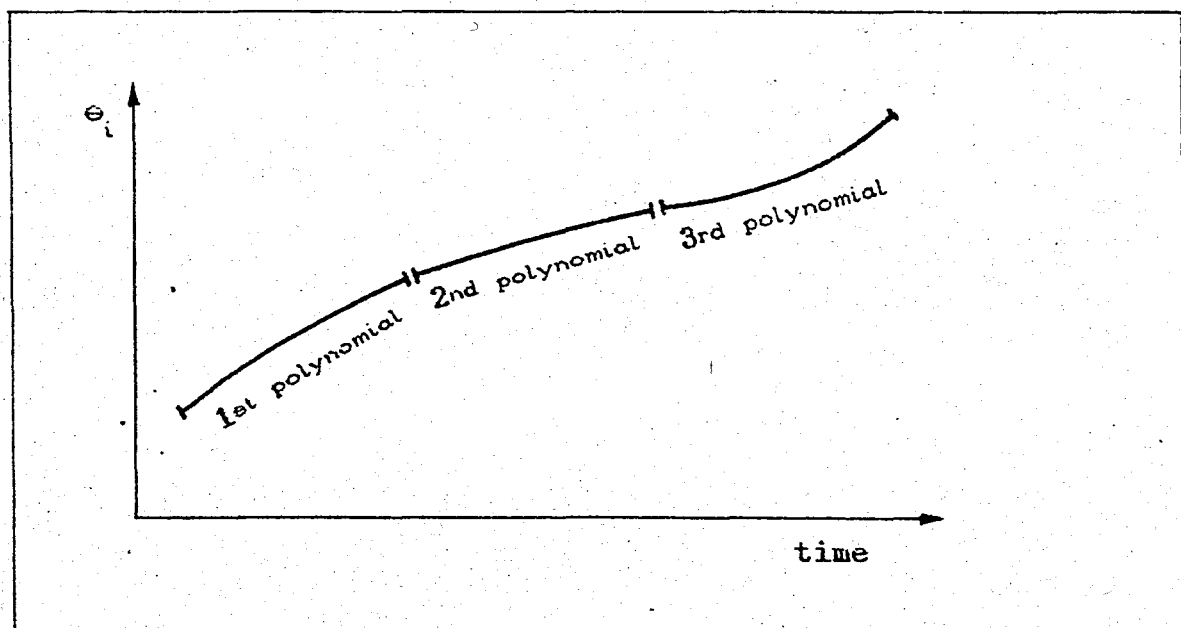


Figure 5.5. - Polynomials attached sequentially

To obtain a path continuous in velocity, the tangent at the junction of two adjacent polynomials must not change direction. This is achieved by taking two knots common to adjacent polynomials. In the same way, three knots are taken to have the path continuous in position, velocity and acceleration. As a result, the 3rd order polynomials put the path forward by overlapping.

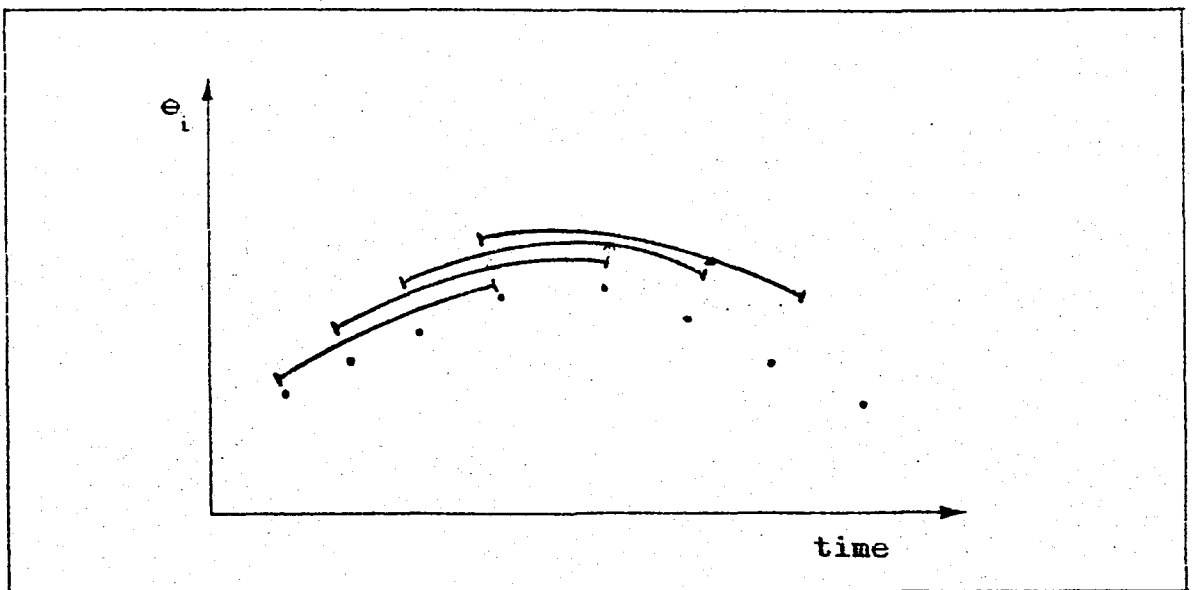


Figure 5.6. - Overlapped polynomials

The coefficients of the polynomials are found as :

$$\begin{bmatrix} a_{9i} \\ a_{2i} \\ a_{1i} \\ a_{0i} \end{bmatrix} = \begin{bmatrix} t_j^3 & t_j^2 & t_j & 1 \\ t_{j+1}^3 & t_{j+1}^2 & t_{j+1} & 1 \\ t_{j+2}^3 & t_{j+2}^2 & t_{j+2} & 1 \\ t_{j+3}^3 & t_{j+3}^2 & t_{j+3} & 1 \end{bmatrix}^{-1} \begin{bmatrix} e_{ij} \\ e_{i,j+1} \\ e_{i,j+2} \\ e_{i,j+3} \end{bmatrix} \quad (5.18)$$

where  $i=1,2,\dots,6$  is the joint number and  $j=1,2,3,\dots$  is the polynomial number.

## VI. SIMULATION OF BEHAVIORS OF THE 6R SPRAY PAINTING ROBOT

### 6.1. STRUCTURE OF THE SIMULATION PROGRAM

A computer simulation program package has been developed for the simulation of a 6R spray painting robot whose wrist configuration is of *Pitch-yaw-roll* type. The program employs 13 subroutines, 6 input and 6 output files simultaneously.

The structure of the program is modular in that, all sub-titles of the subject is formed into a subroutine. But the recursive (N-E) dynamic modelling algorithm involves too many messy matrix and vector products. Therefore, it's been taken as the structure of the main program to which the subroutines are linked.

The program package contains a conic helix, a spatial parabola and a spatial line as three example scenarios in the workspace of a 6R robot of certain dimensions. The paths can not be altered, but they are there to give a demonstrative sight to the user. On the other hand, the program is completely flexible for any 6R robot of any geometric dimensions and physical quantities (mass inertia, etc.) of the same type of structure. Plus, it may be run for any path through teach-in facilities as long as the knots are defined. The flowchart of the program is given in

### Fig.6.1.

The program has been written in FORTRAN and can be run by an AT compatible personal computer.

### 6.2. MAIN PROGRAM

Recursive (N-E) dynamic modelling algorithm has been taken as the major structure of the main program since it involves messy matrix and vector products. It has then been completed with the inputs, user interactive questions, outputs and adjoined subroutines.

Input data read from various files basically are;

- i) Geometric and physical parameters (such as masses and link lengths of the robot..)
- ii) Initial position and orientation of the robot, desired end-effector speed and angular velocity vector of the wrist, length of paths for the conic helix, spatial parabola and line,
- iii) Inertia matrices of each link, force on the end-effector,
- iv) Data related to the control and updating policy,
- v) Some other parameters necessary for the simulation. (such as for DISCR3 subroutine.)

### 6.3. SUBROUTINES

Thirteen subroutines have been linked to the main program to perform the necessary computations for simulation. The required input variables and generated outputs have been explained in detail in the subroutine called HELP. It is also possible to find any information about each individual subroutine in HELP. At the beginning of the program, the user is prompted a list where, he/she may select the HELP subroutine for any enquiries.

DISCR3 is the subroutine used to discretize the continuous, decoupled state model of each link for computer simulation purposes.

MINV is for the computation of the inverse of any given matrix of order  $n$ .

INVERSE subroutine solves the inverse kinematics problem of the 6R spray painting robot.

JAC2 is the subroutine for the construction of *Jacobian* matrix of the robot.

ROT contains the transformation matrices of each coordinate frame attached to the individual joints.

TRAJ, HELIX and PARAB are the subroutines to generate three scenarios as the path to be followed by the spray gun. TRAJ generates a spatial line while HELIX and PARAB create a conic helix and a spatial parabola in the cartesian coordinate frame, respectively.

JINT3 is the subroutine that interpolates the data came from teach-in and creates a path.

DRK is to solve the direct kinematics problem of the robot.

SIM is the subroutine that generates the control vector and computes the new state of the robot.

UPD is the subroutine that contains the adjustable updating limits of the system matrices within the workspace of the given robot.

#### 6.4. USER INTERACTION

The program is user interactive. It directs many questions to the user during execution. It also enables the user to change anything that he/she input or selected before skipping that item. The output is formatted neatly so that it can be understood easily.

JINT3 is the subroutine that interpolates the data came from teach-in and creates a path.

DRK is to solve the direct kinematics problem of the robot.

SIM is the subroutine that generates the control vector and computes the new state of the robot.

UPD is the subroutine that contains the adjustable updating limits of the system matrices within the workspace of the given robot.

#### 6.4. USER INTERACTION

The program is user interactive. It directs many questions to the user during execution. It also enables the user to change anything that he/she input or selected before skipping that item. The output is formatted neatly so that it can be understood easily.

## VII. SIMULATION RESULTS

### 7.1. SCENARIOS

In order to simulate the dynamic behavior of a robot, it is compulsory to define a certain task that has to be performed by the end-effector. In case of spray painting, this task is the path to be followed by the tip of the spray gun while keeping it in the proper orientation across the surface, at all times.

In this study, three basic scenarios besides on-line teach-in with off-line trajectory determination have been selected. After that, a 6R robot with the given features in table 7.1. is used for the simulation purposes. It is important for the path describing the task to be within the workspace, that is; the region in which the robot can manipulate. Therefore, the constant coefficients involved in the scenarios have been adjusted accordingly.

### 7.2. SPATIAL LINE

One of the diagonals of an inclined rectangular surface located in the workspace of the robot has been assumed as the rectilinear path to be followed by the spray gun, leading to have all the joints in motion.

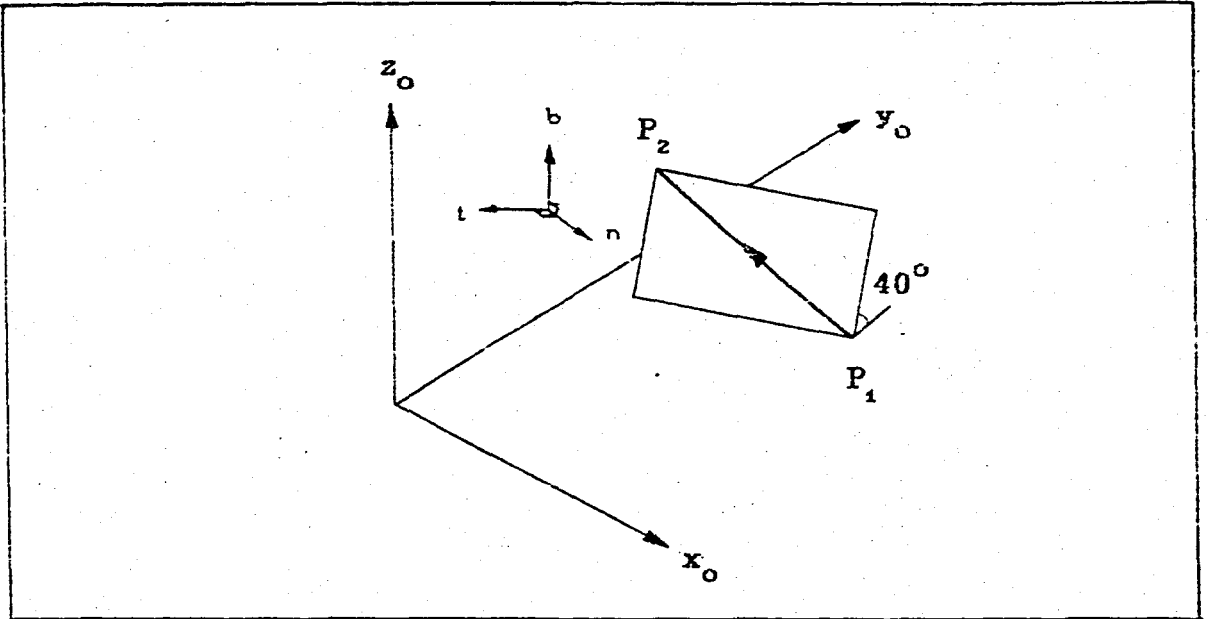


Figure 7.1. - Spatial line

The motion starts at point  $P_1(1;1.54;0)$  and stops at point  $P_2(0.1;2.2;0.56)$ , (Dimensions are in meters). The equation of the line can be found as:

$$\vec{r} = -0.9 \hat{i} + 0.66 \hat{j} + 0.56 \hat{k} \quad (7.1)$$

The orientation of the gun remains constant. Then the orientation matrix of the hand for  $\alpha=40^\circ$  degrees of inclination:

$$\begin{bmatrix} -1 & 0 & 0 \\ 0 & 0.76604 & 0.64279 \\ 0 & 0.64279 & -0.76604 \end{bmatrix}$$

If the unit distance travelled along the line is taken as the parameter, the equation of the path with the direction cosines of the line, is given as:

$$\vec{r}(s) = (1-0.72075s)\hat{i} + (1.54+0.52855s)\hat{j} + (0.44847)\hat{k} \quad (7.2)$$

### 7.3. CONIC HELIX

A conic helix is a space curve which is wrapped around a cone whose vertex is on the ground.

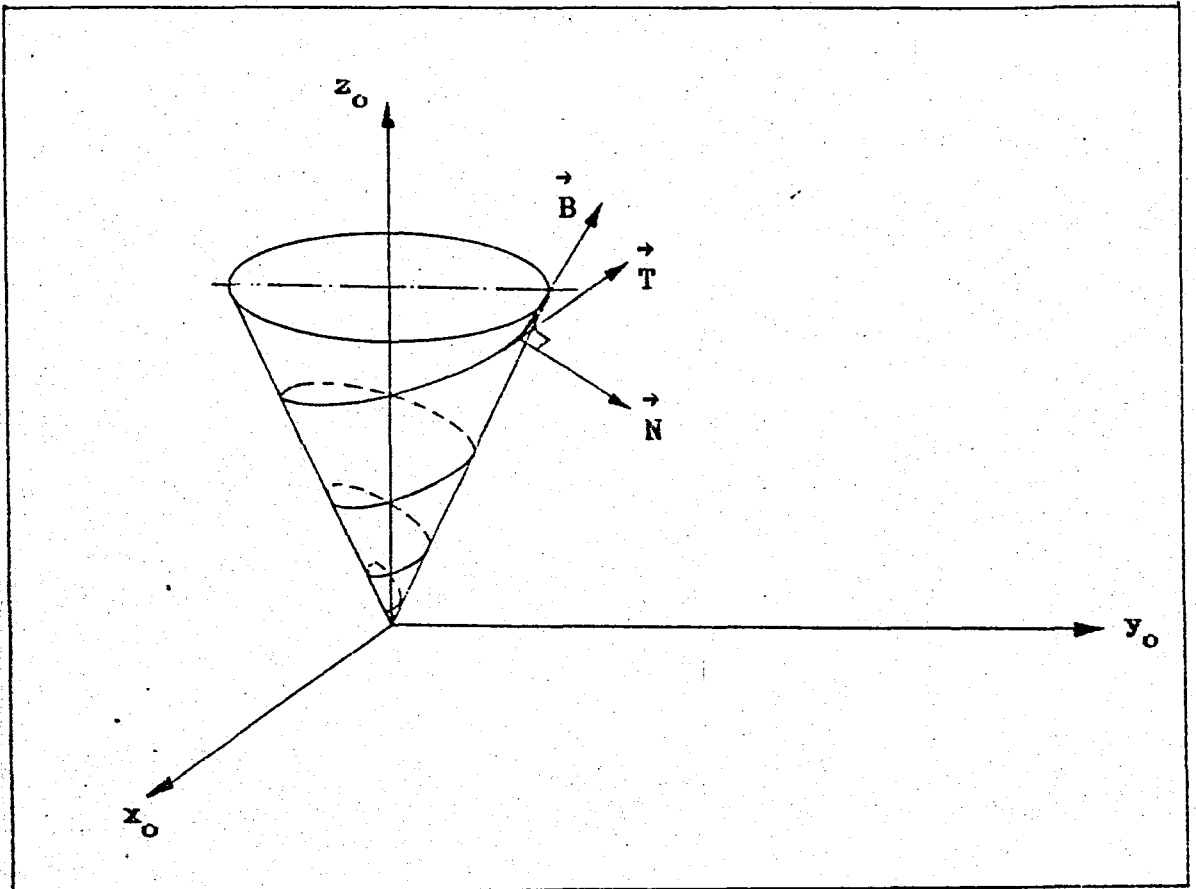


Figure 7.2. - Conic helix

The robot is assumed to be at the center of the conic helix. It is described by the equation :

$$\vec{r}(t) = e^t \cos t \hat{i} + e^t \sin t \hat{j} + e^t \hat{k} \quad (7.3)$$

where  $\vec{r}(t)$  is the position vector of a point on the curve. For the curve to be within the work space of the selected robot, the vertex angle of the cone has been taken as 60 degrees. Then,

$$\vec{r}(t) = e^t \cos t \hat{i} + e^t \sin t \hat{j} + 0.577e^t \hat{k} \quad (7.4)$$

To find the tangent vector, (5.6) is used.

$$\frac{d\vec{r}}{ds} = \frac{d\vec{r}}{dt} \frac{dt}{ds} \quad (7.5)$$

$$\frac{d\vec{r}}{dt} = (e^t \cos t - e^t \sin t) \hat{i} + (e^t \sin t + e^t \cos t) \hat{j} + 0.577e^t \hat{k} \quad (7.6)$$

$$\frac{ds}{dt} = \sqrt{\frac{d\vec{r}}{dt} \cdot \frac{d\vec{r}}{dt}} \quad (7.7)$$

$$\frac{ds}{dt} = \sqrt{2.33} e^t \quad (7.8)$$

Then using (7.4), (7.5) and (7.6),

$$\vec{T} = \frac{1}{\sqrt{2.33}} [(\cos t - \sin t)\hat{i} + (\sin t + \cos t)\hat{j} + 0.577\hat{k}] \quad (7.9)$$

is the equation of the *tangent* vector. In order to find the normal vector (5.8) is used. Through the same way :

$$\frac{d\vec{T}}{dt} = \frac{1}{\sqrt{2.33}} [-(\sin t + \cos t)\hat{i} + (\cos t - \sin t)\hat{j}] \quad (7.10)$$

$$\frac{d\vec{T}}{ds} = \frac{d\vec{T}}{dt} \frac{dt}{ds} \quad (7.11)$$

$$\frac{d\vec{T}}{ds} = \frac{1}{\sqrt{2.33} e^t} [-(\sin t + \cos t)\hat{i} + (\cos t - \sin t)\hat{j}] \quad (7.12)$$

$$\kappa = \left| \frac{d\vec{T}}{ds} \right| = \frac{\sqrt{2}}{2.33 e^t} \quad (7.13)$$

Then using (7.10), (7.11) and (5.8),

$$\vec{N} = \frac{1}{\sqrt{2}} [-(\sin t + \cos t)\hat{i} + (\cos t - \sin t)\hat{j}] \quad (7.14)$$

This is the principle normal of the curve in the direction toward the center. But the hand normal will be in the opposite direction because the robot is inside the curve. Then,

$$\vec{N}_H = \frac{1}{\sqrt{2}} [ (\sin t + \cos t) \hat{i} + (\sin t - \cos t) \hat{j} ] \quad (7.15)$$

Finally, the moving trihedral is constructed by the subroutine as :

$$\vec{B}_H = \vec{N}_H * \vec{T} \quad (7.16)$$

Here the parameter 't' is taken as the base rotation  $e_1$ . The length of the path to be followed is calculated by:

$$S_{(\alpha, \beta)} = \int_{\alpha}^{\beta} |\vec{r}'| dt \quad (7.17)$$

where  $\alpha$  and  $\beta$  are the angles between which the length is to be calculated. They have been chosen as  $\alpha=15$  and  $\beta=45$  degrees. Since  $|\vec{r}'| = ds/dt$ ,

$$S_{(\alpha, \beta)} = \int_{\alpha}^{\beta} \sqrt{2.33} e^t dt \quad (7.18)$$

$$S = 1.363 \text{ m}$$

## 7.4. SPATIAL PARABOLA

The spatial parabola is given by the equation :

$$\vec{r}(t) = t\hat{i} + [a(t-c)^2 + k]\hat{j} + z\hat{k} \quad (7.19)$$

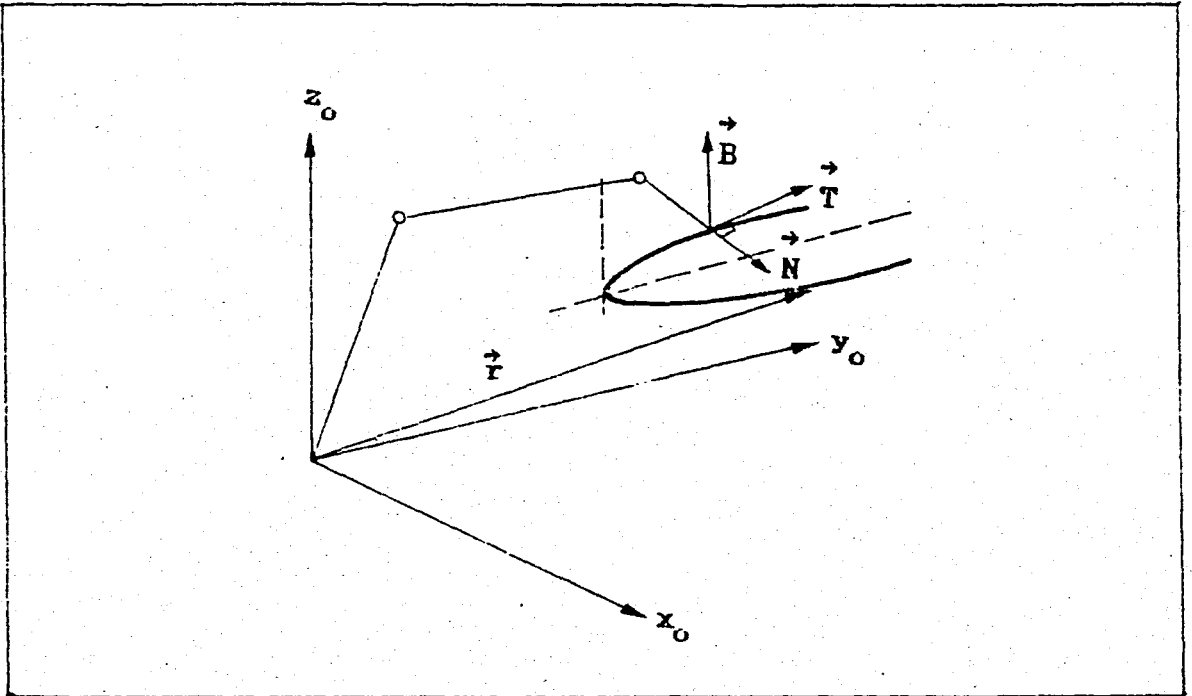


Figure 7.3. - Spatial parabola

The selected parabola has the equation of:

$$\vec{r}(t) = t\hat{i} + [2(t-0.7)^2 + 1]\hat{j} + 0.5\hat{k} \quad (7.20)$$

Through the same procedures given in conic helix,

$$\frac{d\vec{r}}{dt} = \hat{i} + [4(t-0.7)]\hat{j} \quad (7.21)$$

$$\frac{ds}{dt} = \sqrt{16t^2 - 22.4t + 8.84} \quad (7.22)$$

The tangent vector is :

$$\vec{T} = \frac{0.25}{\sqrt{t^2 - 1.4t + 0.5525}} [\hat{i} + (4t - 2.8)\hat{j}] \quad (7.23)$$

To calculate the normal vector :

$$\frac{d\vec{T}}{dt} = (t^2 - 1.4t + 0.5525)^{-3/2} [-(0.25t - 0.175)\hat{i} + 0.0625\hat{j}] \quad (7.24)$$

$$\frac{d\vec{T}}{ds} = \frac{0.25}{(t^2 - 1.4t + 0.5525)^2} [-(0.25t - 0.175)\hat{i} + 0.0625\hat{j}] \quad (7.25)$$

$$\kappa = \left| \frac{d\vec{T}}{ds} \right| = \frac{\sqrt{(0.25t - 0.175)^2 + 0.0625^2}}{4(t^2 - 1.4t + 0.5525)^2} \quad (7.26)$$

$$\vec{N} = \frac{1}{\sqrt{0.0625t^2 - 0.0875t + 0.0345}} [-(0.25t - 0.175)\hat{i} + 0.0625\hat{j}] \quad (7.27)$$

Here the principle normal of the curve and the normal of the hand are in the same direction since the robot is outside the curve. The parameter  $t$  is taken as the increments in the  $x_0$  direction of the base frame. The subroutine computes the moving trihedral by taking the cross-product of  $\vec{T}$  and  $\vec{N}$  to

find the bi-normal vector  $\vec{B}$ .

$$\vec{B} = \vec{N} \times \vec{T} \quad (7.28)$$

The arc length to be travelled is found by the line integral

$$S = \int_{0.1}^{1.3} \sqrt{16t^2 - 22.4t + 8.84} \, dt \quad (7.29)$$

where the robot sweeps the linear projected distance between the 0.1 th and 1.3 th meters of the  $x_0$  axis of base frame.

### 7.5. TEACH-IN ON THE CONIC HELIX

This scenario has been used to see whether the trajectories in joint coordinates determined by the on line teach-in, off-line path computation facilities of the program are satisfactory or not. For this purpose 16 arbitrarily distributed knots on the same conic helix described before, have been taught the robot, (Fig.7.4).

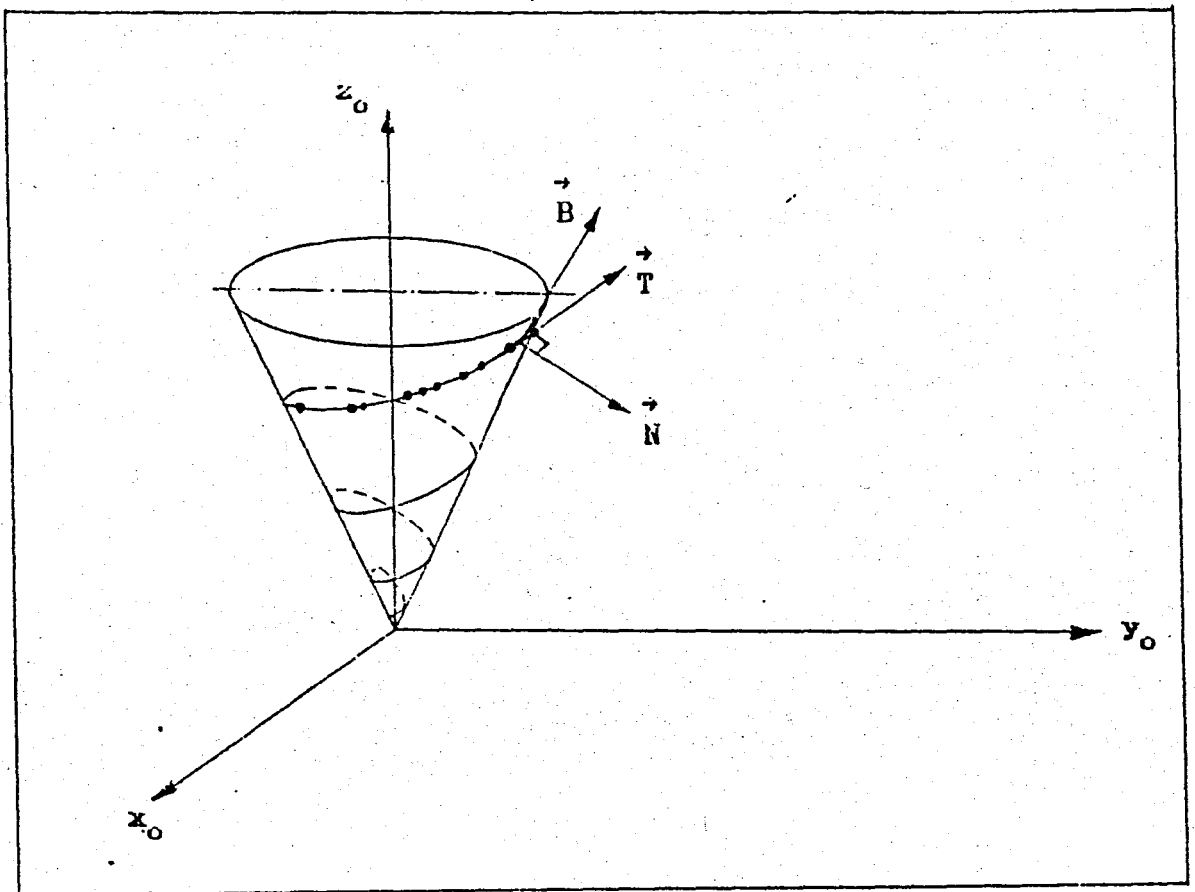


Figure 7.4. - Teach-in on the conic helix

### 7.6. TEACH-IN ON A RECTANGULAR SURFACE

In order to paint a surface, the path must first be taught the robot. For this reason, the path given by Fig. 7.5 is specified by 44 unevenly distributed knots. The surface has the dimensions of  $30 \times 50 \text{ cm}^2$ . The spray pattern width has been taken as 30 cm. The job will be completed with 3 passes over the surface. Required average speed has been taken as 0.5 m/s.

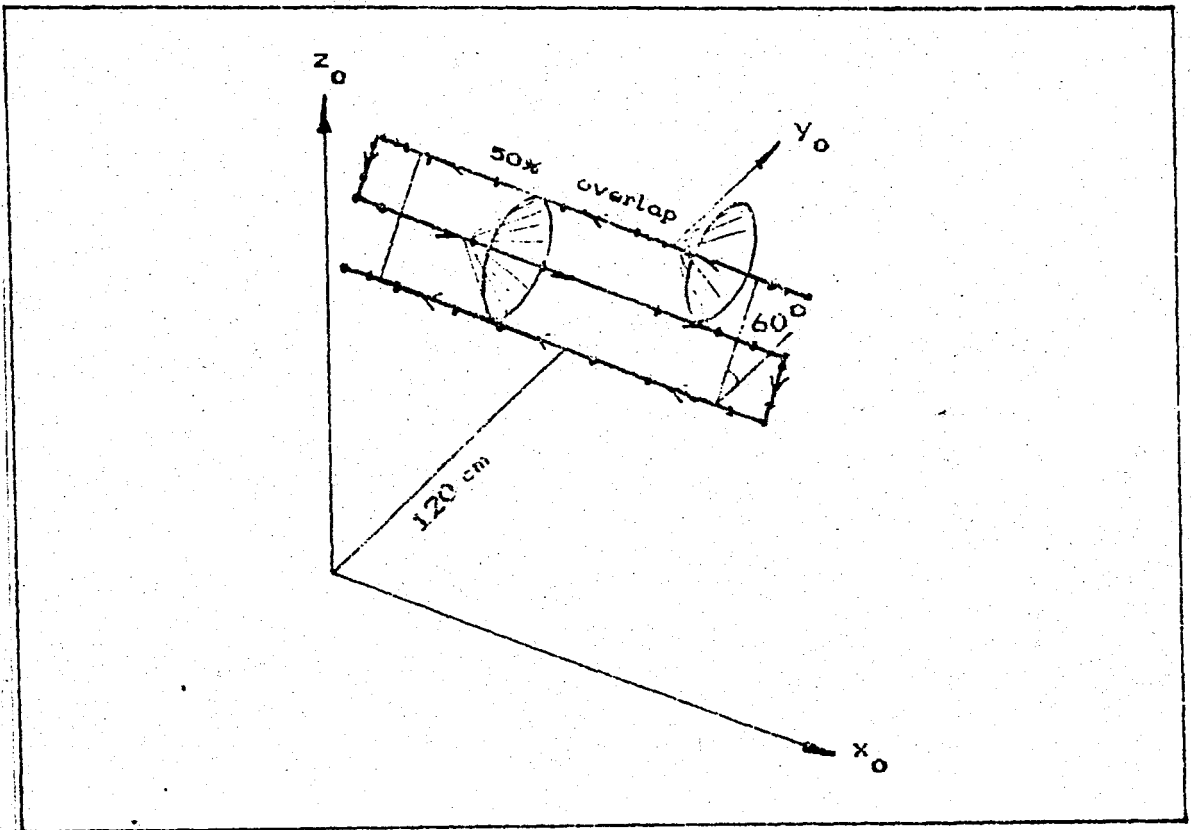


Figure 7.5. - Teach-in on a rectangular surface

The moving trihedral of the end-effector has been specified as follows:

$$\begin{aligned} \vec{T} = -\hat{j} \quad \text{and} \quad \vec{B} = 0.5\hat{j} + 0.866\hat{k}, \text{ then} \\ \vec{N} = \vec{B} * \vec{T} \end{aligned} \quad (7.30)$$

is the principle normal of the surface,

$$\vec{N}_H = -\vec{N} \quad (7.31)$$

$$\vec{N}_H = 0.866\hat{j} - 0.5\hat{k} \quad (7.32)$$

N, T and B will remain unchanged during the process. The knots have been sampled more often nearby the corners of the path.

link #	Length (cm)	Mass (kg)
1	30	20
2	100	20
3	120	20
4	30	4
5	30	4
6	10	1

Table 7.1. - Dimensions of the selected robot

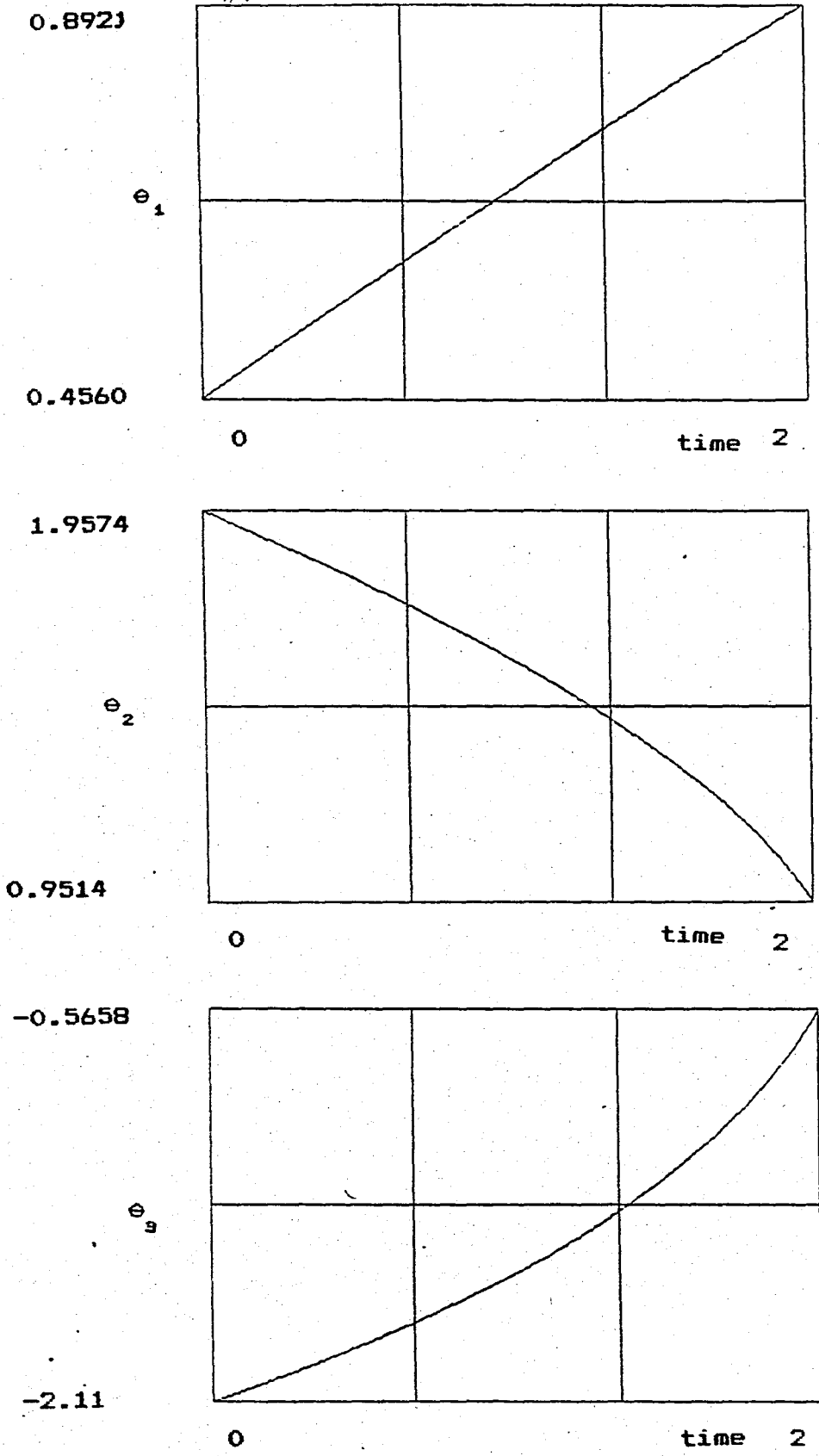


Figure 7.6. - First three joint displacements (rad) for conic helix path. Time in sec.

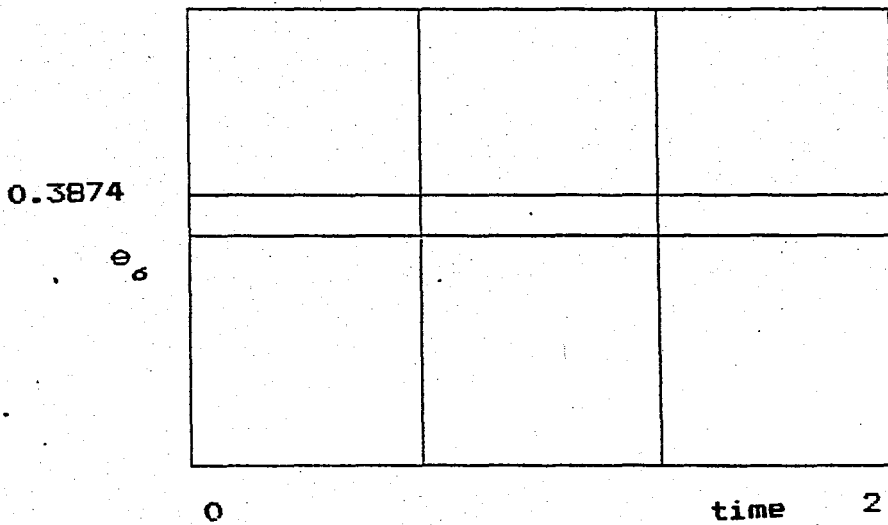
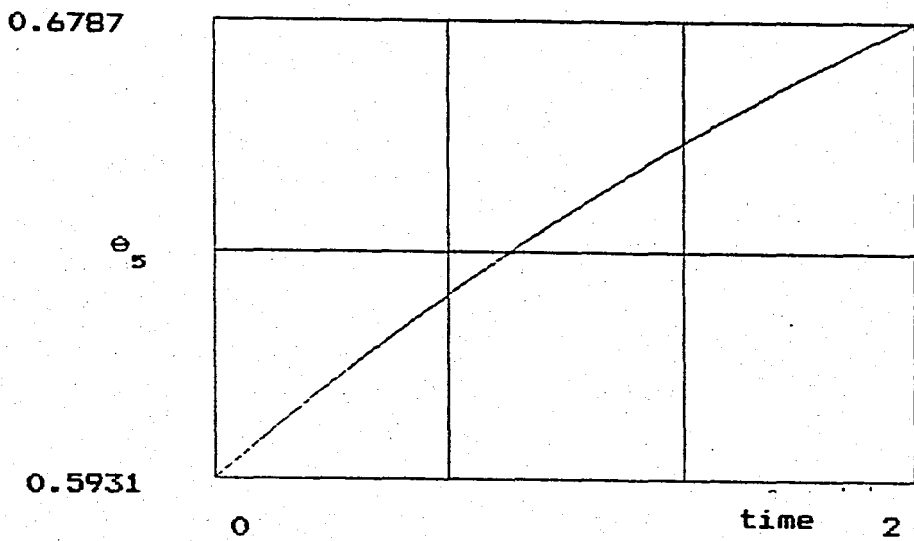
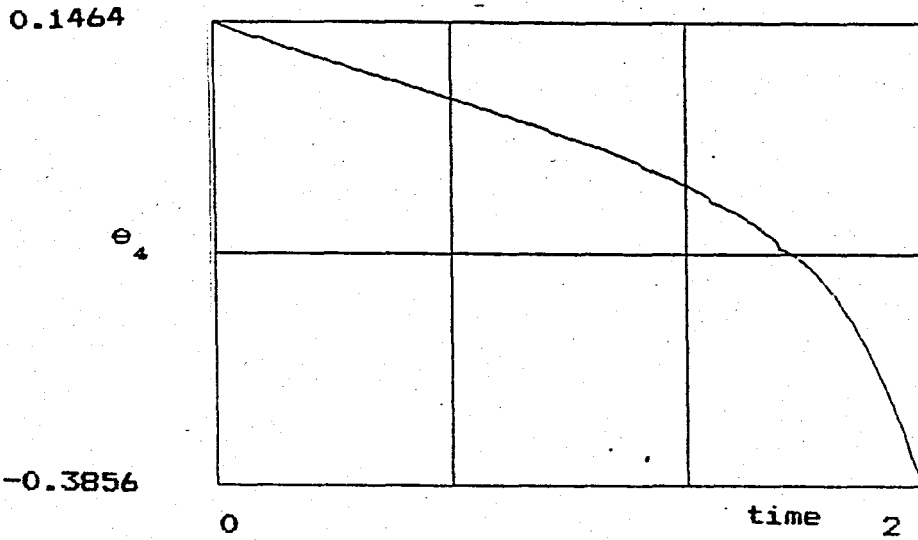


Figure 7.7. - Wrist joint displacements (rad) for conic helix path. Time in sec.

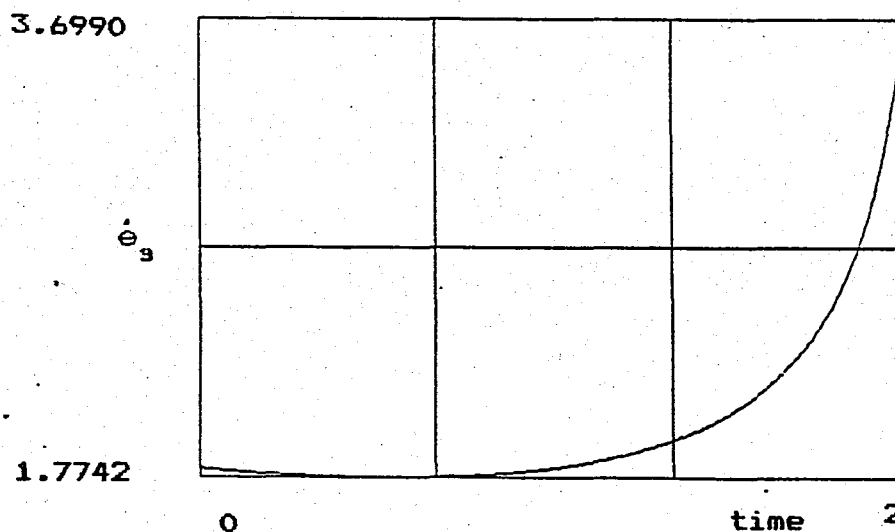
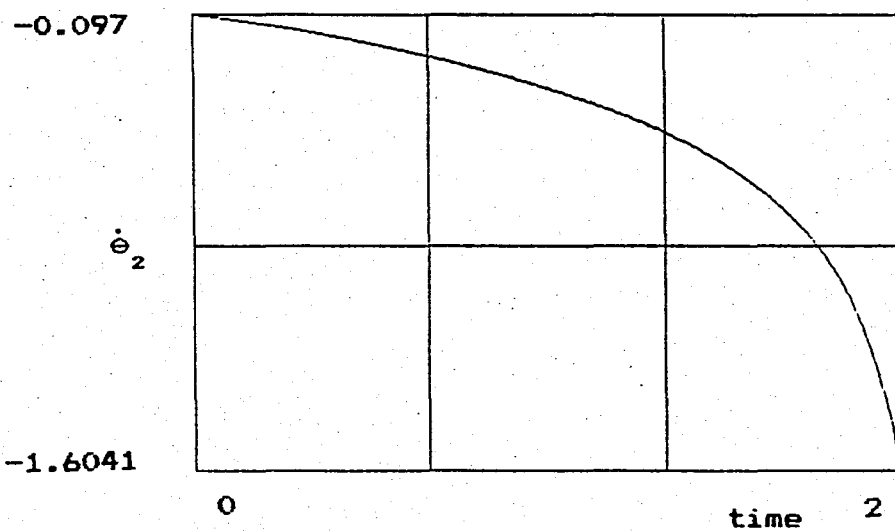
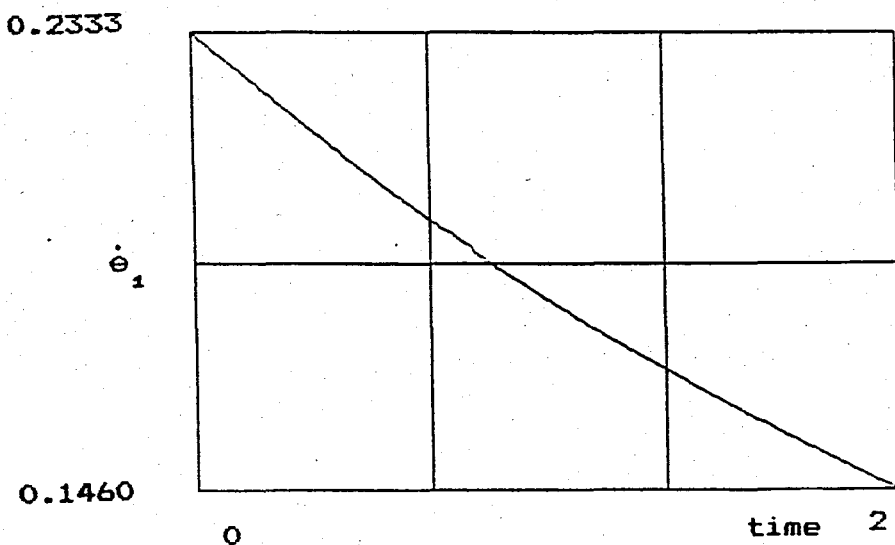


Figure 7.8. - First three joint velocities (rad/sec) for conic helix path. Time in sec.

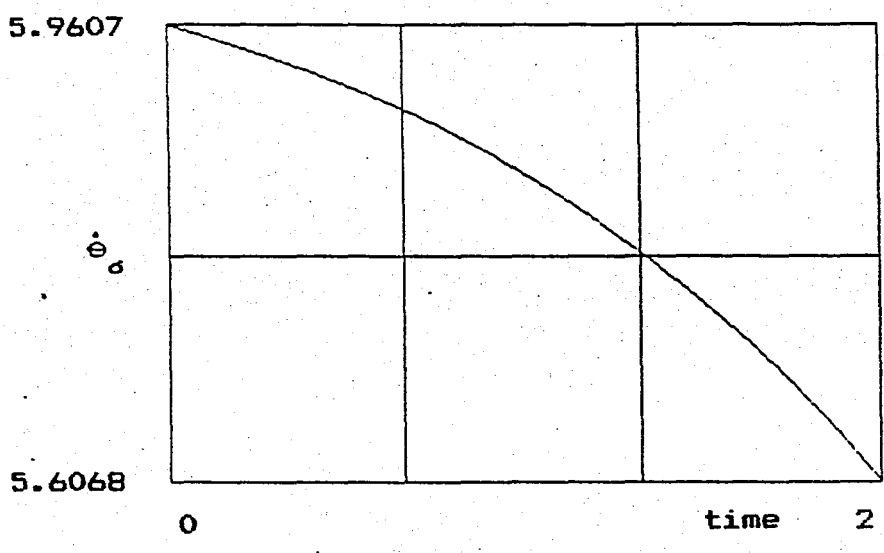
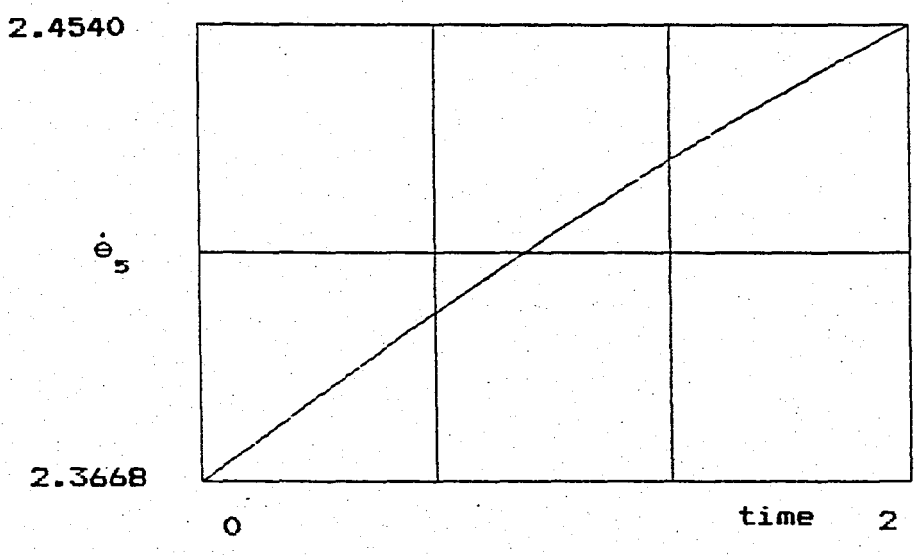
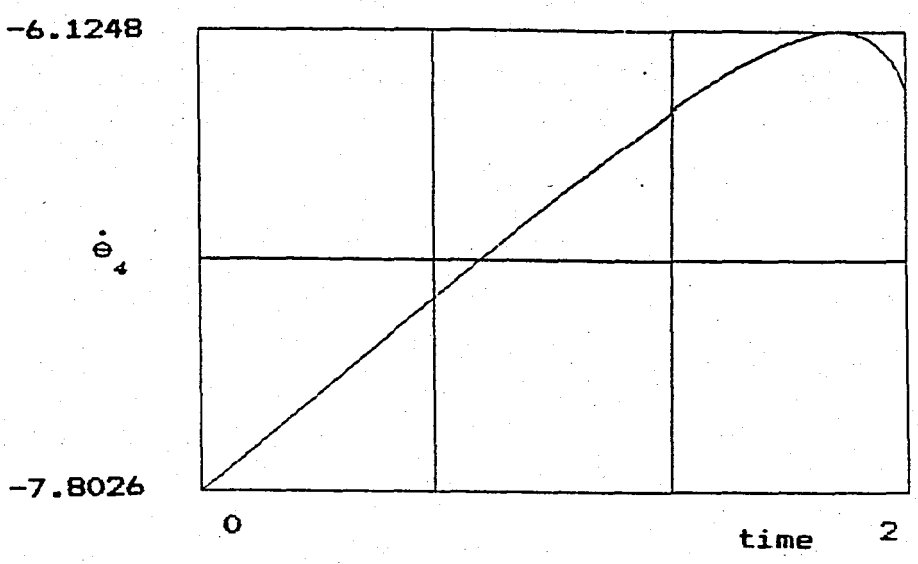


Figure 7.9. - Wrist joint velocities (rad/sec) for conic helix path. Time in sec.

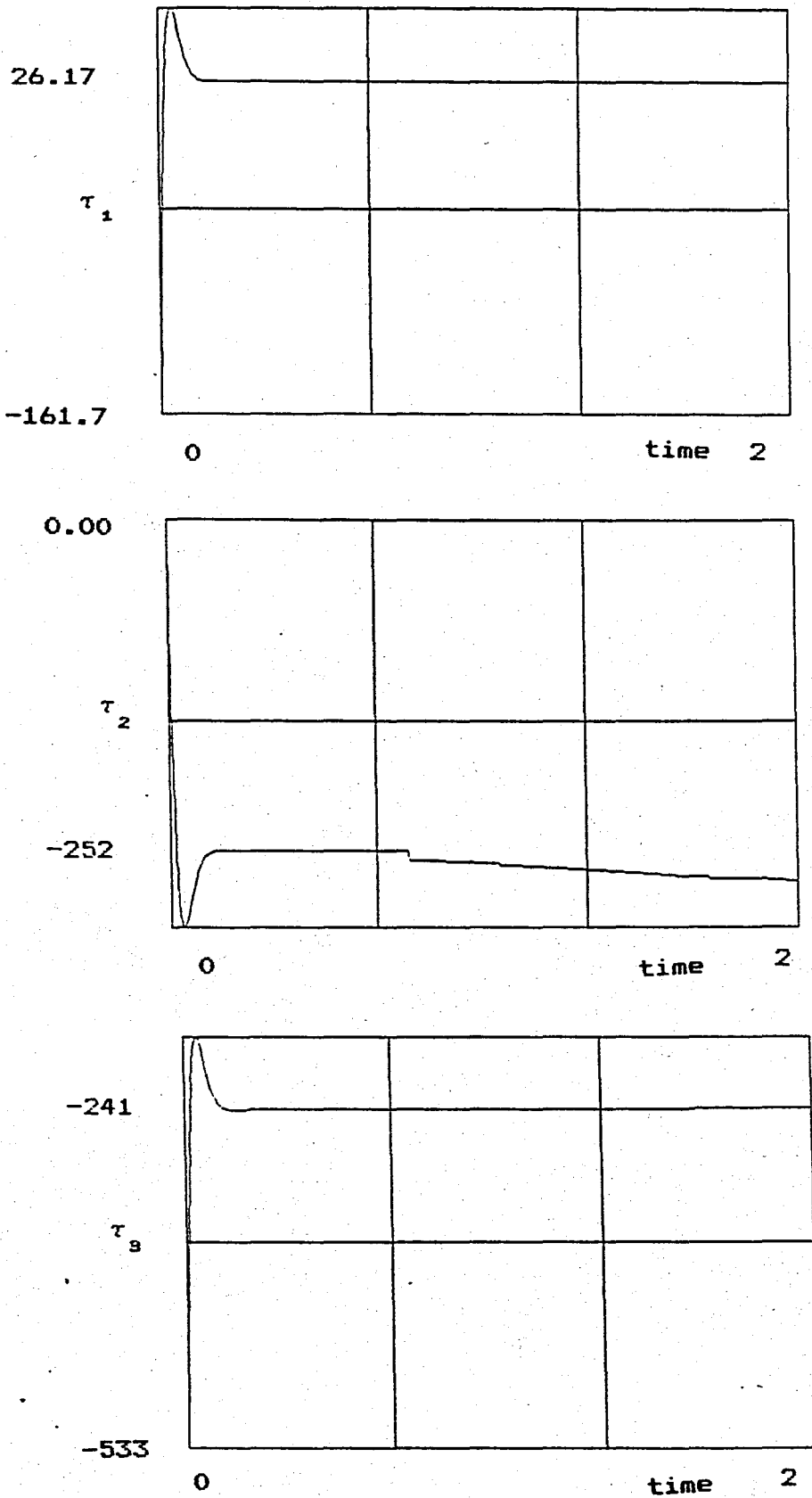


Figure 7.10.- First three joint torques (Nt) for conic helix path. Time in sec.

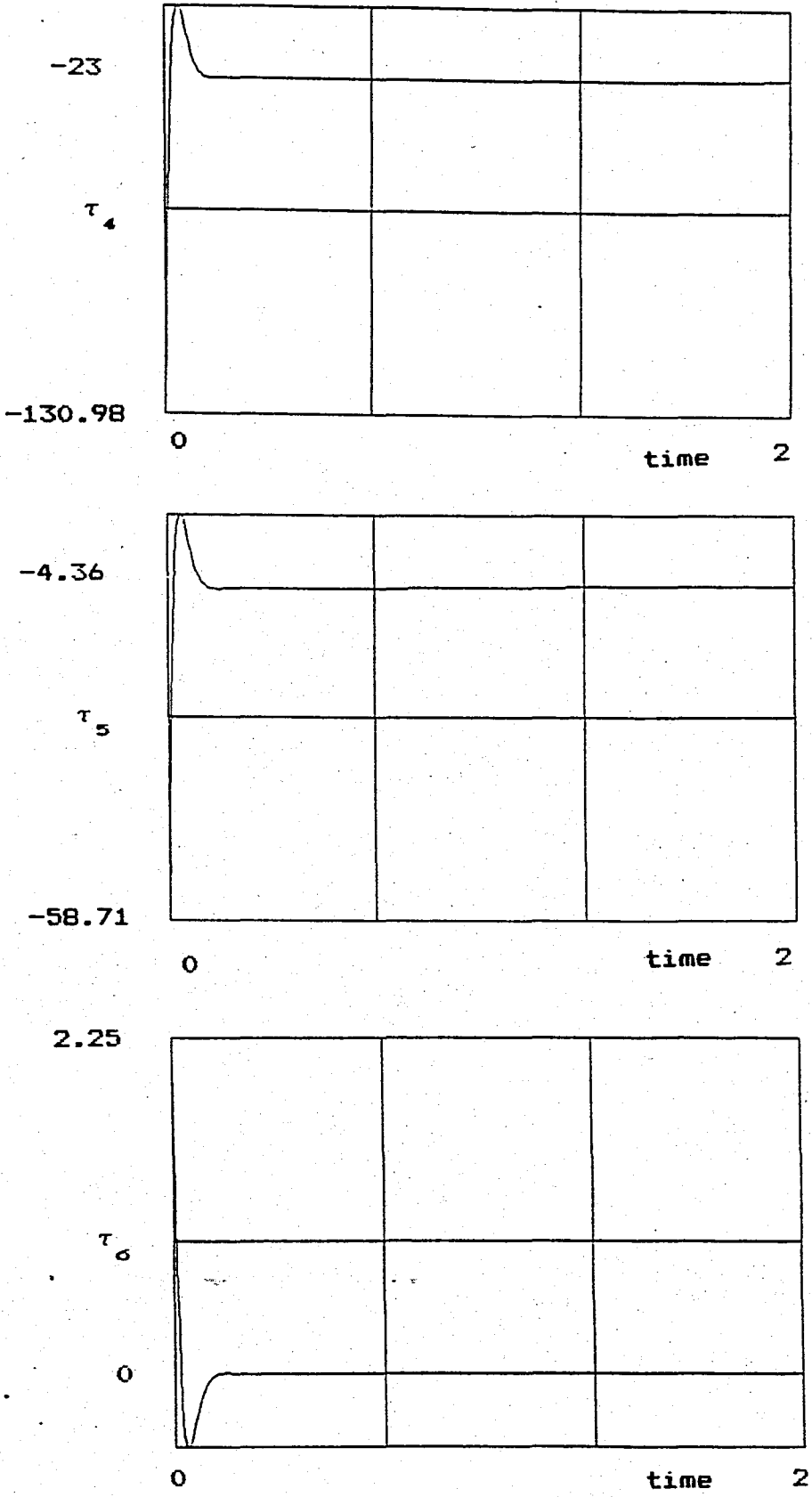


Figure 7.11.- Wrist joint torques (Nt) for conic helix path.  
Time in sec.

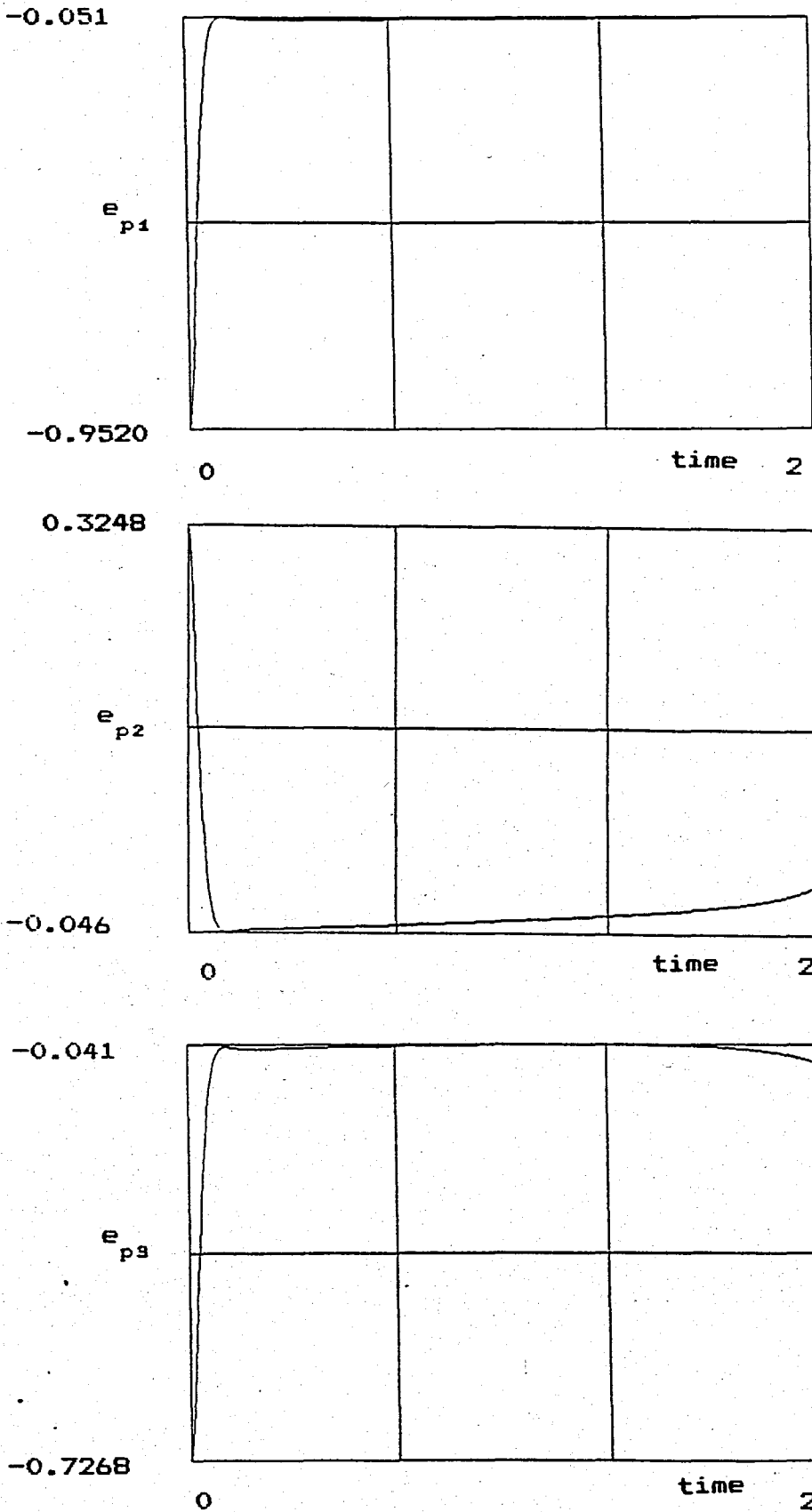


Figure 7.12.- Position errors (rad) of the first three joints following conic helix path. Time in sec.

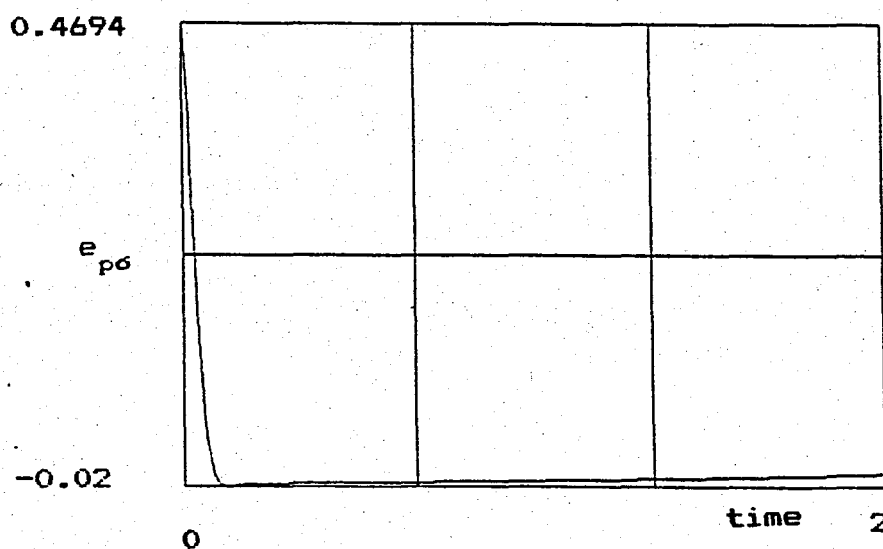
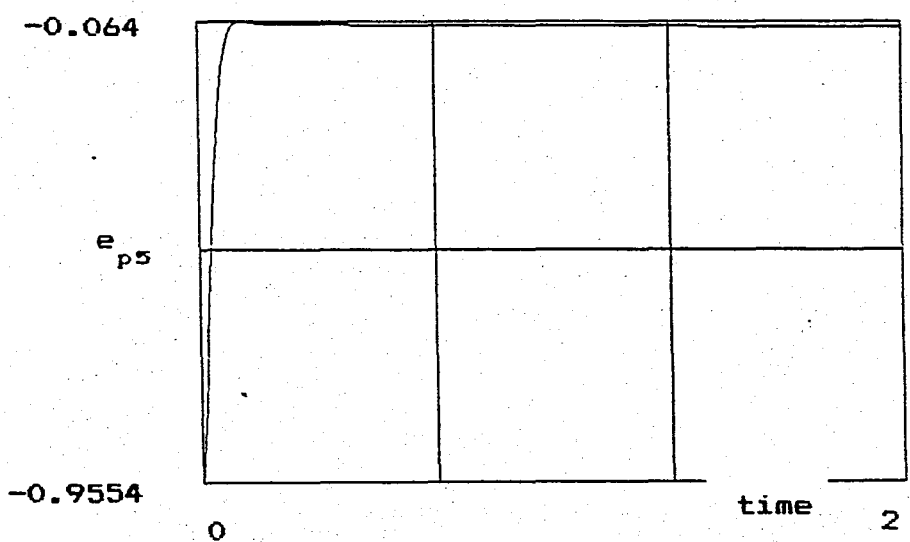
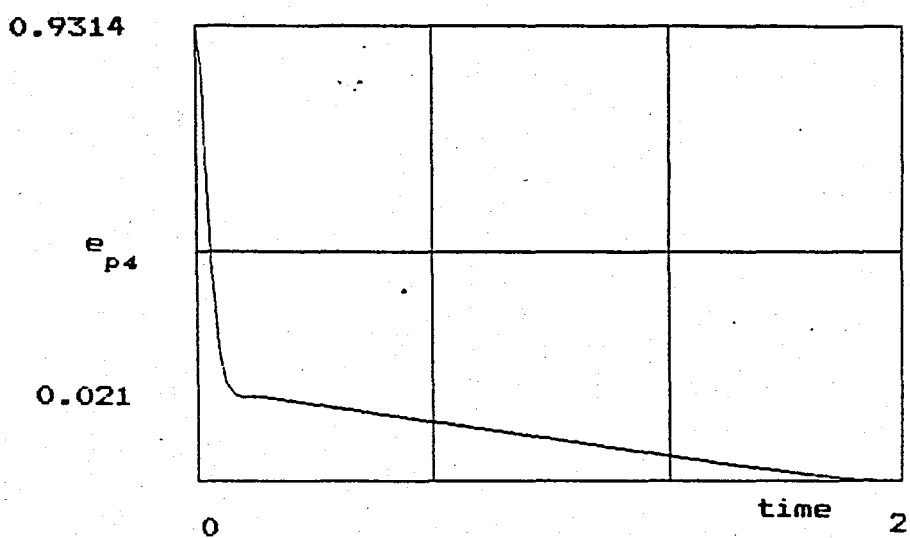


Figure 7.13.- Position errors (rad) of wrist joints following conic helix path. Time in sec.

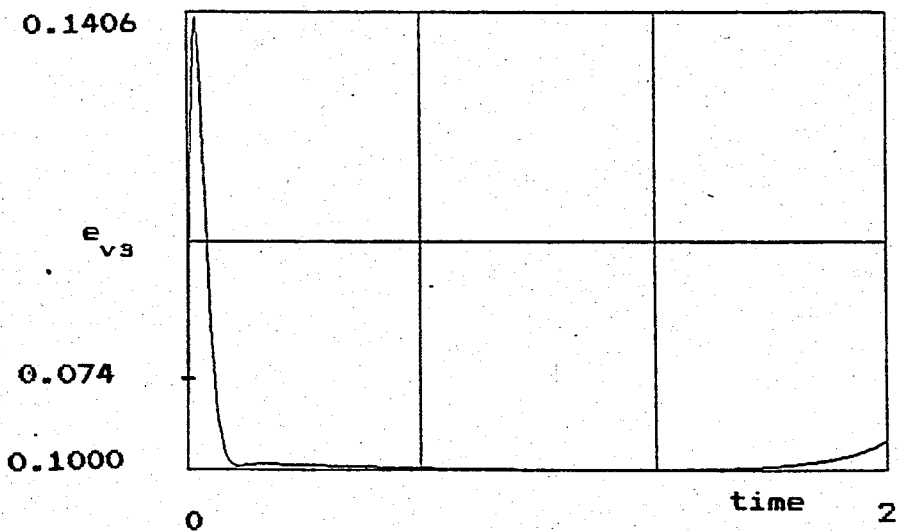
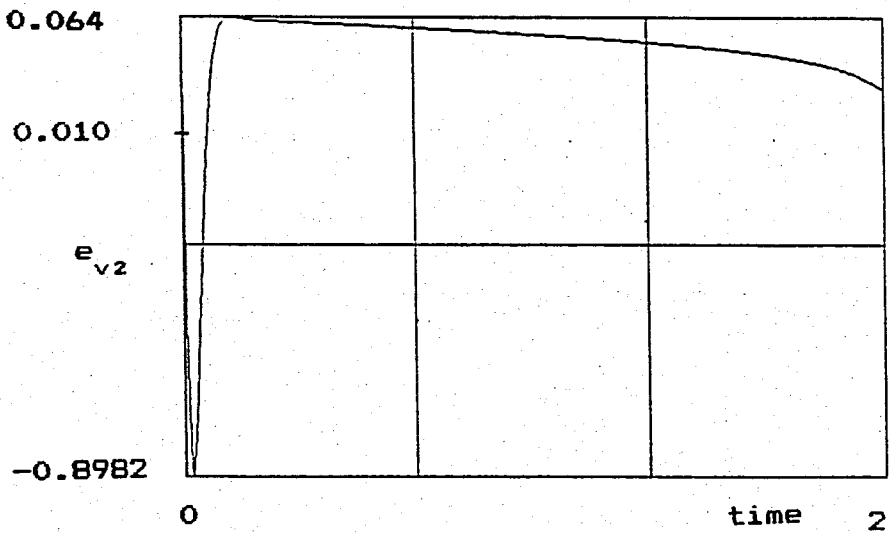
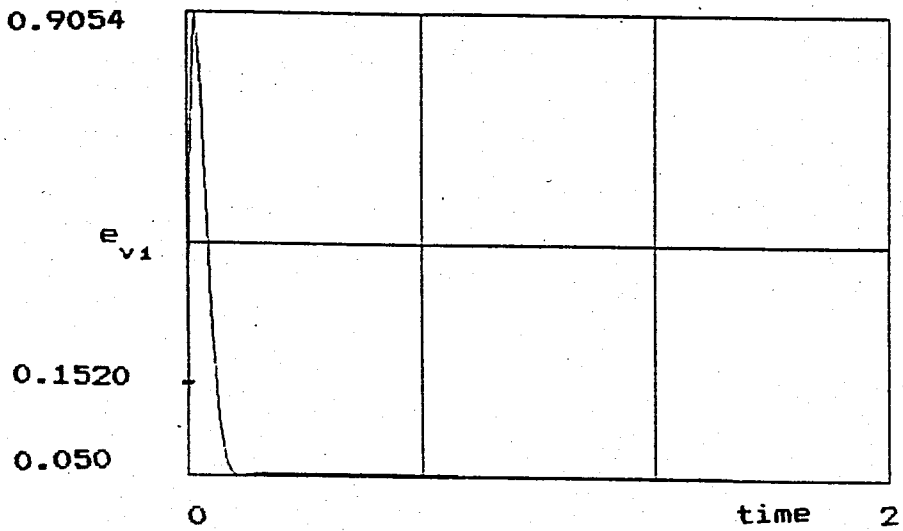


Figure 7.14.- Speed errors (rad/sec) of the first three joints following conic helix path. Time in sec.

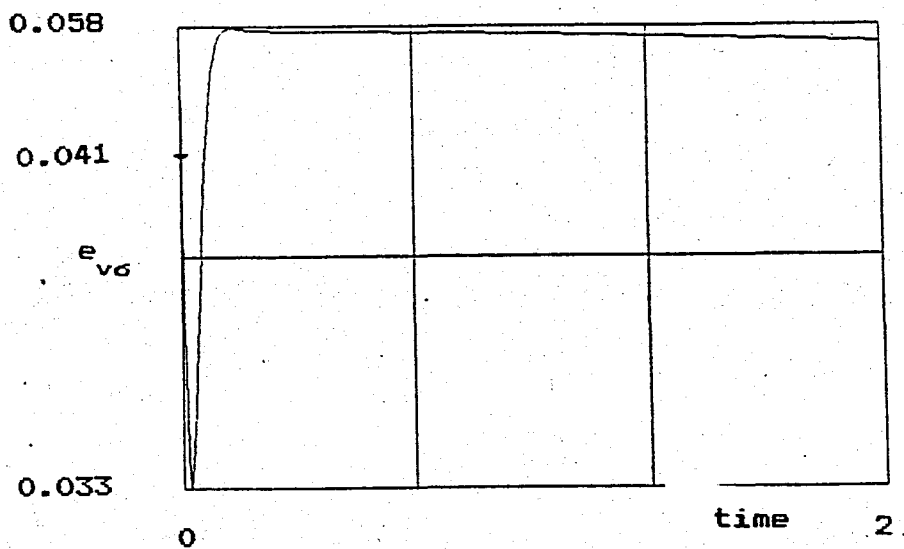
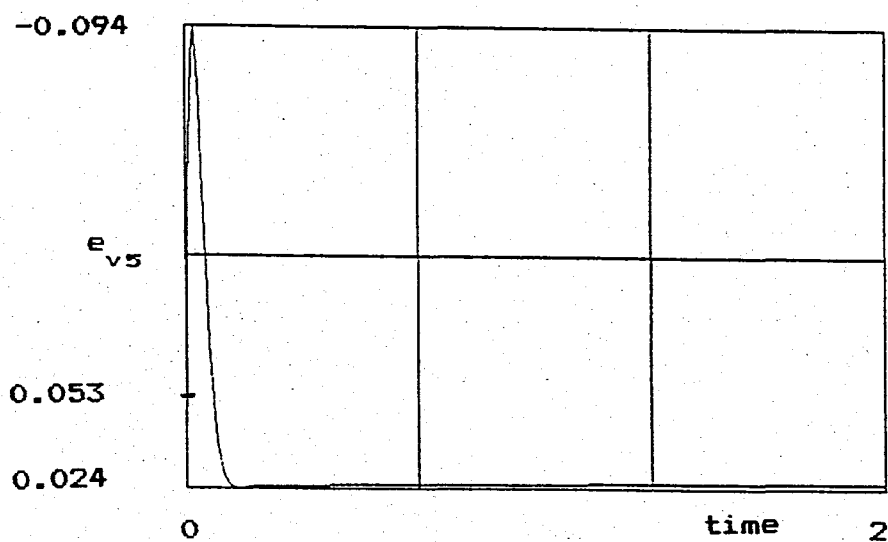
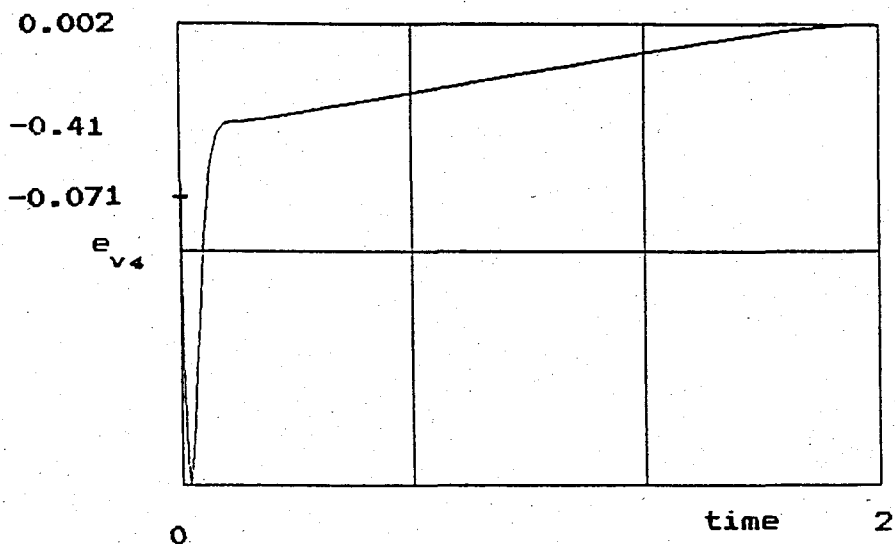
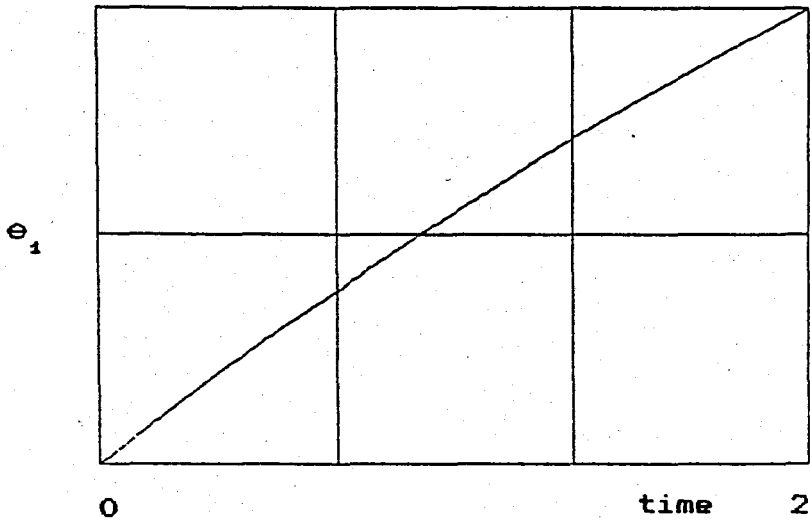
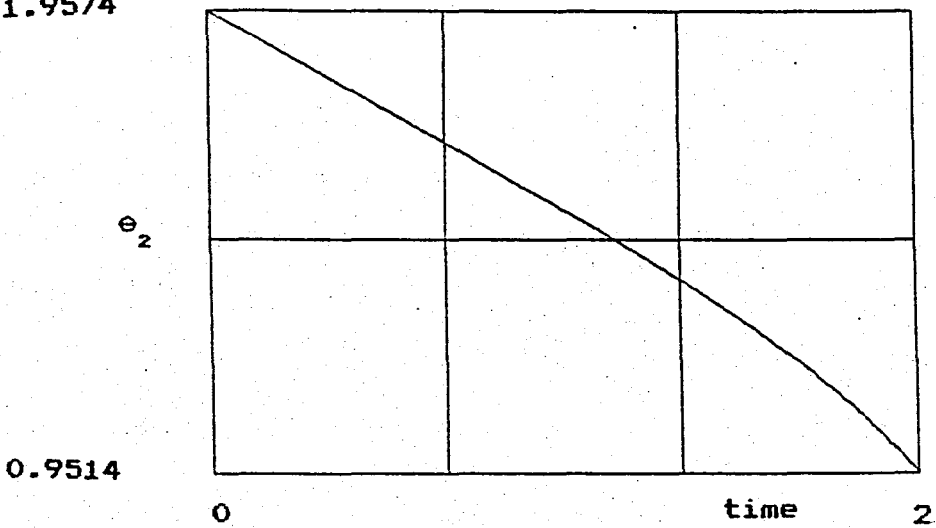


Figure 7.15.- Speed errors (rad/sec) of wrist joints following conichelix path. Time in sec.

0.8921



1.9574



-0.5658

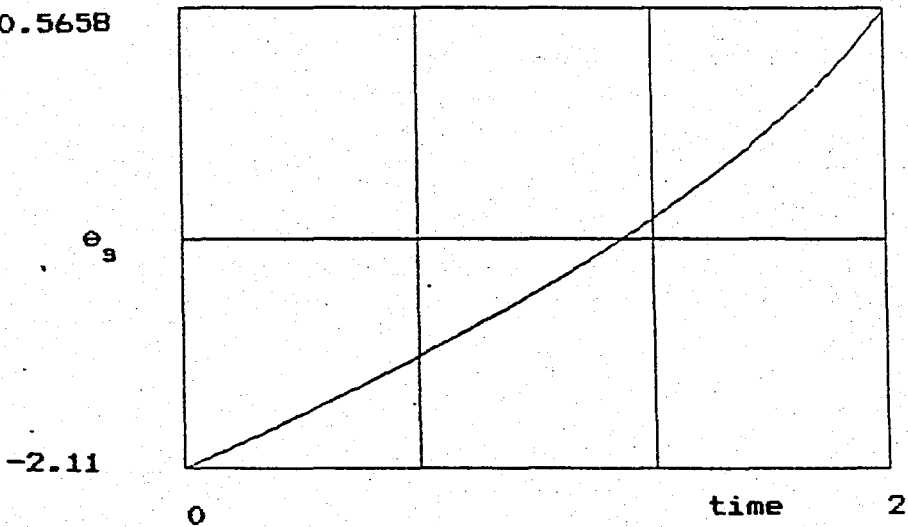


Figure 7.16.--Teach-in, first three joint displacements (rad) on the conic helix path. Time in sec.

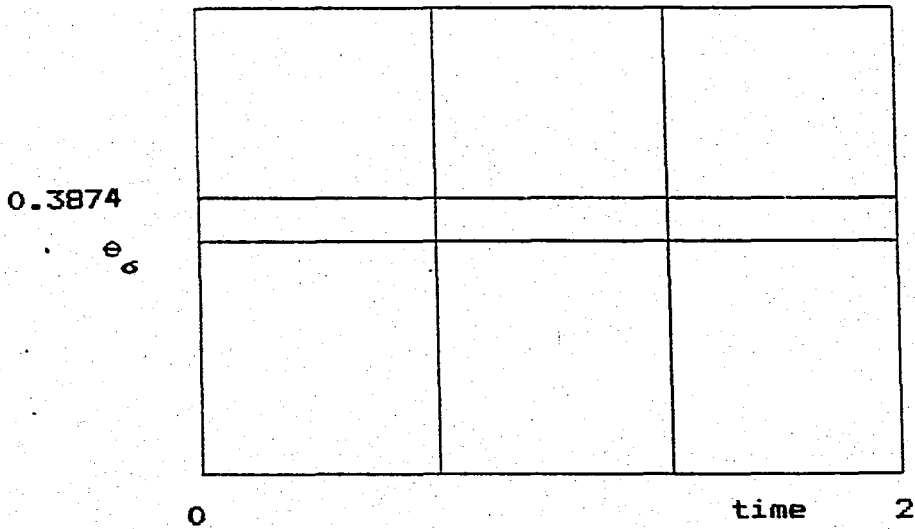
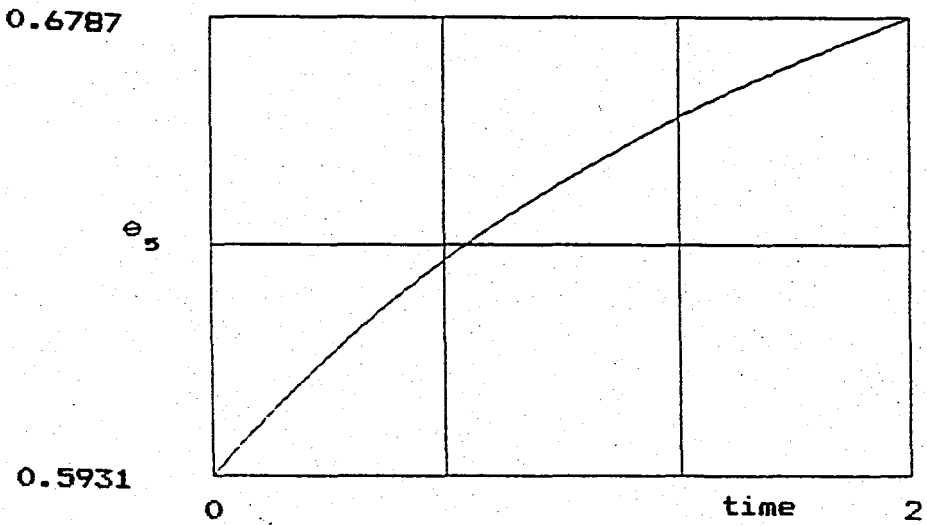
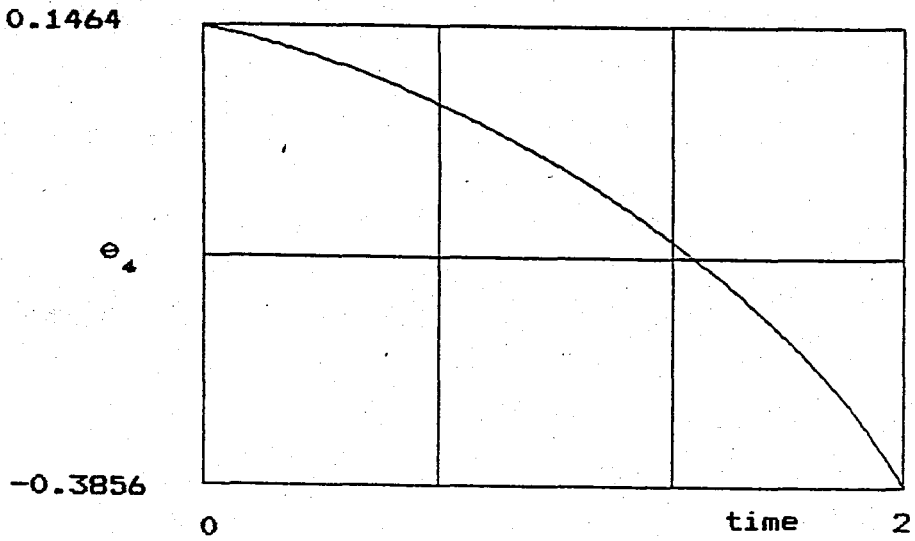


Figure 7.17.- Teach-in, wrist joint displacements (rad) on the conic helix path. Time in sec.

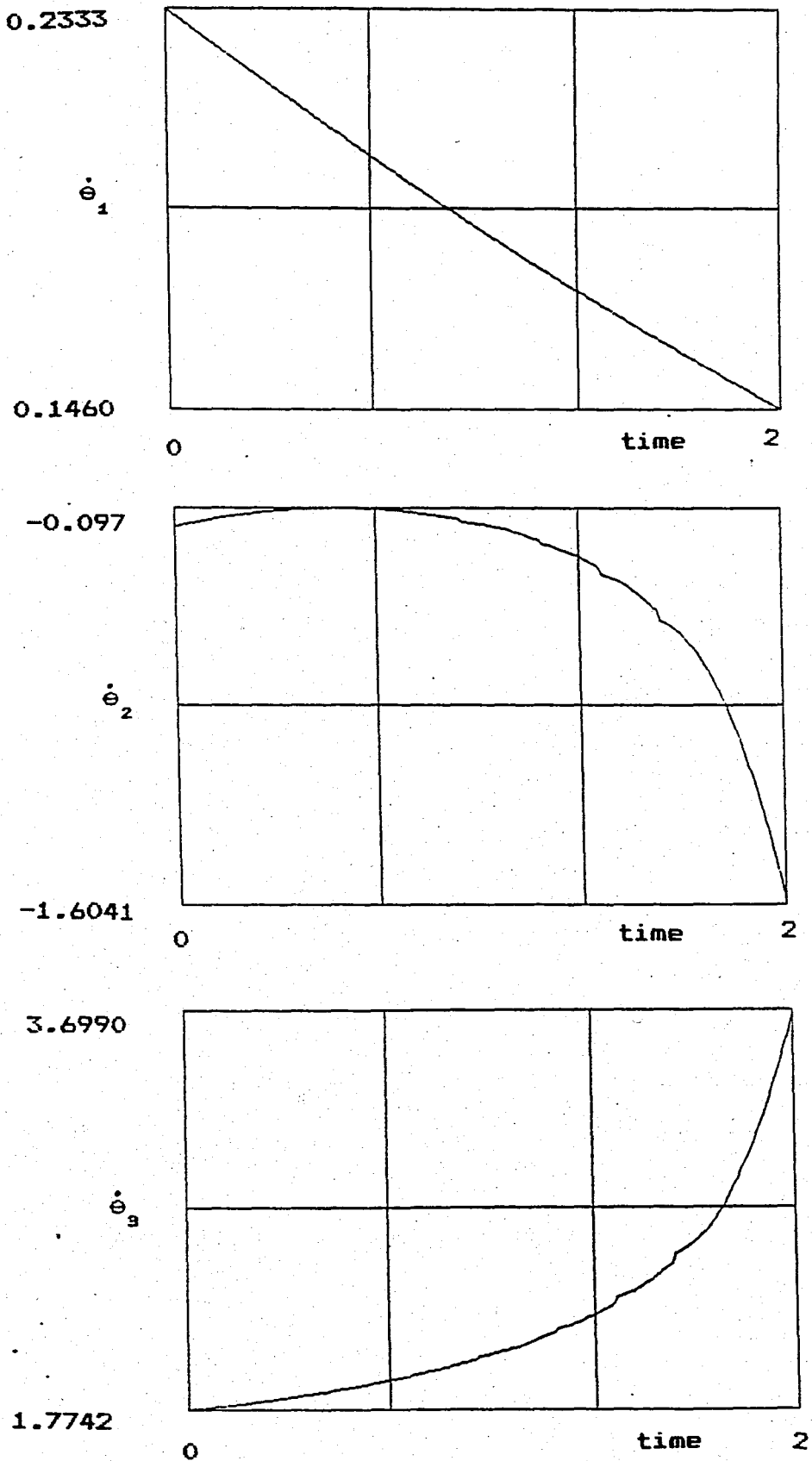


Figure 7.18.—Teach-in, first three joint velocities (rad/sec) on the conic helix path. Time in sec.

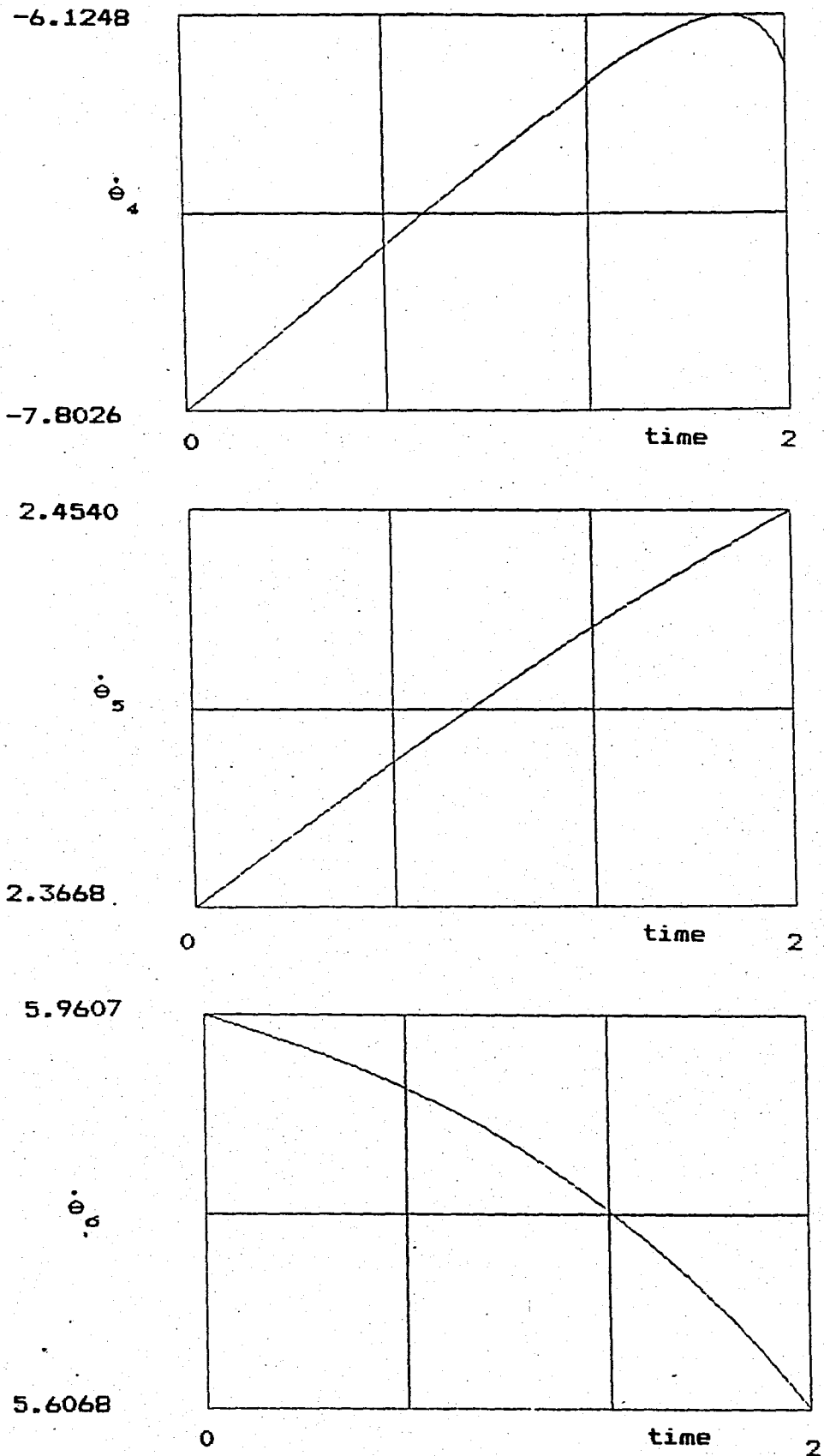


Figure 7.19.- Teach-in, wrist joint velocities (rad/sec) on the conic helix path. Time in sec.

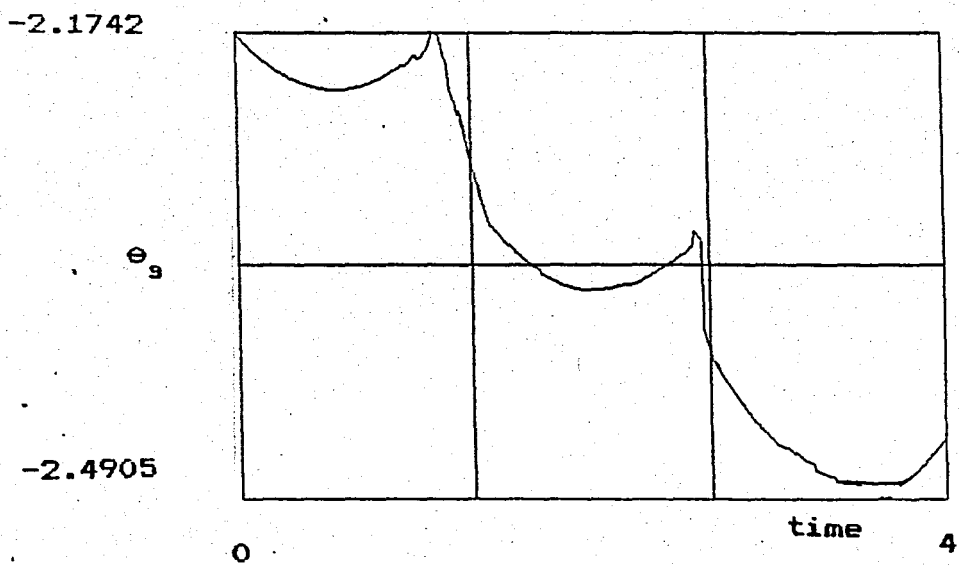
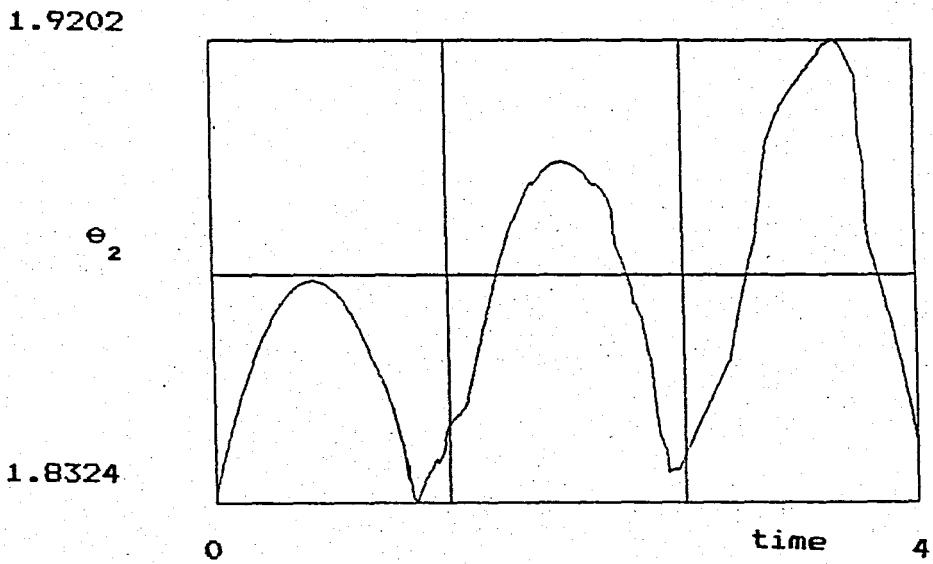
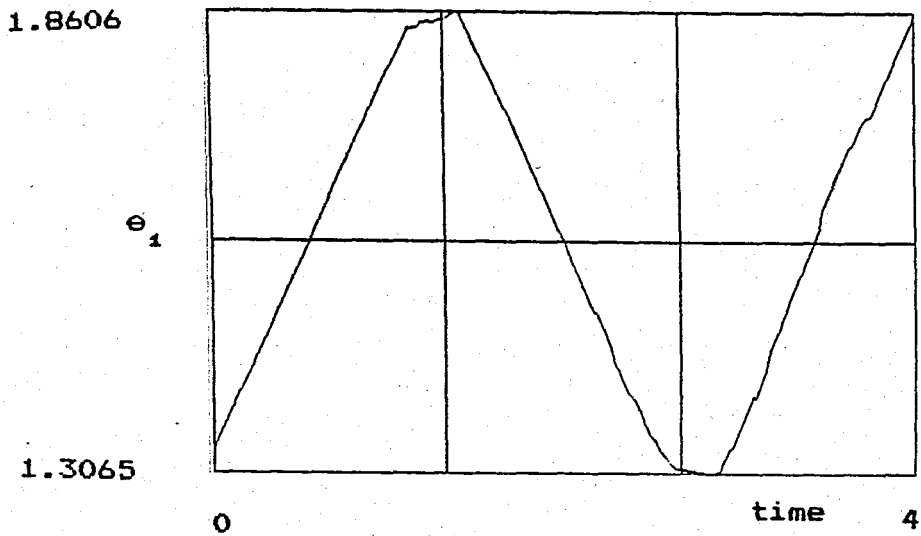


Figure 7.20.—Teach-in, first three joint displacements (rad) on the rectangular plate. Time in sec.

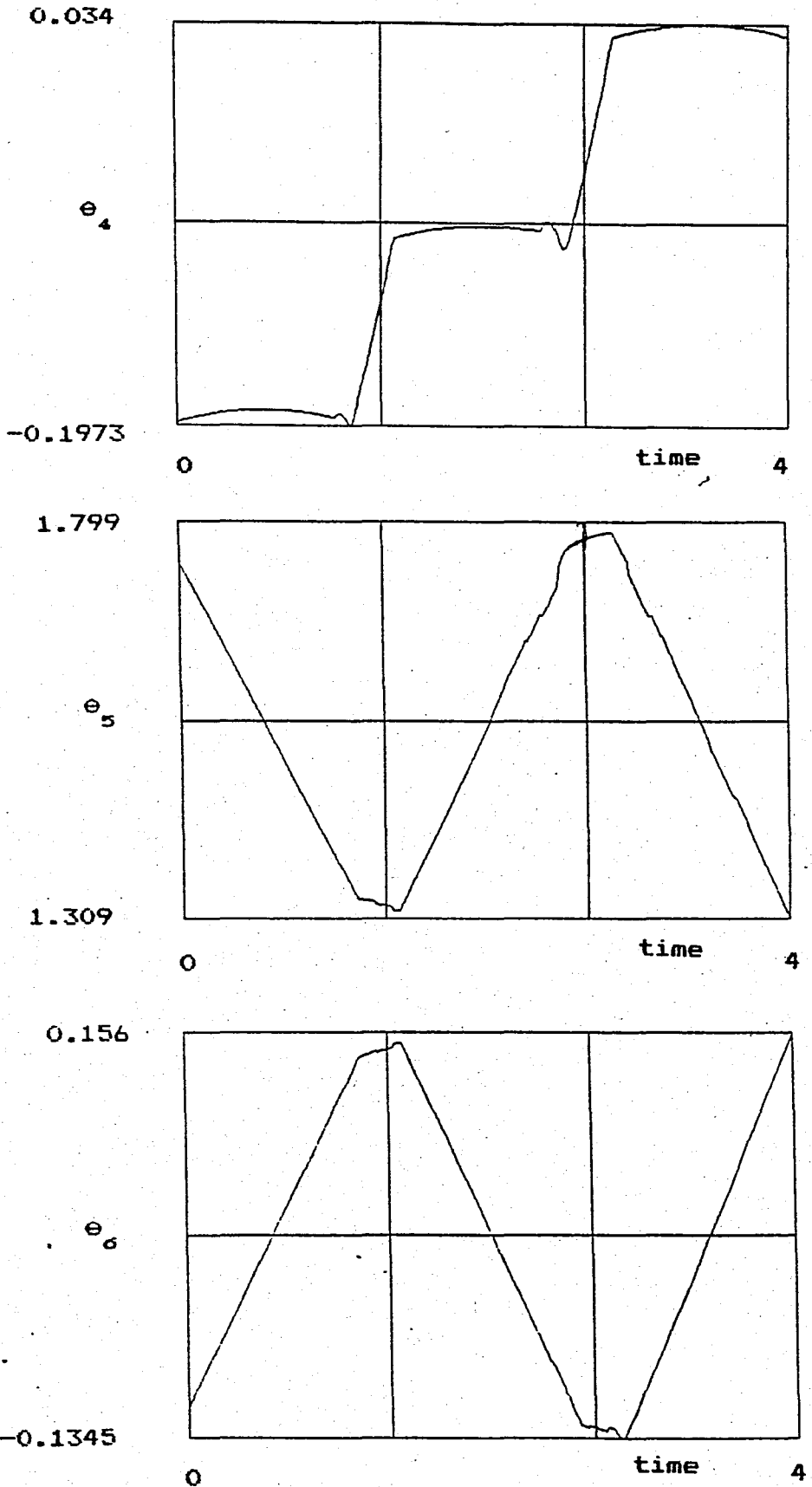


Figure 7.21.- Teach-in, wrist joint displacements (rad) on the rectangular plate. Time in sec.

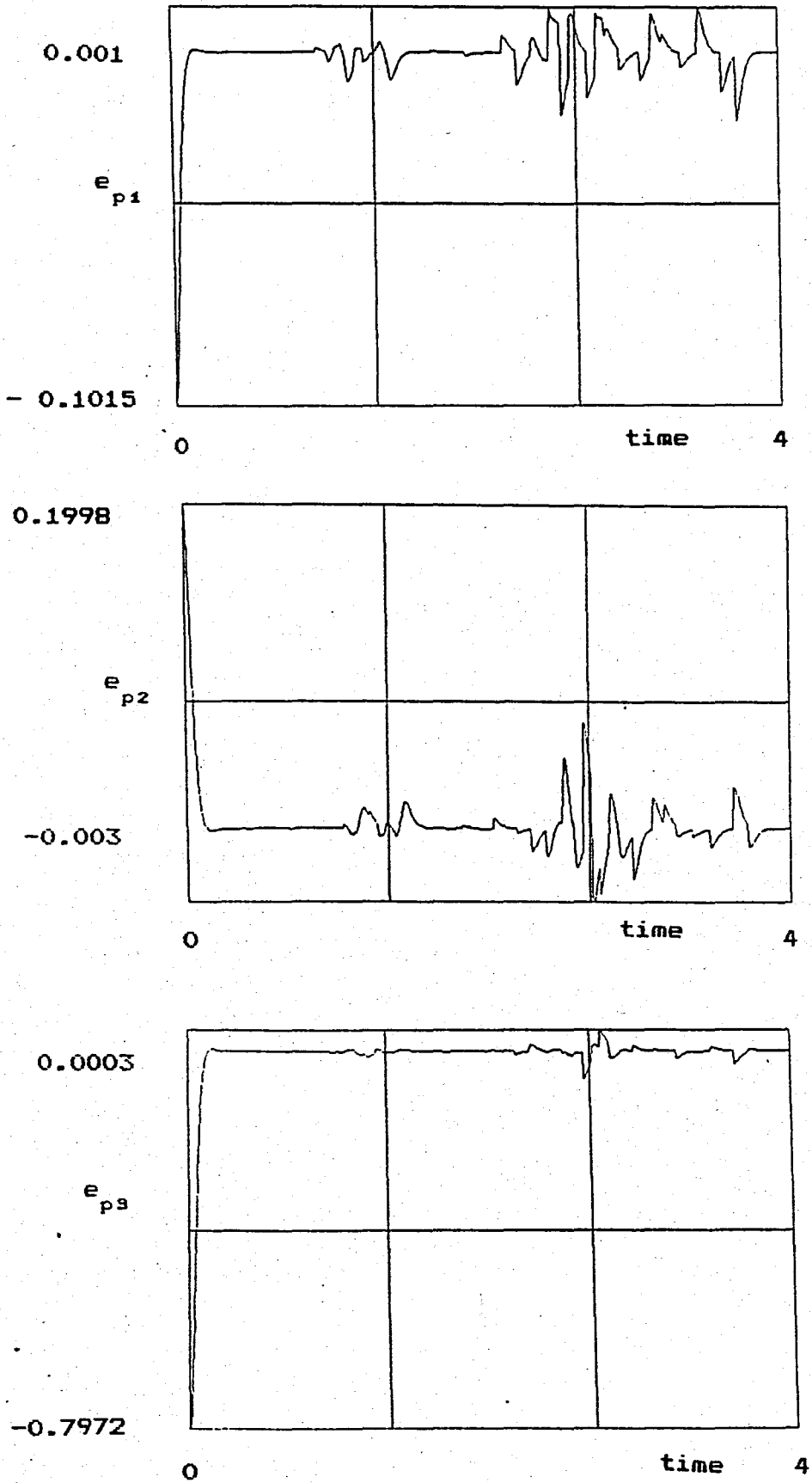


Figure 7.22.- Position errors (rad)of the first three joints following the path for rectangular plate. Time in sec.

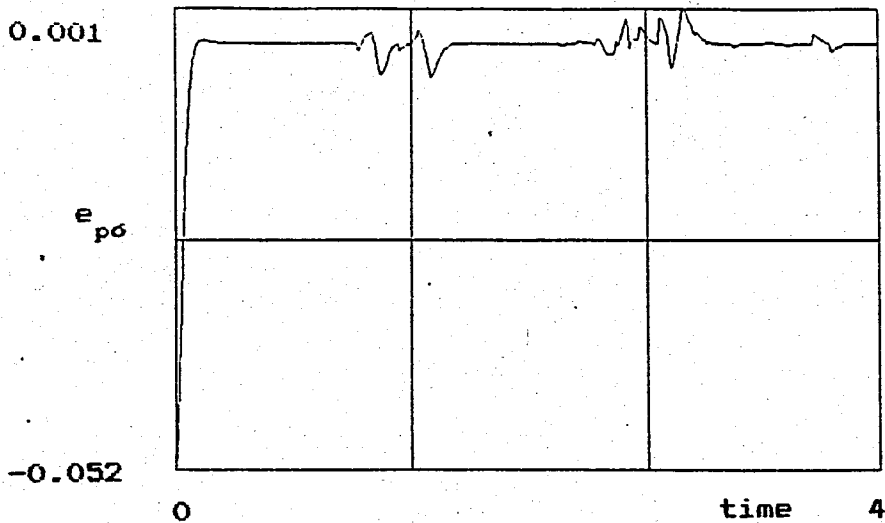
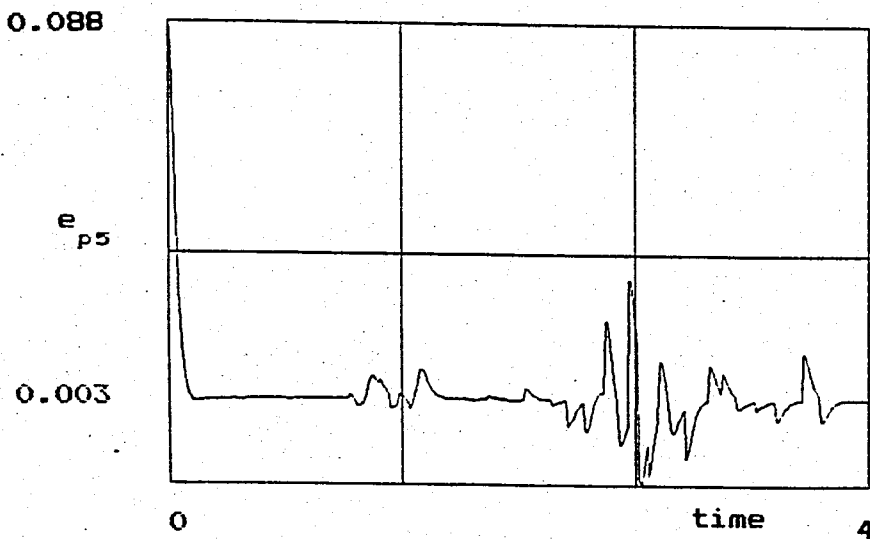
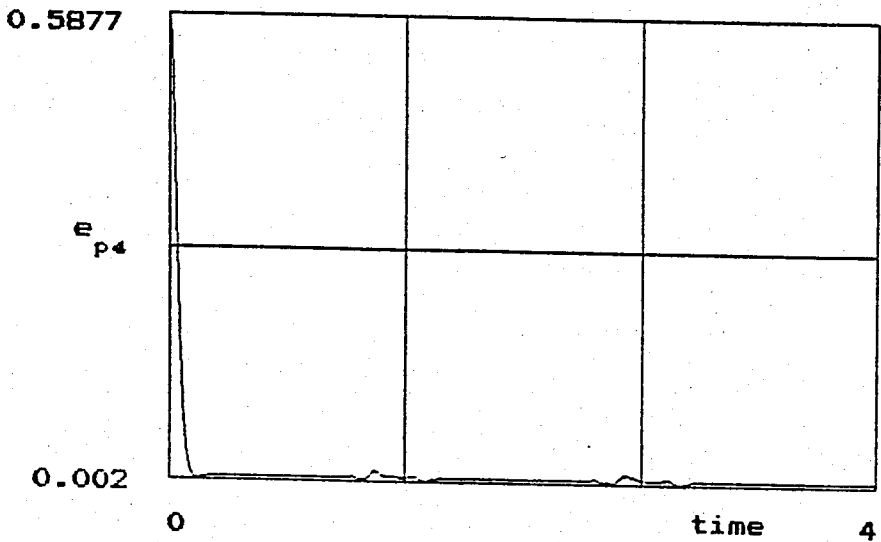


Figure 7.23.- Position errors (rad) of the wrist joints following the path for rectangular plate. Time in sec.

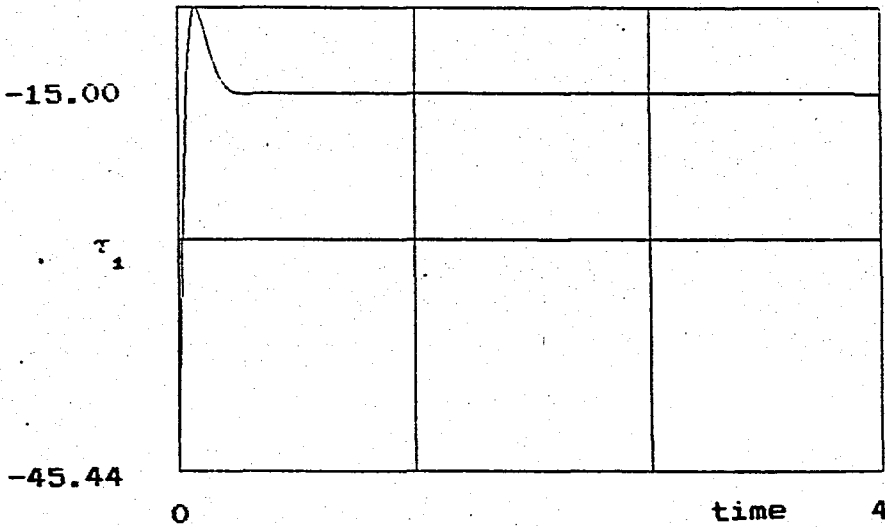
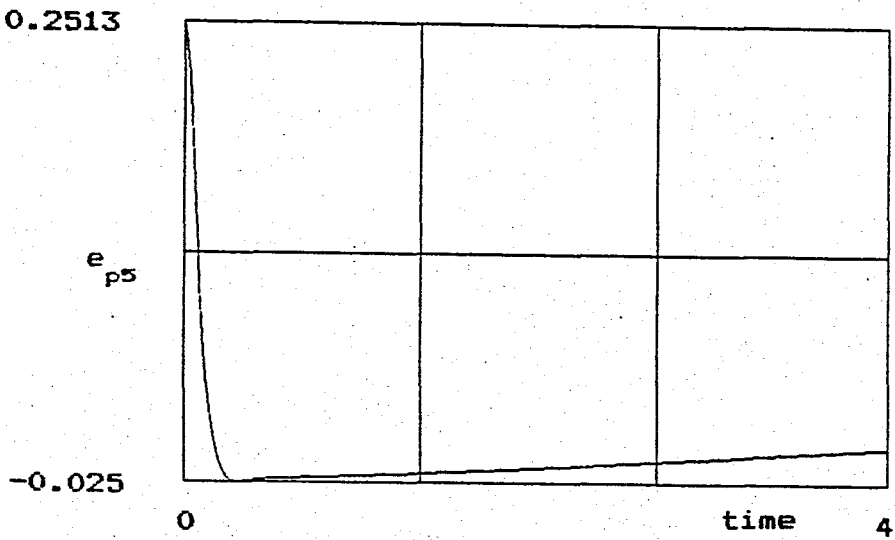
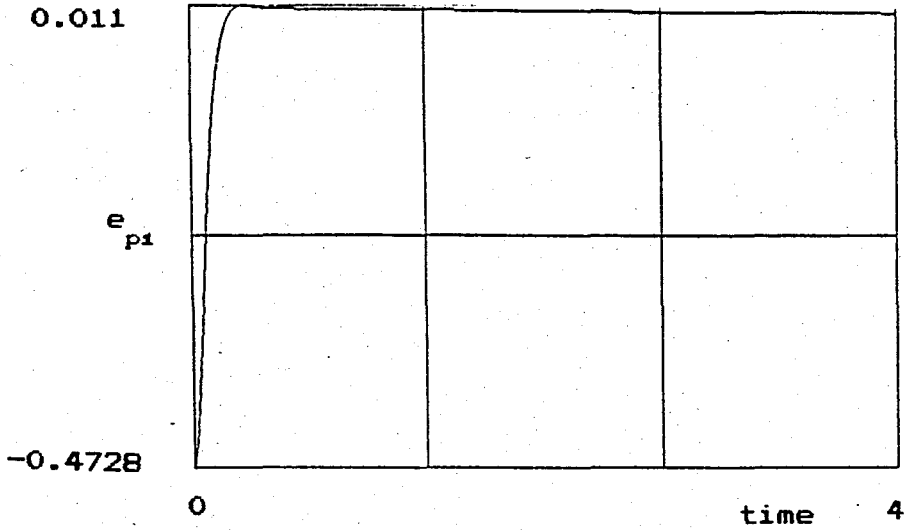


Figure 7.24.- Torque (Nt) of the first, position errors (rad) of the first & fifth joints following the spatial line. Time in sec.

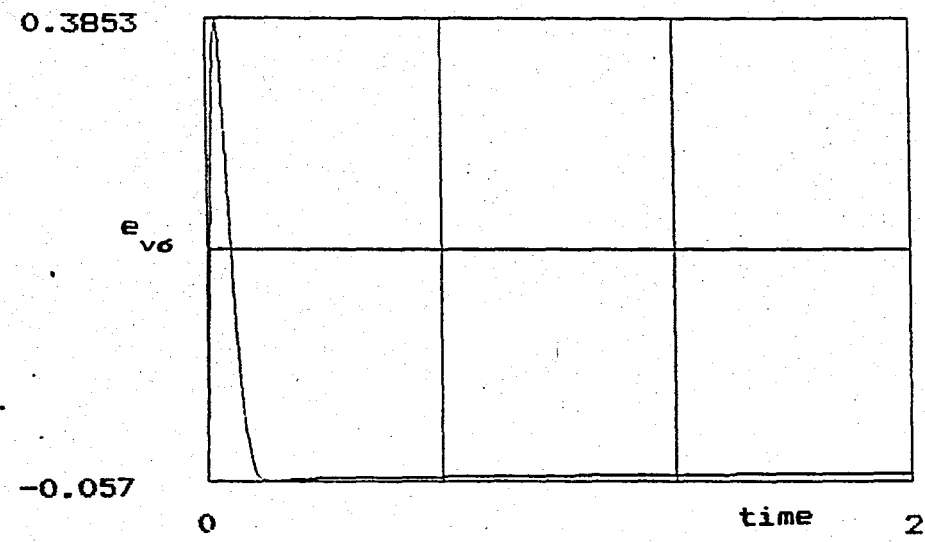
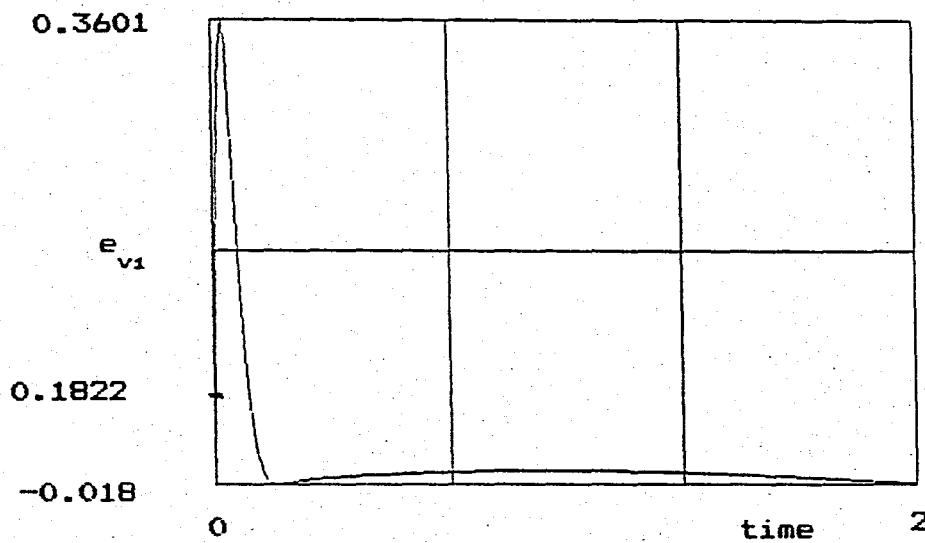
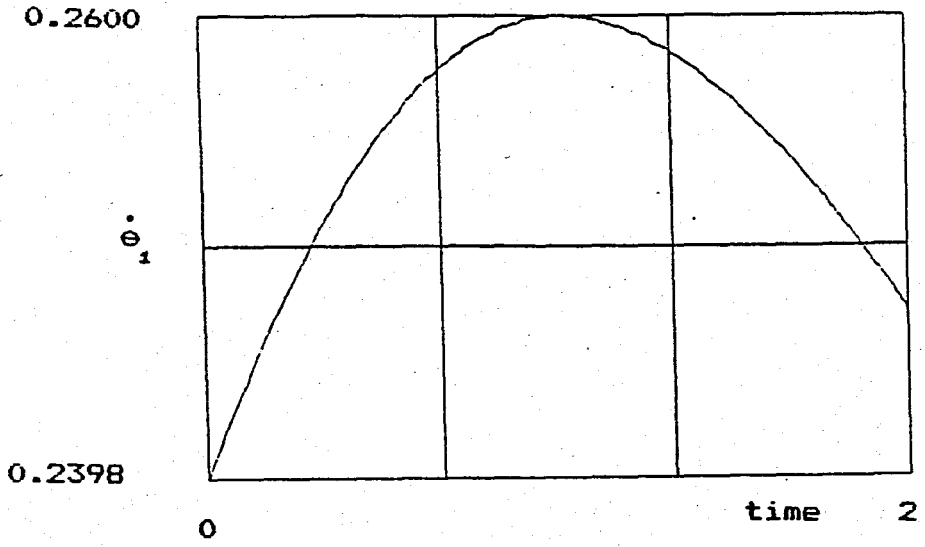


Figure 7.25.—Speed of the first(rad/sec), speed error (rad/sec) of the first & sixth joints on the spatial line. Time in sec.

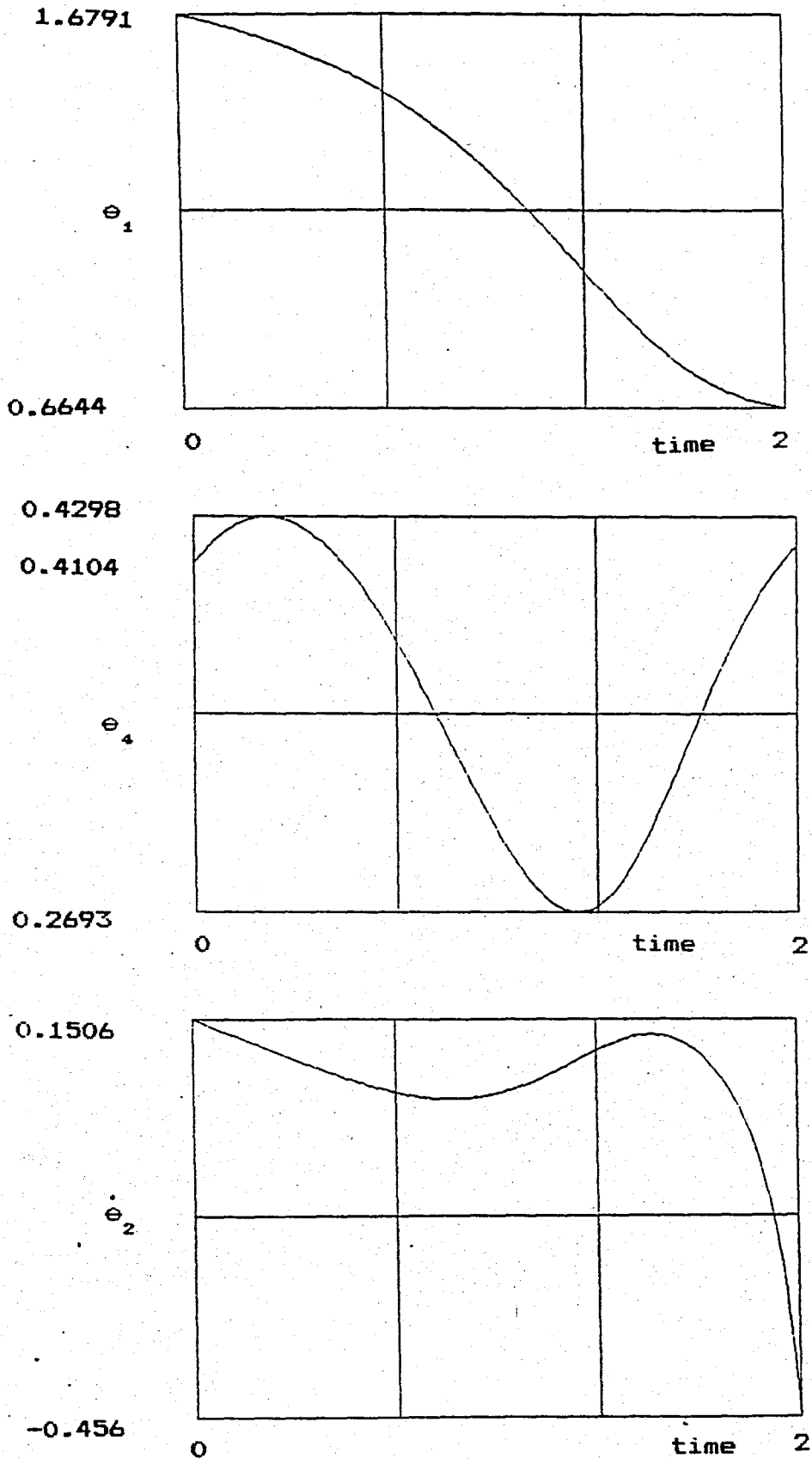


Figure 7.26.—First & fourth joint displacements (rad), velocity (rad/sec) of the second joint on the spatial parabola. Time in sec.

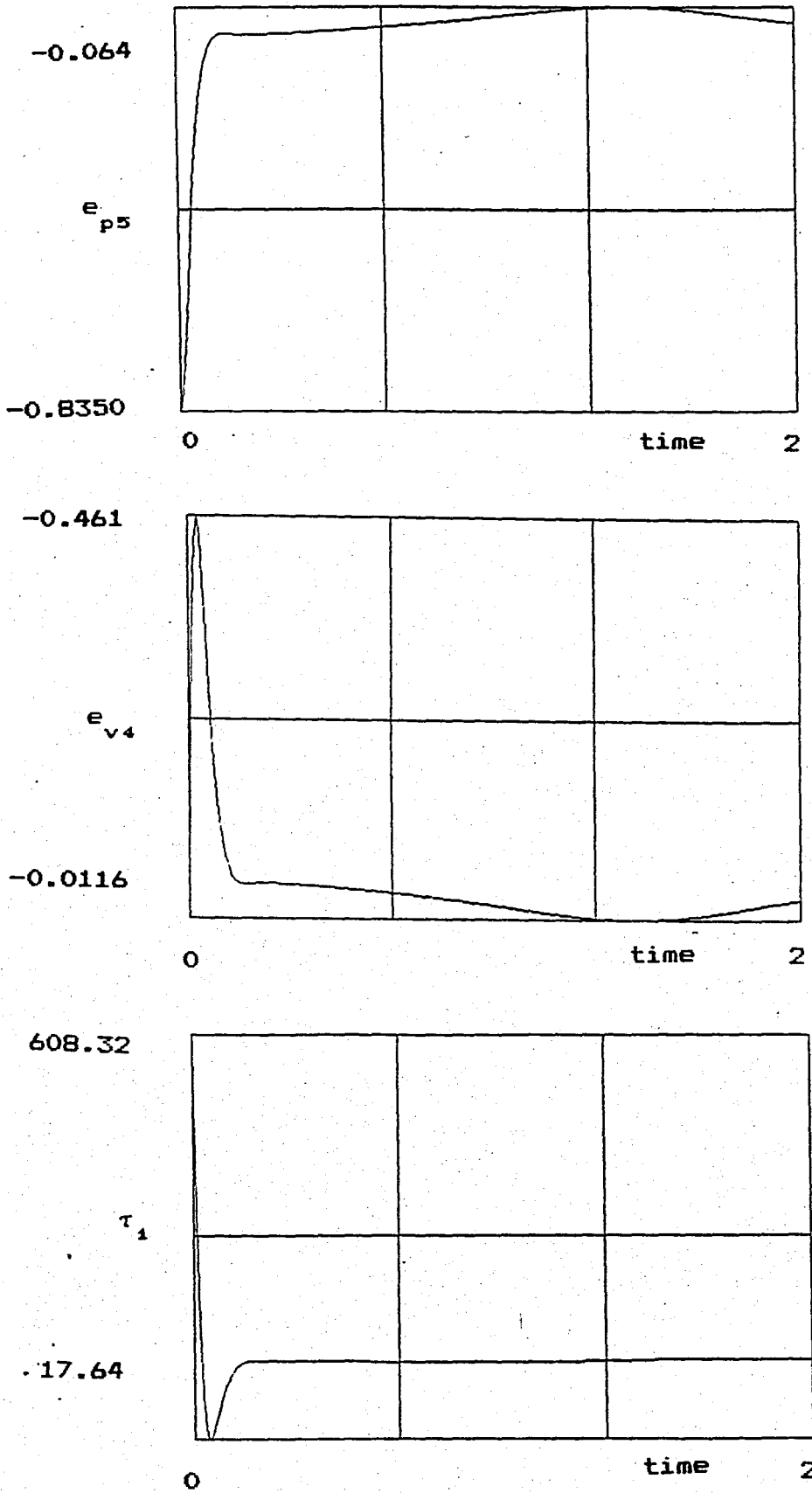


Figure 7.27.- Position (rad) & speed errors (rad/sec) of the fifth & fourth joints & torque (Nt) for the first one on spatial parabola. Time in sec.

## VIII. CONCLUSIONS

Associated with the robotic applications to the spray painting process, the problem of defining the time history of the spray gun for task completion became indisputably important. Because, a spray painting manipulator can even be economically justified if the special requirements of spray painting process which lead to saving material that had been previously wasted as overspray mist, are met. For this reason, a hybrid method namely on-line teach-in with off-line trajectory determination has been developed to teach a robot the desired path for completing a task.

In order to simulate the dynamic behavior of a spray painting robot, it is compulsory to define a dynamic model as well as a suitable control policy. N-E recursive dynamic modelling algorithm has been adopted to a six degree of freedom spray painting robot having a wrist configuration of pitch-yaw-roll type. The proposed control algorithm on the other hand is, computed torque technique. Both had been preferred for their conformity to computer simulation. Furthermore, to complete the simulation program

computation of the manipulator Jacobian have been investigated.

Computation of the system matrices defining the dynamic model involves too many messy matrix and vector products. Among them, the inertia matrix is the one having the biggest influence on the system behavior. An updating policy, taking the trace of the inertia matrix as the basis of decision for when to update, has been developed. It's been observed that this divides the workspace of the robot into sub-regions which are concentric spherical stratum. In a particular stratum the values of the system matrices tend to remain constant. The algorithm updates the system matrices if the end-effector passes from one stratum to another. This resulted in considerable save in time and made the program run faster.

Three basic scenarios, a spatial line, a conic helix and a spatial parabola have been selected. They all cause all the joints of the robot to move. Besides this, teach-in facilities have been used to simulate the robot painting an inclined surface located in the workspace. In addition, the same conic helix has been this time taught the robot to see the effectiveness of the hybrid trajectory planning algorithm. It's been observed that the proposed algorithm resulted in smooth curves which are continuous in position, speed and acceleration. The approximated paths in joint coordinates for the conic helix have only

infinitesimal deviations from the analytically calculated ones. Position and speed errors are negligibly small. The overshoots at the torque diagrams are because of making the manipulator which is stationary at its initial position move at the desired speed. An acceleration profile may be defined to reduce the peaks.

The developed algorithm for off-line trajectory determination is fast enough and occupies not very much of memory capacity. Therefore, it can be used for planning any trajectory to be followed by constant speed, for continuous path robots.

## BIBLIOGRAPHY

- [1] DeVilbiss , The ABC's of Spray Equipment for Refinishing.
- [2] Critchlow, Arthur J., Introduction to Robotics.  
New York : Macmillan Publishing Comp., 1985.
- [3] Asada, H. and Slotine, J.-J.E., Robot Analysis and Control. New York : A Wiley-Interscience Publ.. 1986.
- [4] Fu, K.S., Gonzalez, R.C., Lee, C.S.G., Robotics.  
New York : McGraw Hill International Editions, 1987.
- [5] Lee, C.S.G., "Robot Arm Kinematics, Dynamics and Control", IEEE 0018-9112/1200 pp.62-80, 1982.
- [6] Kuzucu, A., Akmehmet, A., "Computer Aided Determination of Robot Arm Dynamics and Adaptive Control Algorithms", 1984.
- [7] Meriam, J.L., Statics and Dynamics.  
New York : John Wiley & Sons, 1980.
- [8] Luh, J.Y.S., Walker, M.W., and Paul, R.P.C. "On-line Computational Schemes for Mechanical Manipulators", J. Dynamic Syst. Measurement, Contr., Vol.102 pp 69-76, 1980.
- [9] Vukobratovic, M., and Stepanenko, Yu., "Dynamics of Articulated Open-Chain Active Mechanisms".  
Math. Biosciences, Vol.28, pp 137-170, 1976.

- [10] Kuzucu,A., "Kayan Ufuklu Kontrol ve Uygulamalari",  
J. 1. Ulusal Otomatik Kontrol Sempozyumu,pp 207-217,  
1982.
- [11] Spigel,M.R., Vector Analysis,  
New York : Schaum Publishing Comp.,1959.
- [12] Reis Robot, Catalog for Reis Robot products.  
1426 Davis Road,ELGIN, IL 60120 USA.
- [13] Zecher.,J.E., "Generation of cubic polynomial  
splines".Machine Design,Feb.1989.Publ.Penton  
Publishing,Ohio.(ISSN 0024-2114).
- [14] Asada,H., "Automatic Program Generation from Teaching  
Data for the Hybrid Control of Robots".IEEE Trans.  
on robotics & Automation,Vol.5,No.2 Apr.1989.
- [15] Andersson,R.,L., "Aggressive Trajectory Generation  
for a Robot Ping-Pong player".IEEE Control Syst.Mag.  
0200-0015,1989.